High-Precision Measurement of the W Boson Mass with the CDF II Detector

Ashutosh V. Kotwal
Duke University

For the CDF Collaboration

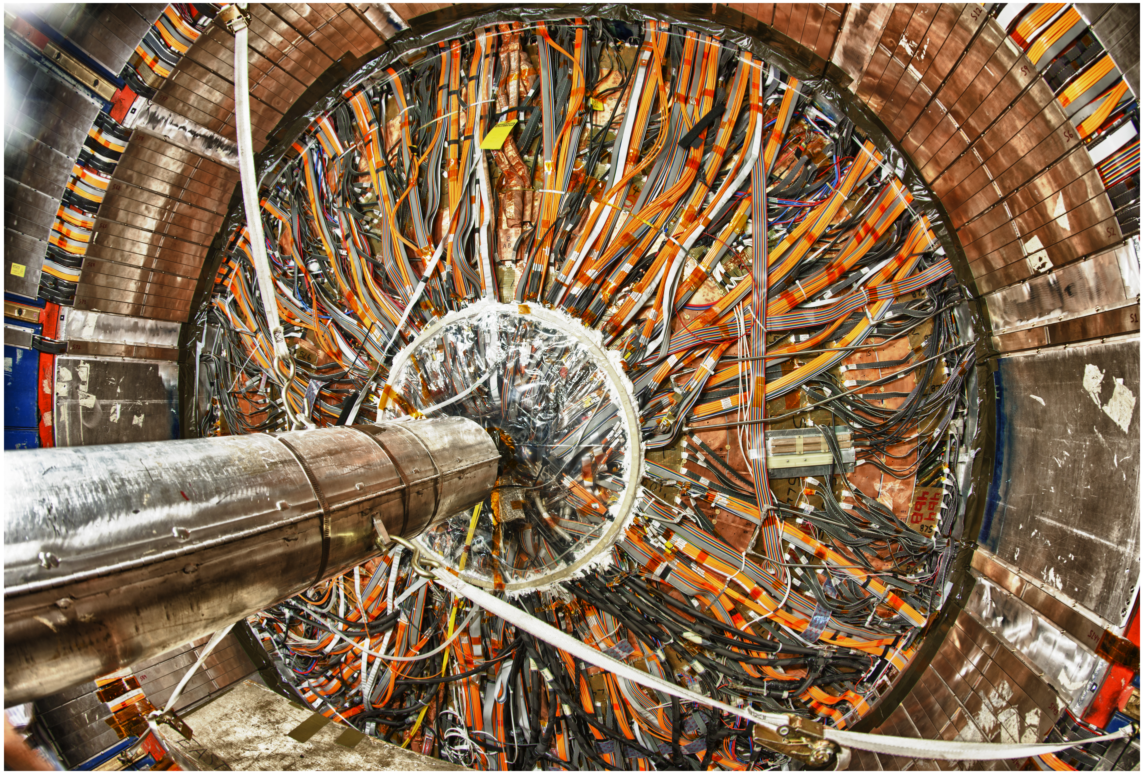

50th SLAC Summer Institute
August 10, 2022

A Century of Particle Physics

- Success # 1: discovery of 6 quarks and 6 leptons
- 12 fundamental fermions: matter particles (and their antimatter counterparts) derived by combining quantum mechanics and special relativity

Quarks

$$\begin{array}{lll} u < 1 \text{ GeV} & c \sim 1.5 \text{ GeV} & t \sim 175 \text{ GeV} \\ d < 1 \text{ GeV} & s < 1 \text{ GeV} & b \sim 4.5 \text{ GeV} \end{array}$$

But the intriguing pattern of mass values is assigned to their Higgs interaction

Leptons

$$\begin{array}{lll} \nu_e < 1 \text{ eV} & \nu_\mu < 0.17 \text{ MeV} & \nu_\tau < 24 \text{ MeV} \\ e\ 0.5 \text{ MeV} & \mu\ 106 \text{ MeV} & \tau\ 1.8 \text{ GeV} \end{array}$$

How to Predict Fundamental Forces

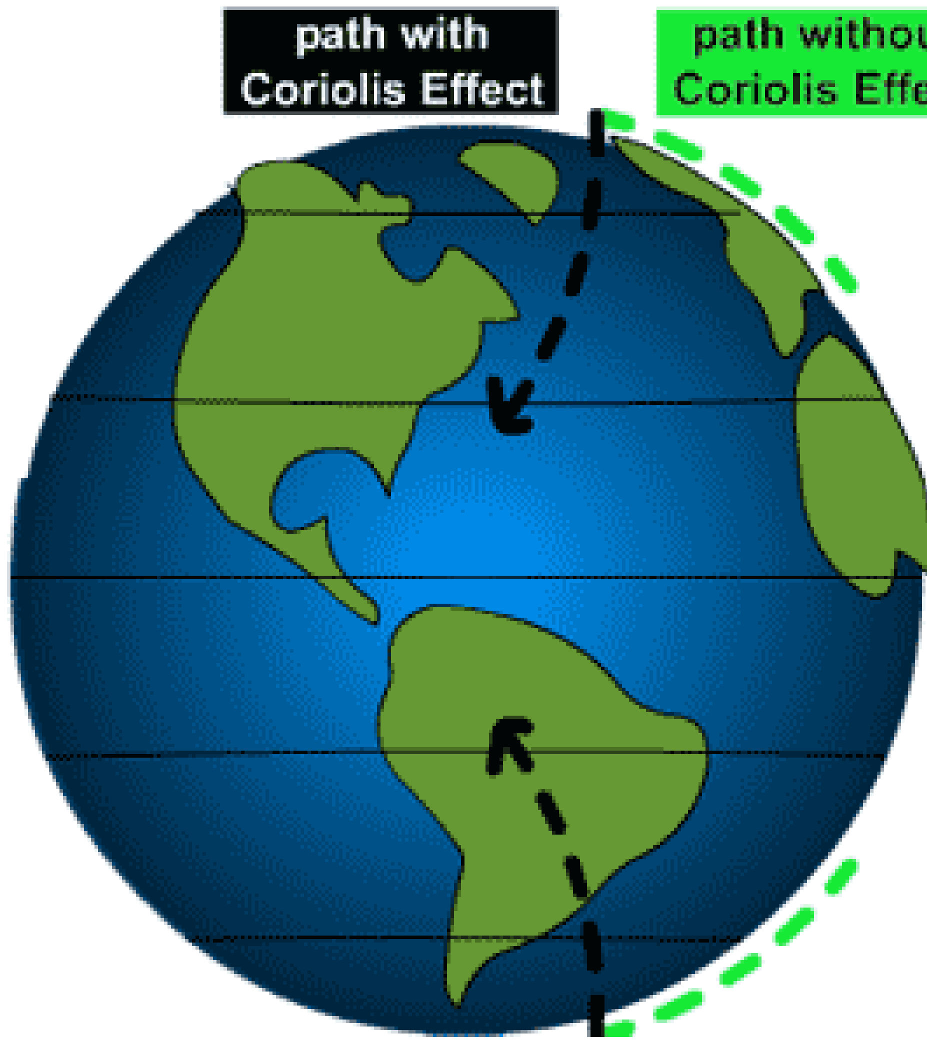

"fictitious" forces observed in accelerating frame of reference

Manifestation of Coriolis Force

Hurricanes appear to rotate in Earth's frame of reference

A Century of Particle Physics

- Success # 2: principle of gauge invariance for *predicting* the nature of fundamental forces
  - matter particles (quarks and leptons) transform in *curved* internal spaces
  - The equations of motion predict terms that describe particle interactions with force fields

Gauge sector $$L = i\bar{\psi}\gamma^{\mu}D_{\mu}\psi - \frac{1}{2}F_{\mu\nu}F^{\mu\nu}$$

Weak Nuclear Decay

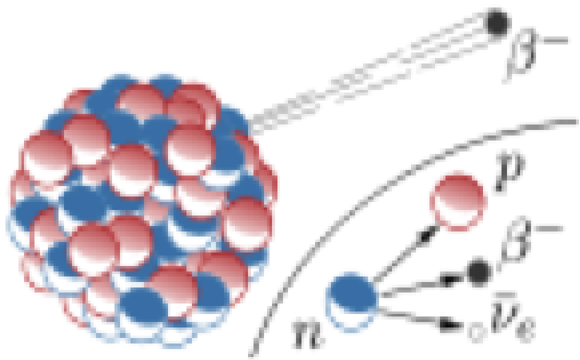

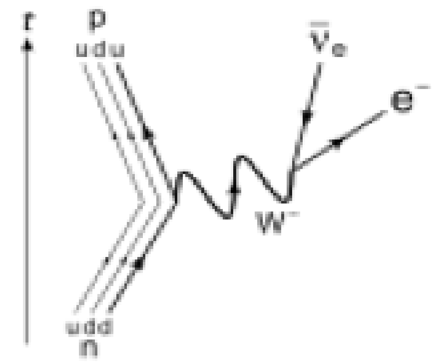

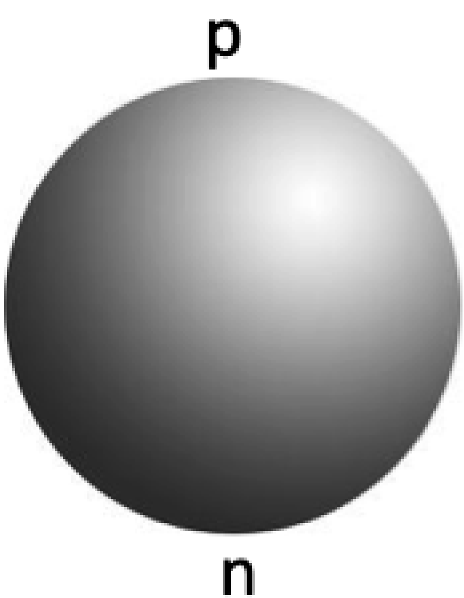

The force causing this interaction is described by particles making transitions on a "mathematical sphere"

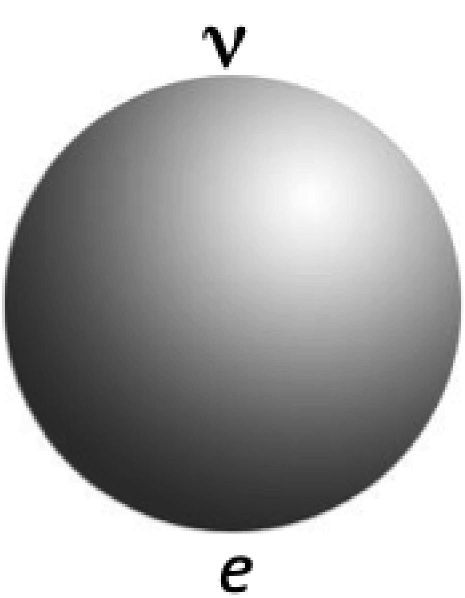

How does the W boson Acquire Mass?

- Fill all of space with “Higgs” field

- Particles propagating through “empty space” actually propagating though Higgs field

- Interaction of particles with Higgs field slows down the particle ⇔ imparting the property of mass to it

Light versus Heavy Particles – like moving through water

Streamlined

- Moves fast through water
- analogous to light particle

Not streamlined

- Moves slowly through water
- analogous to heavy particle

Quantum Ground State Breaks Gauge Symmetry

- Gauge Symmetry predicts all particles should be massless
- Solution: scalar Higgs field develops a ground state that violates the symmetry and generates particle masses via Higgs interactions

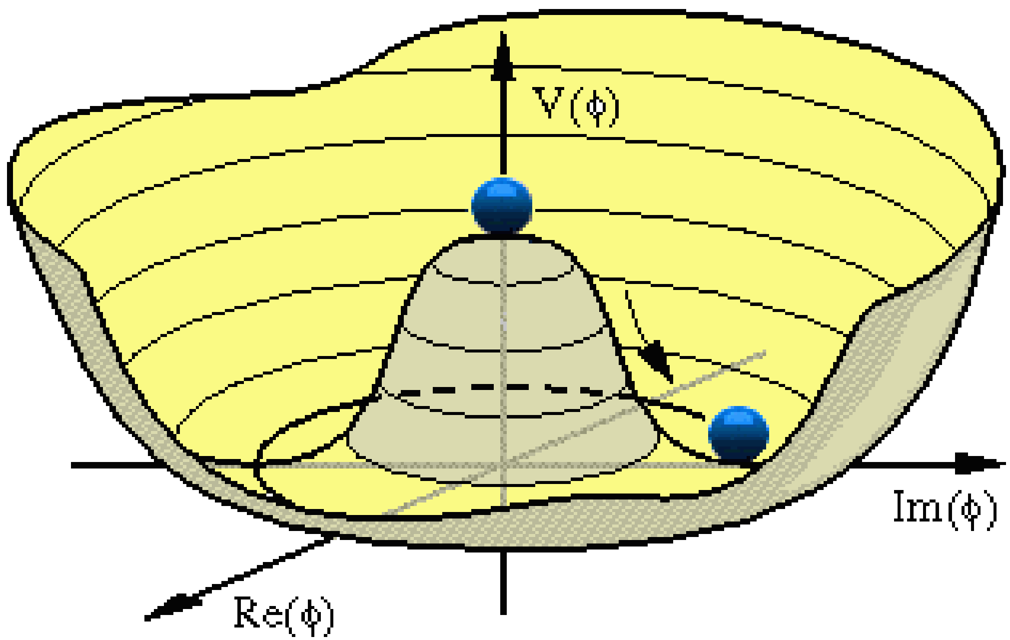

- Phase transition → vacuum state possesses non-trivial quantum numbers
  - Dynamical origin of this phase transition is not known
  - Implies vacuum is a condensed, superconductor-like state

Fundamental *vs* Parametric Physics

- Fundamental principles lead to
  - Chiral fermions from irreducible representations of Lorentz group
    - fermions as spin ½ representations of Lorentz group
    - Fermi-Dirac statistics → Pauli Exclusion Principle
    - why matter occupies volume
  - Massless force mediators (gauge bosons) from gauge invariance
  - Massive gauge bosons and fermions from spontaneous breaking of gauge symmetry

- In comparison, the breaking of gauge symmetry by the Higgs is parametrically induced
  - No dynamic or underlying principle behind it in the Standard Model

Why is Higgs Puzzling

Gauge sector $$L = i\bar{\psi}\gamma^{\mu}D_{\mu}\psi - \frac{1}{2}F_{\mu\nu}F^{\mu\nu}$$

particle	spin
quark: u, d,...	1/2
lepton: e...	1/2
photon	1
W,Z	1
gluon	1
Higgs	0

h: a new kind of
elementary particle

Higgs sector

$$L = \left(h_{ij}\bar{\psi}_i\psi_j H + \text{h.c.}\right) - \lambda|H|^4 + \mu^2|H|^2 - \Lambda_{CC}^4$$

Why is Higgs Puzzling

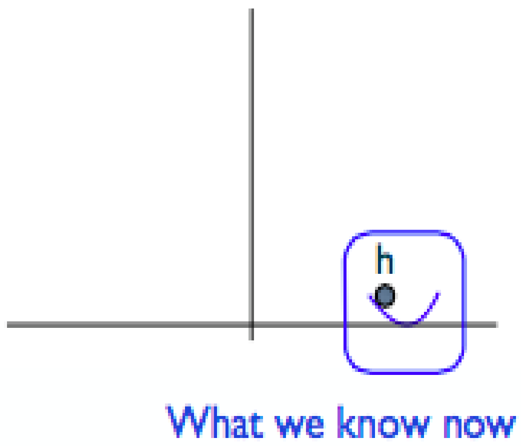

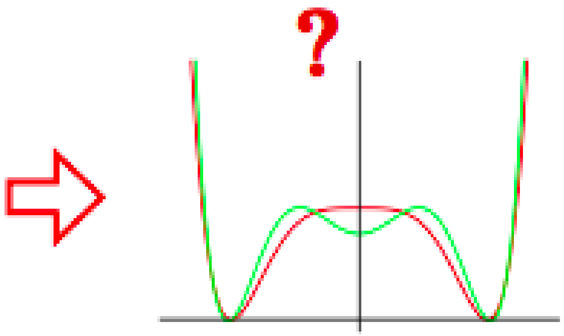

$$V(h) = \frac{1}{2}\mu^2 h^2 + \frac{\lambda}{4}h^4 \quad \text{or} \quad V(h) = \frac{1}{2}\mu^2 h^2 + \frac{\lambda}{4}h^4 + \frac{1}{\Lambda^2}h^6$$

Ad-hoc potential, similar to and motivated by Landau-Ginzburg theory of superconductivity

Standard Model Higgs potential can be extrapolated to the high-energy of quantum gravity without additional parameters

but no a-priori reason for a parameterization to respect this condition

Why is the Higgs Boson so Light?

$$m_H^2 - m_{\text{bare}}^2 =$$

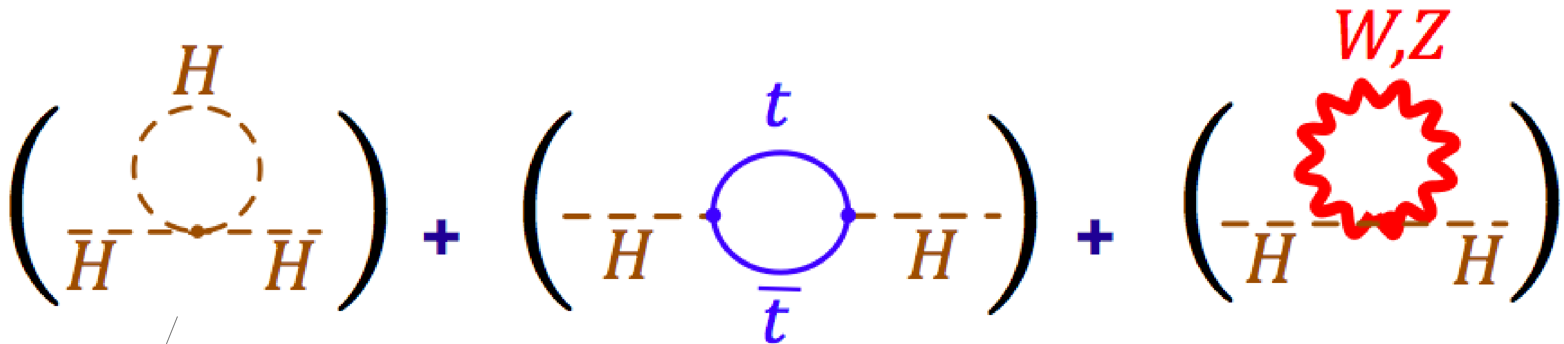

$$\lambda \int^{\Lambda} d^4k \, (k^2 - m_H^{\;2})^{-1} \;\sim\; \Lambda^2 \lambda$$

For the first time, we have additive corrections to parameters which are quadratically divergent

The Higgs boson ought to be a very heavy particle, naturally

However, observed $m_H << \Lambda$

Fine-tuning Problem of Higgs Boson Mass

- The large quantum corrections must be regulated by some very high-energy physics such as energy associated with quantum gravity, $M_{planck} \sim 10^{19}$ GeV
  - Loop calculation gives Higgs boson mass correction $\sim M^2_{planck}$

Top quark loop

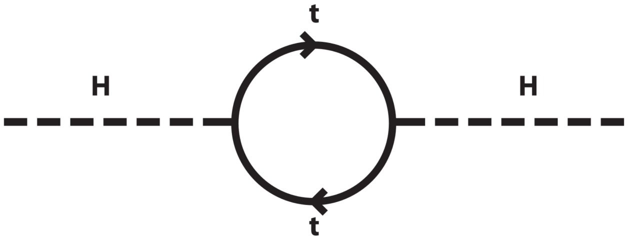

- physical Higgs boson mass $\sim$ 125 GeV

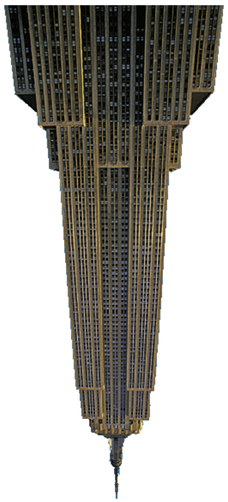

- Therefore need extreme "fine-tuning" of theoretical parameters at high energy
  - Conceptual weakness of Higgs theory as a quantum theory

Higgs boson puzzles

- First fundamental (?) scalar field to be discovered
- Spontaneous symmetry breaking by development of a ground state
  - But ground state is induced parametrically by ad-hoc Higgs potential, no dynamics
- Parameters of Higgs potential are not stable under quantum corrections
  - First time that the quantum correction to a particle mass is additive and quadratically divergent
  - Gauge boson masses are protected by gauge invariance
  - Fermion masses are protected by chiral symmetry of massless fermions
- Single scalar Higgs field is a strange beast, compared to fermions and gauge bosons
- Additional symmetries and/or dynamics strongly motivated by Higgs discovery

Detecting New Physics through Precision Measurements

- Willis Lamb (Nobel Prize 1955) measured the difference between energies of $^2S_{1/2}$ and $^2P_{1/2}$ states of hydrogen atom
  - 4 micro electron volts difference compared to few electron volts binding energy
  - States should be degenerate in energy according to tree-level calculation
- Harbinger of vacuum fluctuations to be calculated by Feynman diagrams containing quantum loops
  - Modern quantum field theory of electrodynamics followed (Nobel Prize 1965 for Schwinger, Feynman, Tomonaga)

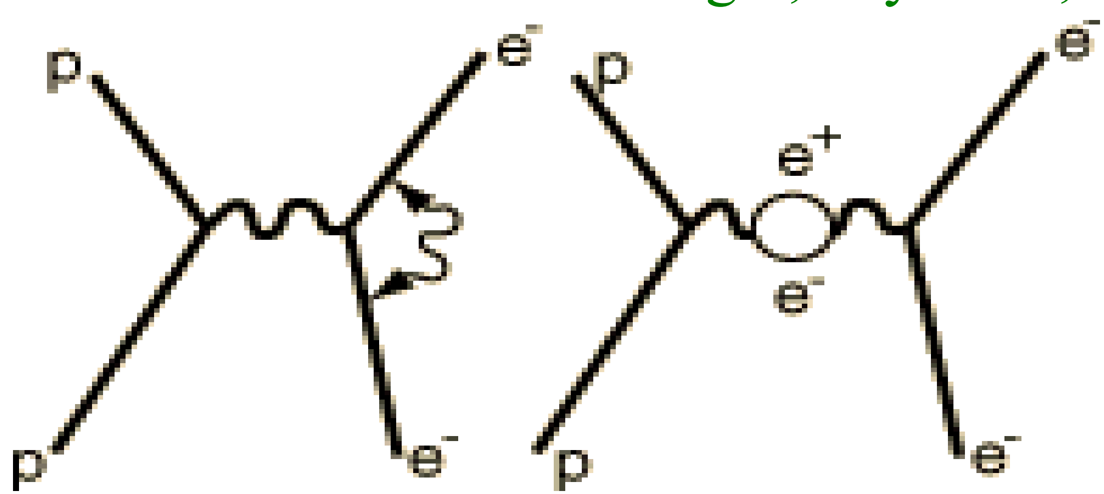

Parameters of Electro-Weak Interactions

- Gauge symmetries related to the electromagnetic and weak forces in the standard model, extension of QED
  - $U(1)_{\text{hypercharge}}$ gauge group with gauge coupling g
  - $SU(2)_{\text{weak}}$ gauge group with gauge coupling g'
- And gauge symmetry-breaking via vacuum expectation value of Higgs field $v \neq 0$
- Another interesting phenomenon in nature: the U(1) generator and the neutral generator of SU(2) get mixed (linear combination) to yield the observed gauge bosons
  - Photon for electromagnetism
  - Z boson as one of the three gauge bosons of weak interaction
- Linear combination is given by Weinberg mixing angle ϑ_W

Parameters of Electro-Weak Interactions

At tree level, all of the observables can be expressed in terms of *three* parameters of the SM Lagrangian: $v,\ g,\ g'$ or, equivalently, $v,\ e,\ s \equiv \sin\theta_W$ (also $c \equiv \cos\theta_W$)

$$\alpha = \frac{e^2}{4\pi}, \qquad G_F = \frac{1}{2\sqrt{2}v^2}, \qquad m_Z = \frac{e\,v}{\sqrt{2}sc}, \qquad m_W = \frac{e\,v}{\sqrt{2}s}, \qquad s^2_{\text{eff}} = s^2,$$

Radiative corrections to the relations between physical observables and Lagrangian params:

$$m_Z^2 = \frac{e^2v^2}{2\,s^2c^2} + \Pi_{ZZ}(m_Z^2)$$

$$m_W^2 = \frac{e^2v^2}{2\,s^2} + \Pi_{WW}(m_W^2)$$

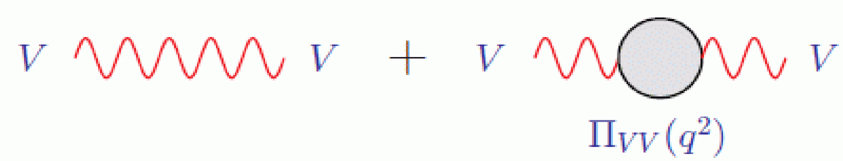

$$G_F = \frac{1}{2\sqrt{2}v^2}\left[1 - \frac{\Pi_{WW}(0)}{m_W^2} + \delta_{\text{VB}}\right]$$

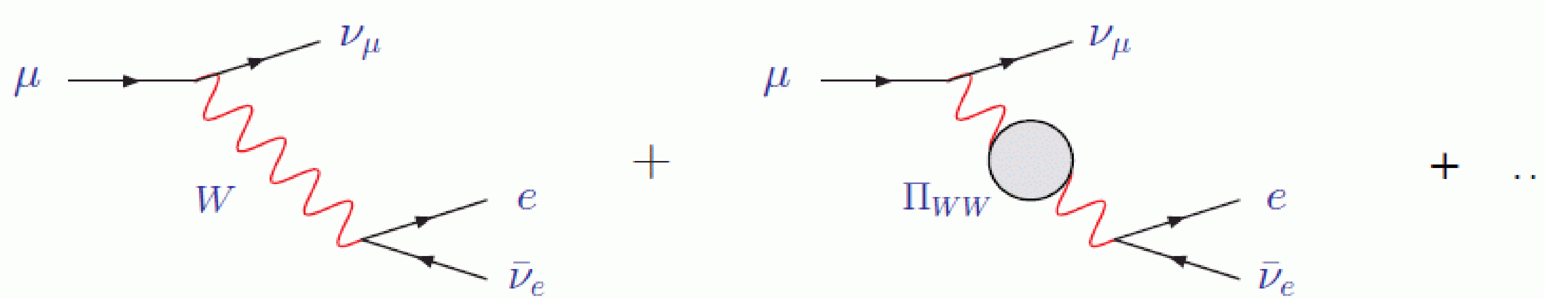

Radiative Corrections to Electromagnetic Coupling

$$\alpha = \frac{e^2}{4\pi}\left[1 + \lim_{q^2 -> 0} \frac{\Pi_{\gamma\gamma}(q^2)}{q^2}\right]$$

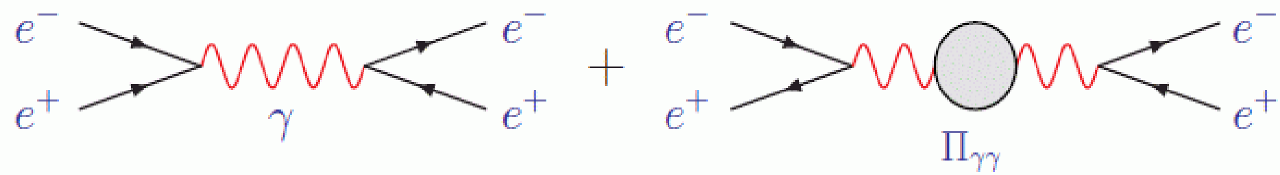

this one is tricky: the hadronic contribution to $\Pi'_{\gamma\gamma}(0)$ cannot be computed perturbatively

We can however trade it for another experimental observable: $R_{\rm had}(q^2) = \dfrac{\sigma_{\rm had}(q^2)}{\sigma_{\ell^+\ell^-}(q^2)}$

$$\alpha(m_Z) = \frac{e^2}{4\pi}\left[1 + \frac{\Pi_{\gamma\gamma}(m_Z)}{m_Z{}^2}\right] = \frac{\alpha}{1 - \Delta\alpha(m_Z)}$$

$$\Delta\alpha(m_Z) = \underbrace{\Delta\alpha_\ell(m_Z) + \Delta\alpha_{\rm top}(m_Z)}_{\text{calculable}} + \Delta\alpha^{(5)}_{\rm had}(m_Z)$$

$$\Delta\alpha^{(5)}_{\rm had}(m_Z) = -\frac{m_Z^2}{3\pi}\int_{4m_\pi^2}^{\infty} \frac{R_{\rm had}(q^2)\mathrm{d}q^2}{q^2\,(q^2 - m_Z^2)} = 0.02758 \pm 0.00035$$

(This hadronic contribution is one of the biggest sources of uncertainty in EW studies)

Radiative Corrections to W Boson Mass

All these corrections can be combined into relations among physical observables, e.g.:

$$m_W^2 = m_Z^2 \left[\frac{1}{2} + \frac{1}{2}\sqrt{1 - \frac{2\sqrt{2}\,\pi\alpha}{G_F\, m_Z^2}\,(1+\Delta r)} \right]$$

Δr can be parametrized in terms of two universal corrections and a remainder:

$$\Delta r \;=\; \Delta\alpha(m_Z) \;-\; \frac{c^2}{s^2}\Delta\rho \;+\; \Delta r_{\rm rem}$$

The leading corrections depend quadratically on m_t but only logarithmically on m_H :

$$\Delta\rho \;=\; \frac{\Pi_{ZZ}(0)}{m_Z^2} - \frac{\Pi_{WW}(0)}{m_W^2} \;\approx\; \frac{3\,\alpha}{16\pi c^2}\left(\frac{m_t^2}{s^2 m_Z^2} \;+\; \log\frac{m_H^2}{m_W^2} \;+\; \ldots\right)$$

$$\frac{\delta m_W^2}{m_W^2} \;\approx\; \frac{c^2}{c^2-s^2}\,\Delta\rho\;, \qquad \delta\,\sin^2\theta_{\rm eff} \;\approx\; -\,\frac{c^2\,s^2}{c^2-s^2}\,\Delta\,\rho$$

Contributions from Supersymmetric Particles

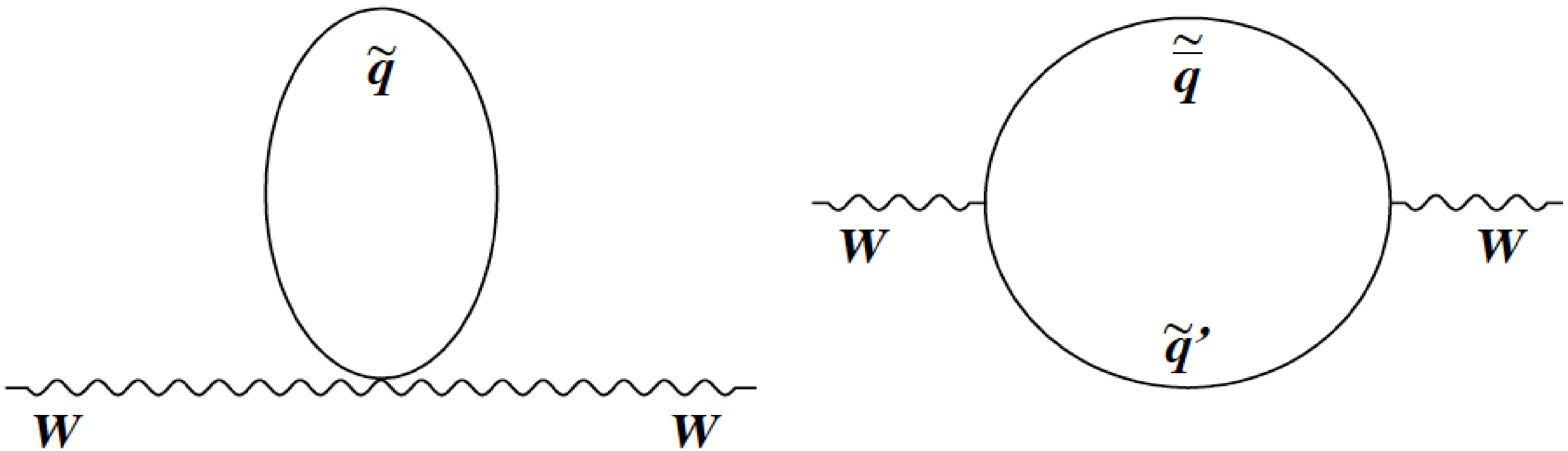

- Quantum correction to W boson mass depends on mass splitting (Δm^2) between supersymmetric quarks
- SUSY loops can contribute tens of MeV to M_W
  - Even with significant exclusions from Large Hadron Collider
  - Supersymmetric particle could constitute dark matter

Motivation

- Generic parameterization of new physics contributing to W and Z boson self-energies through radiative corrections in propagators
  - *S, T, U* parameters (Peskin & Takeuchi, Marciano & Rosner, Kennedy & Langacker, Kennedy & Lynn)

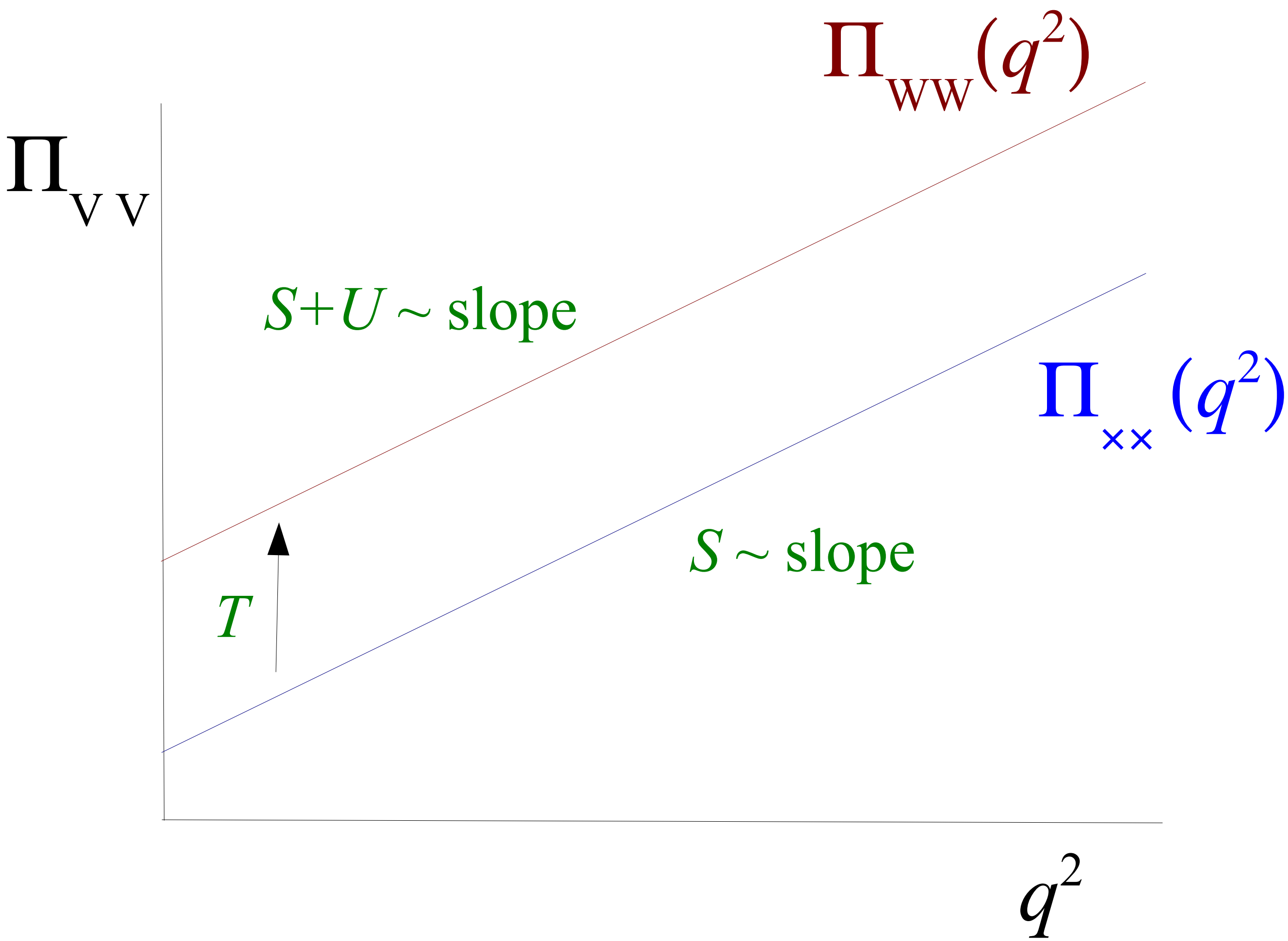

A_{FB} and A_{LR} Observables

- Asymmetries definable in electron-positron scattering sensitive to Weinberg mixing angle ϑ_W

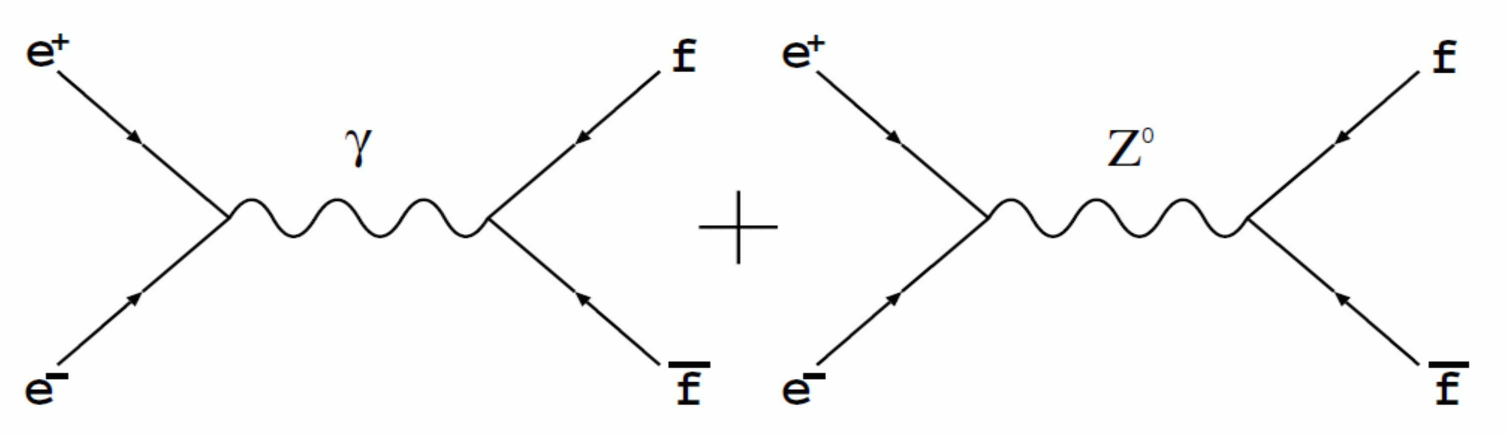

- Fermions, Higgs (and possible new physics) also contribute radiative corrections to ϑ_W via quantum loops

- A_{FB} is the angular (forward – backward) asymmetry of the final state

- A_{LR} is the asymmetry in the total scattering probability for different polarizations of the initial state (measured very precisely at SLAC's SLC by SLD)

S-T plane

- Generic parameterization of new physics contributing to W and Z boson self-energies: *S, T, U* parameters

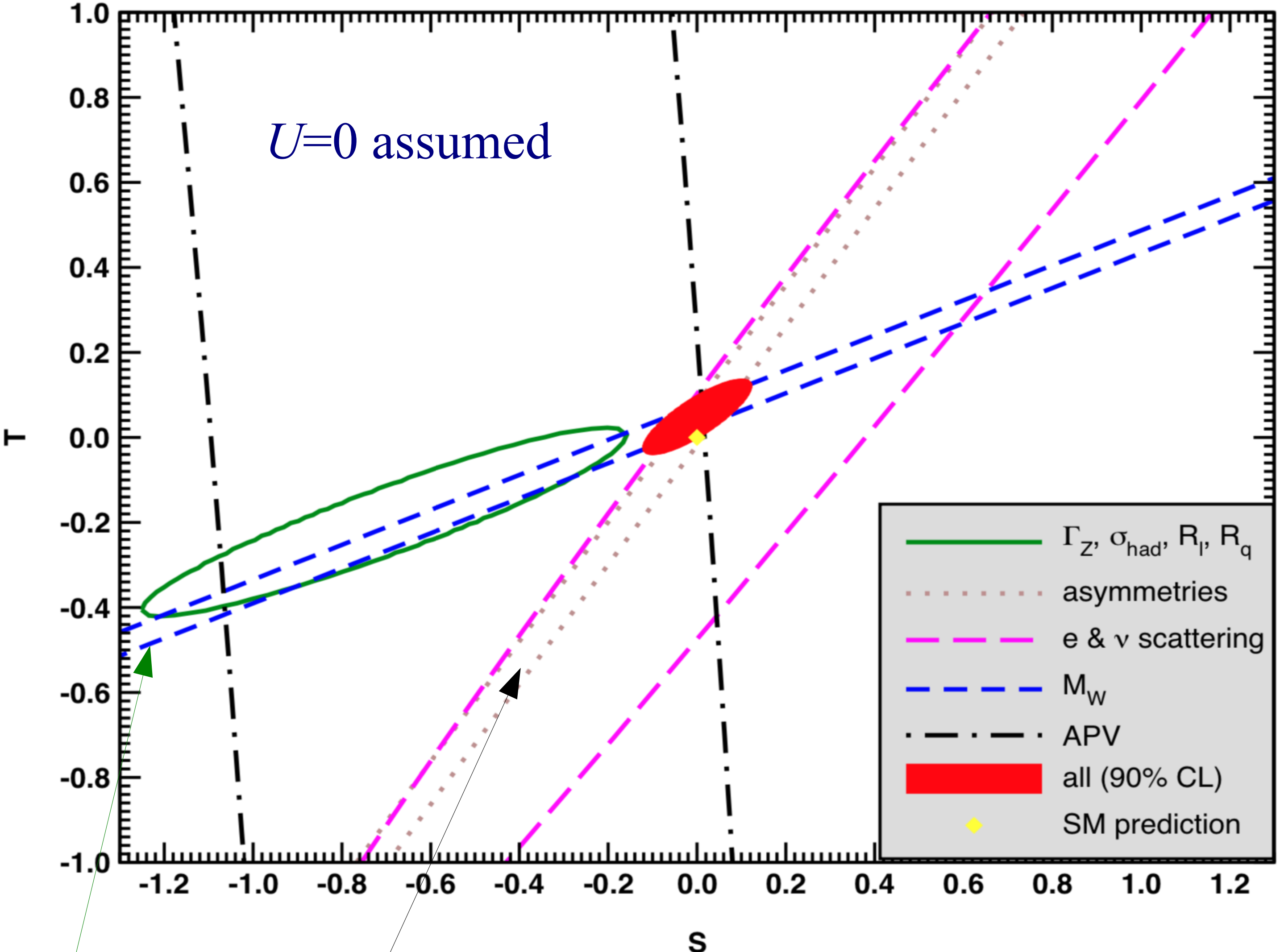

Additionally, M_W is the only measurement which constrains *U*

(From PDG 2021)

M_W and Asymmetries are the most powerful observables

Motivation for Precision Measurements

- The electroweak gauge sector of the standard model is constrained by precisely known parameters
  - $\alpha_{EM}(M_Z) = 1 / 127.918(18)$
  - $G_F = 1.16637\ (1) \times 10^{-5}\ \mathrm{GeV}^{-2}$
  - $M_Z = 91.1876\ (21)\ \mathrm{GeV}$
  - $m_{top} = 172.89\ (59)\ \mathrm{GeV}$
  - $M_H = 125.25\ (17)\ \mathrm{GeV}$
- At tree-level, these parameters are related to M_W
  - $M_W^2 = \pi\alpha_{EM} / \sqrt{2}G_F \sin^2\vartheta_W$
    - Where ϑ_W is the Weinberg mixing angle, defined by

$$\cos\vartheta_W = M_W/M_Z$$

Motivation for Precision Measurements

- Radiative corrections due to heavy quark and Higgs loops and (potentially) undiscovered particles

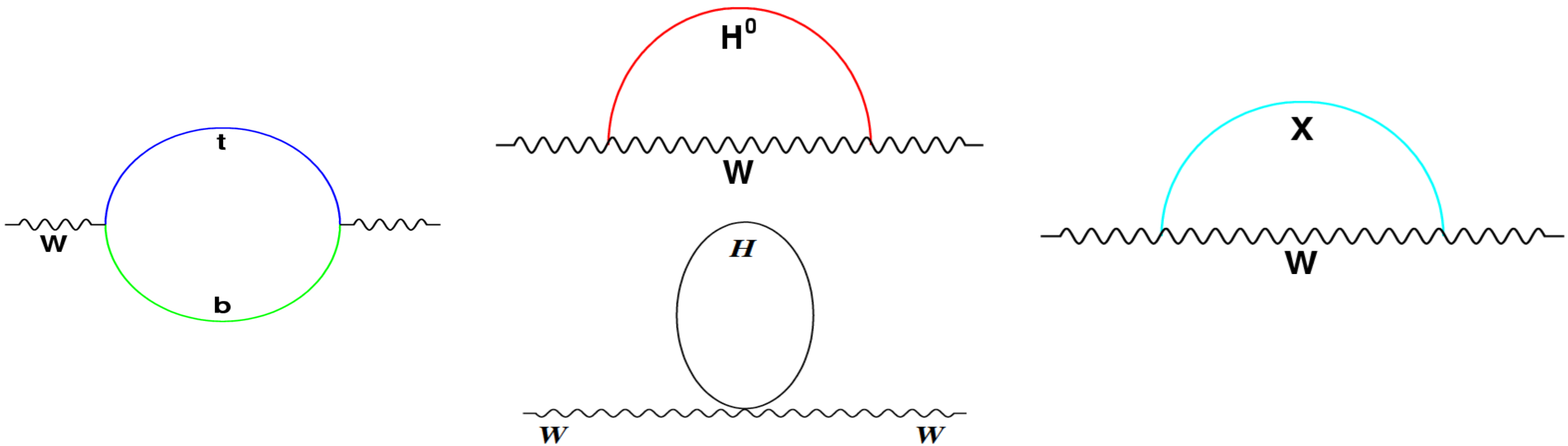

Motivate the introduction of the ρ parameter: $M_W^2 = \rho\,[M_W(\text{tree})]^2$
with the predictions $\Delta\rho = (\rho-1) \sim M_{top}^2$ and $\Delta\rho \sim \ln M_H$

Motivation for Precision Measurements

- The mass of the W boson is tightly constrained by the symmetries of the standard model, in conjunction with M_{top} and M_{Higgs}
  - The Higgs boson was the last missing component of the model
  - Following the observation of the Higgs boson, a measurement of the W-boson mass provides a stringent test of the model

- The W boson mass is presently constrained by SM global fits to a relative precision of 0.01%
  - provides a strong motivation to test the SM by measuring the mass to the same level of precision
  - SM expectation $M_W = 80{,}357 \pm 4_{inputs} \pm 4_{theory}$ MeV
  - Inputs include Z- and Higgs boson and top-quark masses, EM coupling and muon lifetime measurements

Beyond-SM Modifications to Expected M_W

- Hypotheses to provide a deeper explanation of the Higgs field, its potential and the Higgs boson, include
  - Supersymmetry
  - Compositeness
  - New strong interactions
  - Extended Higgs sector

- Hypothetical sources of particulate dark matter

- Extended gauge sector

W mass measurement – decay kinematics

- Main complication: invariant mass cannot be reconstructed from 2-body leptonic decay mode
  - Because neutrino is not detectable directly
- Exploit the "Jacobian edge" in lepton transverse momentum spectrum

$$\frac{d\sigma}{d\cos\hat{\theta}} = \sigma_0(\hat{s})\left[\frac{1}{2}(1+\cos\hat{\theta})^2 + \frac{1}{2}(1-\cos\hat{\theta})^2\right]$$

$$= \sigma_0(\hat{s})(1+\cos^2\hat{\theta})$$

W boson rest frame

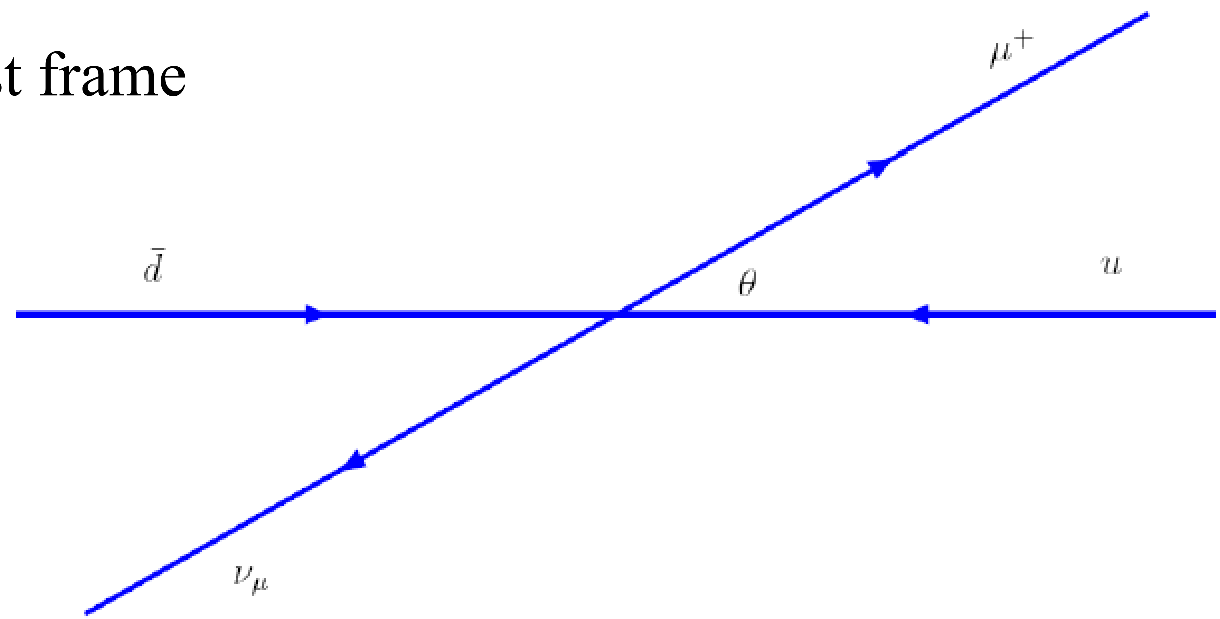

W mass measurement – decay kinematics

- Main complication: invariant mass cannot be reconstructed from 2-body leptonic decay mode
  - Because neutrino is not detectable directly
- Exploit the "Jacobian edge" in lepton transverse momentum spectrum

$$
\begin{aligned}
\frac{d\sigma}{dp_T} &= \frac{d\sigma}{d((m_W/2)\sin\hat{\theta})} \\
&= \frac{2}{m_W}\frac{d\sigma}{d\sin\hat{\theta}} \\
&= \frac{2}{m_W}\frac{d\sigma}{d\cos\hat{\theta}}\left|\frac{d\cos\hat{\theta}}{d\sin\hat{\theta}}\right| \\
&= \frac{2}{m_W}\sigma_0(\hat{s})(1+\cos^2\theta)|\tan\hat{\theta}| \\
&= \sigma_0(\hat{s})\frac{4p_T}{m_W^2}(2-4p_T^2/m_W^2)\left(\frac{1}{\sqrt{1-4p_T^2/m_W^2}}\right)
\end{aligned}
$$

Invariant under longitudinal boost

W mass measurement – decay kinematics

- Main complication: invariant mass cannot be reconstructed from 2-body leptonic decay mode
  - Because neutrino is not detectable directly
- Exploit the "Jacobian edge" in lepton transverse momentum spectrum

We can transfer $\frac{d\sigma}{dp_T}$ to $\frac{d\sigma}{dm_T}$ by using $m_T = 2p_T$:

$$\begin{aligned}\frac{d\sigma}{dm_T} &= \frac{1}{2}\frac{d\sigma}{dp_T} \\ &= \sigma_0(\hat{s})\frac{m_T}{m_W}(2 - \frac{m_T^2}{m_W^2})\left(\frac{1}{\sqrt{1 - m_T^2/m_W^2}}\right)\end{aligned}$$

W mass measurement – decay kinematics

- Lepton transverse momentum not invariant under transverse boost
- But measurement resolution on leptons is good

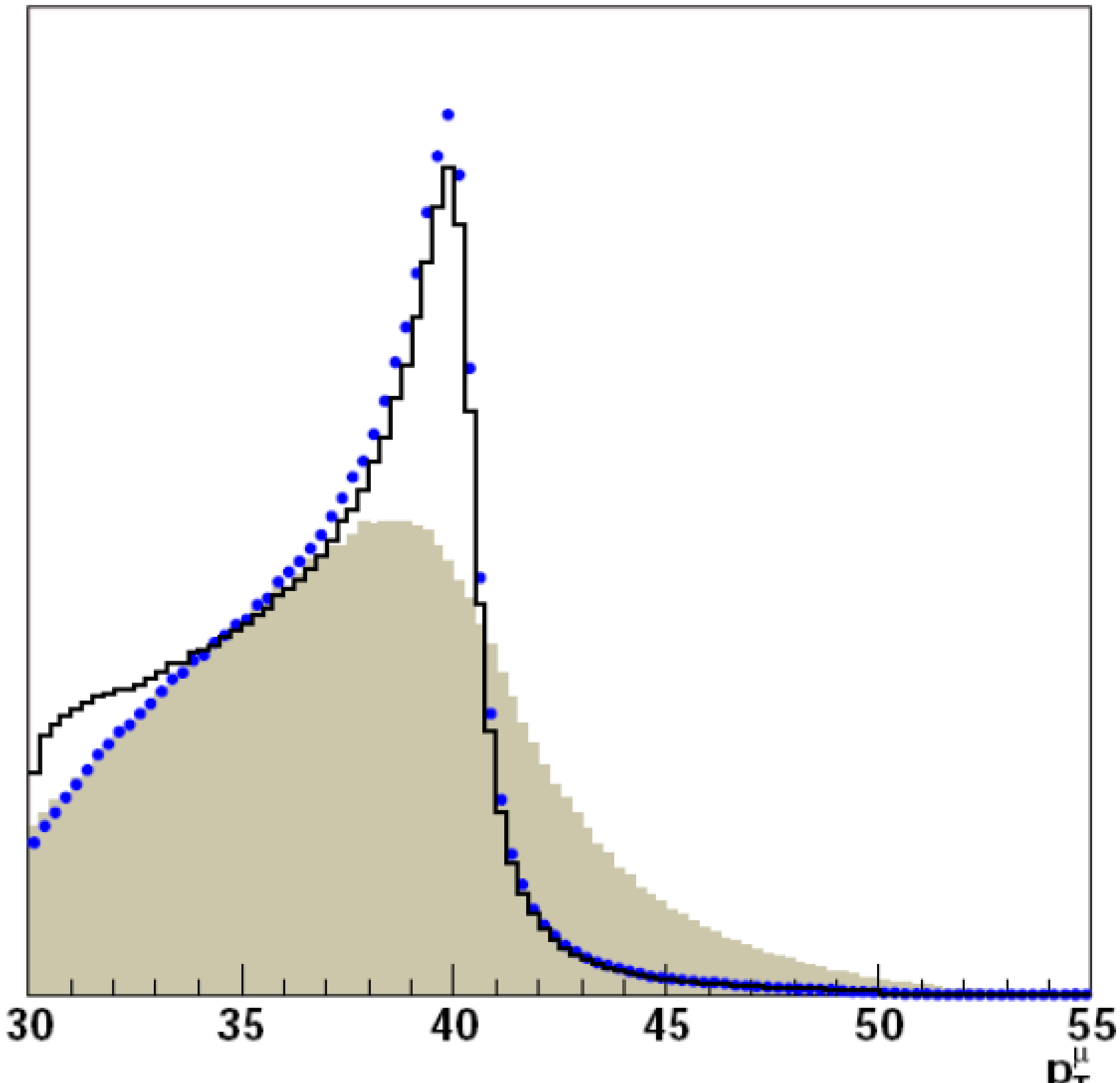

Black curve: truth level, no $p_T(W)$

Blue points: detector-level with lepton resolution and selection, But no $p_T(W)$

Shaded histogram: with $p_T(W)$

W mass measurement – decay kinematics

- Define "transverse mass" → approximately invariant under transverse boost
- But measurement resolution of "neutrino" is not as good due to recoil

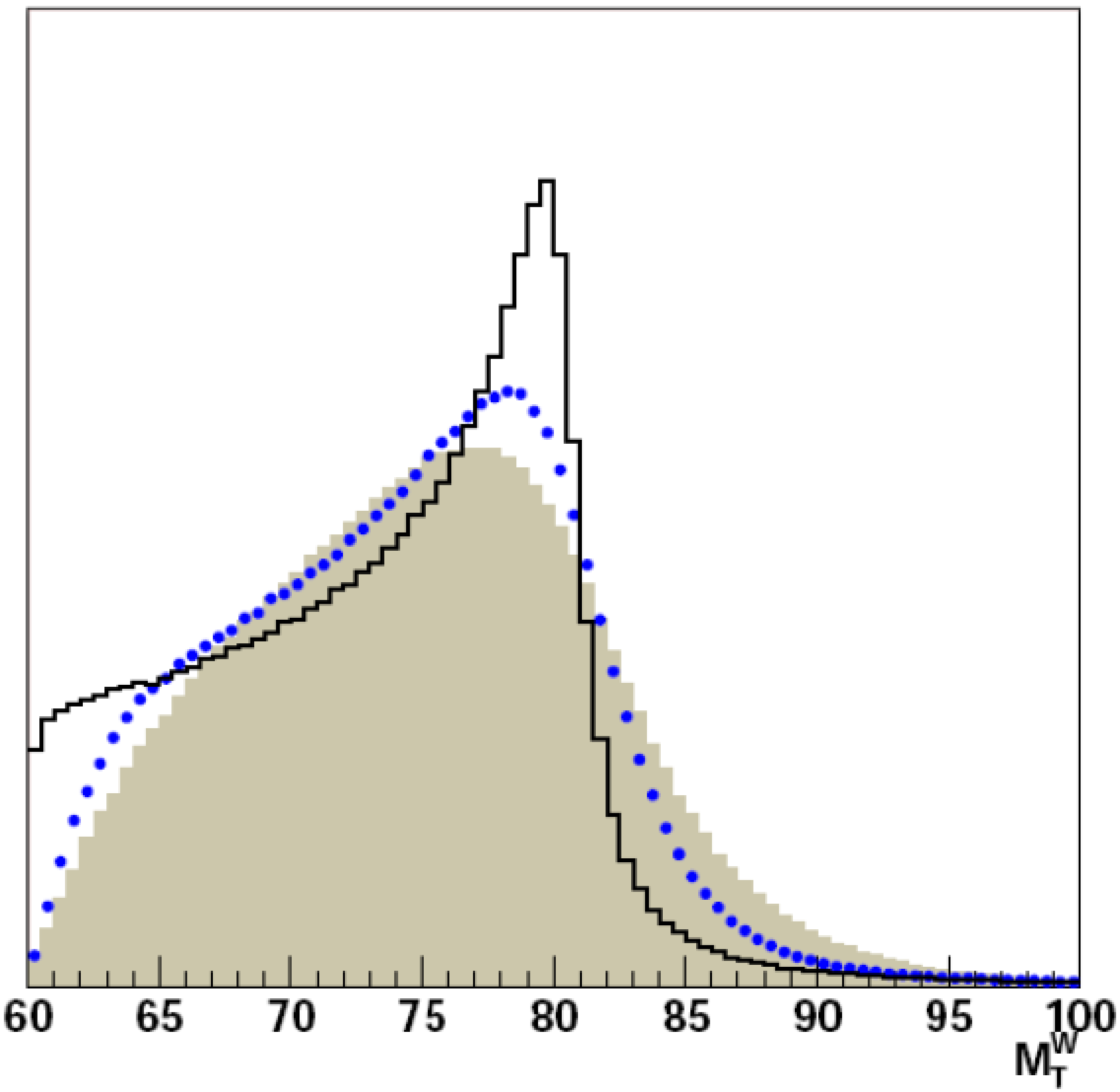

Black curve: truth level, no $p_T(W)$

Blue points: detector-level with lepton resolution and selection, But no $p_T(W)$

Shaded histogram: with $p_T(W)$

$$m_T = \sqrt{\left(E_T^l + E_T^\nu\right)^2 - \left(\vec{p}_T^{\,l} + \vec{p}_T^{\,\nu}\right)^2}$$

$$= \sqrt{2 p_T^\mu p_T^\nu (1 - \cos \Delta\phi)}$$

Signal Simulation and Template Fitting

- All signals simulated using a Custom Monte Carlo
  - Generate finely-spaced templates as a function of the fit variable
  - perform binned maximum-likelihood fits to the data
- Custom fast Monte Carlo makes smooth, high statistics templates
  - And provides analysis control over key components of the simulation

$$L = \prod_{i=1}^{N} \frac{e^{-m_i} {m_i}^{n_i}}{n_i!}$$

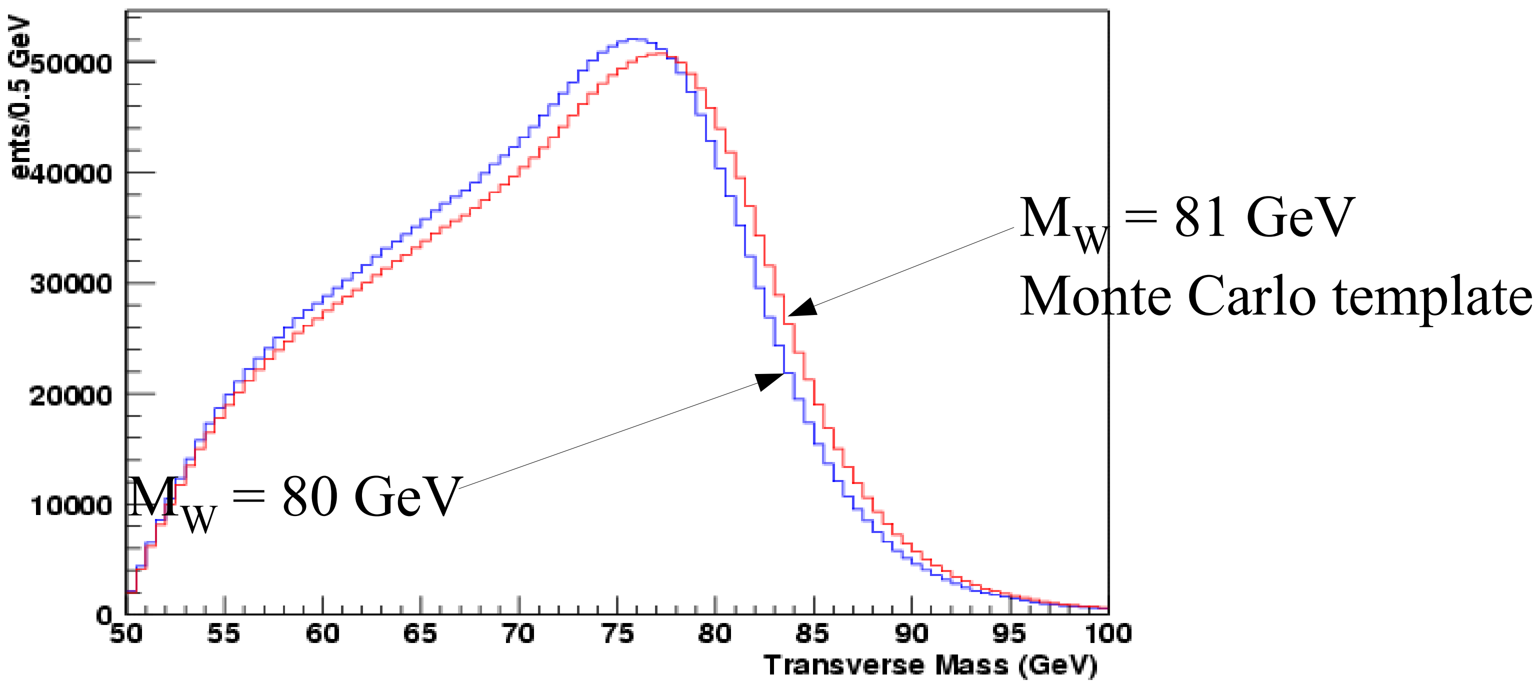

- We will extract the W mass from six kinematic distributions: Transverse mass, charged lepton p_T and missing E_T using both electron and muon channels

W Boson Production at the Tevatron

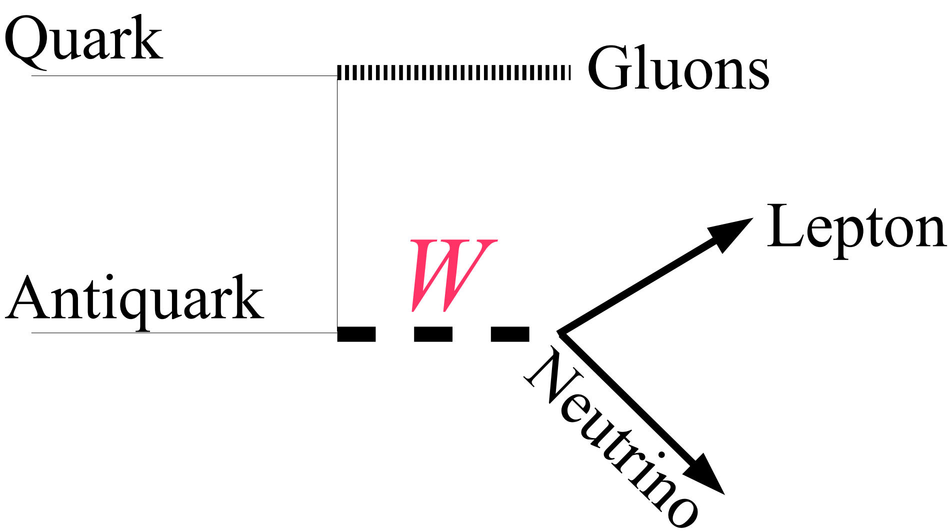

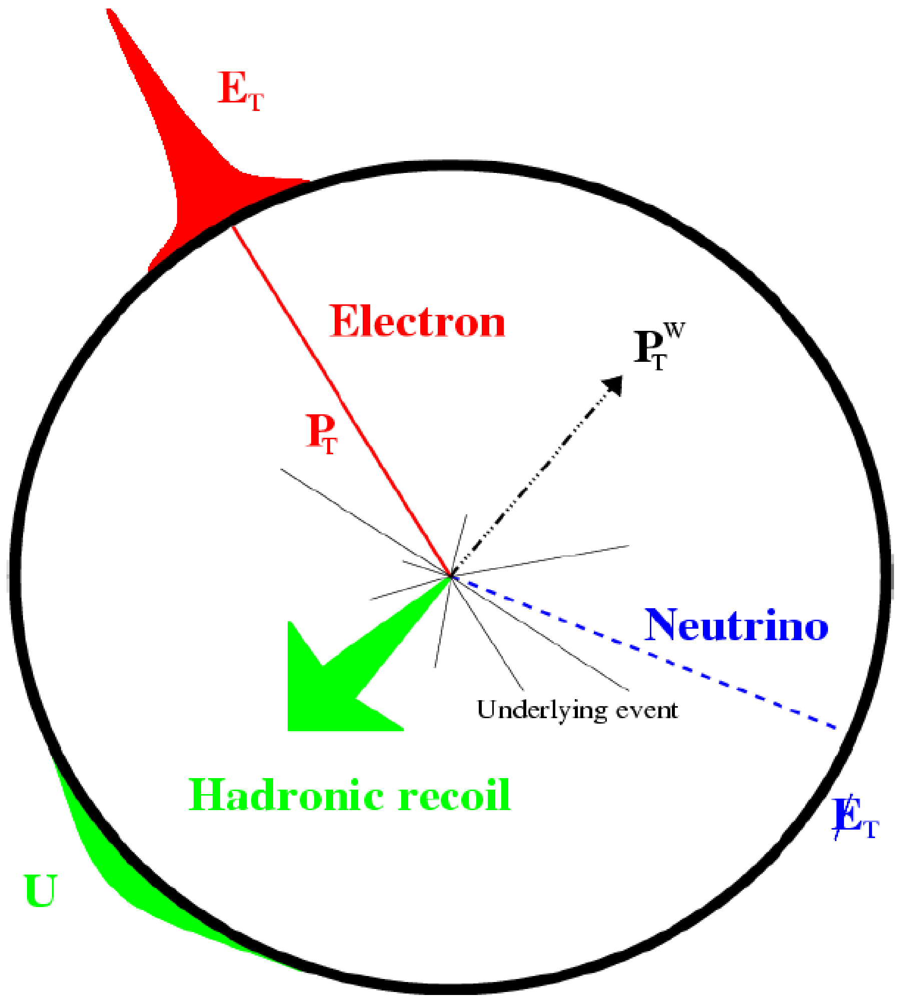

Quark-antiquark annihilation dominates (80%)

Lepton p_T carries most of *W* mass information, can be measured precisely (achieved 0.004%)

Initial state QCD radiation is *O*(10 GeV), measure as soft 'hadronic recoil' in calorimeter (calibrated to ~0.2%)

dilutes *W* mass information, fortunately $p_T(W) \ll M_W$

W Boson Production at the Tevatron

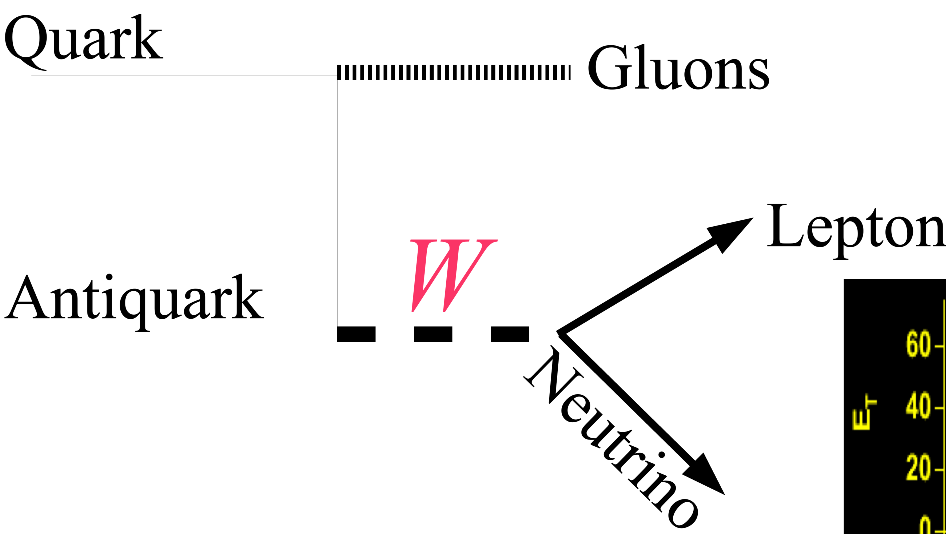

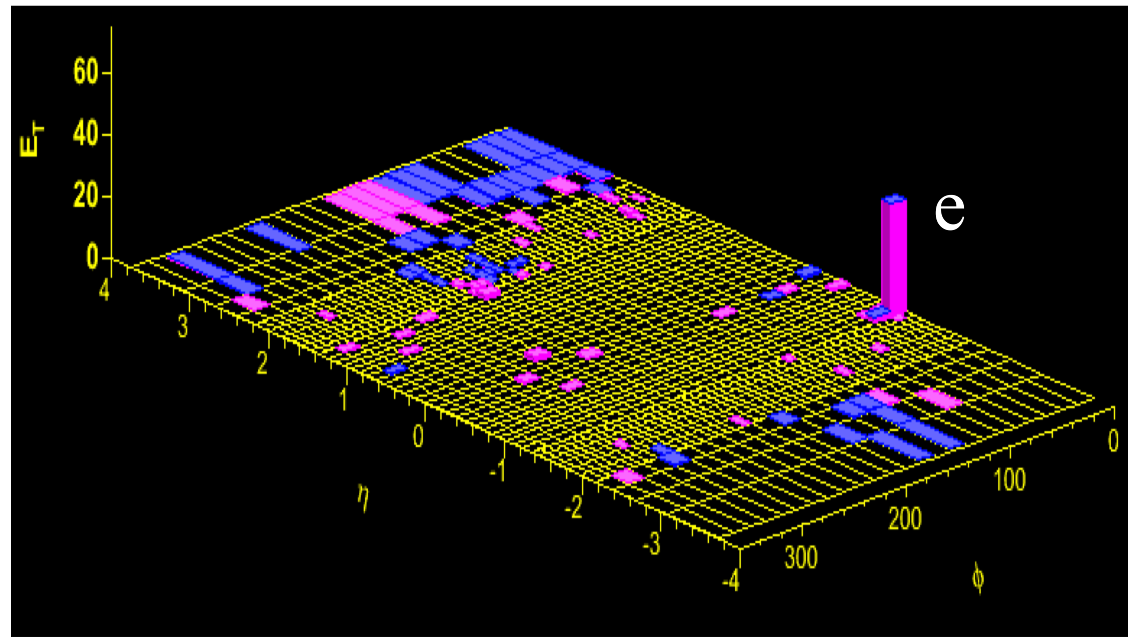

Quark-antiquark annihilation dominates (80%)

Lepton p_T carries most of W mass information, can be measured precisely (achieved 0.004%)

Initial state QCD radiation is O(10 GeV), measure as soft 'hadronic recoil' in calorimeter (calibrated to ~0.2%)
dilutes W mass information, fortunately $p_T(W) << M_W$

Quadrant of Collider Detector at Fermilab (CDF)

EM calorimeter provides precise electron energy measurement

COT provides precise lepton track momentum measurement

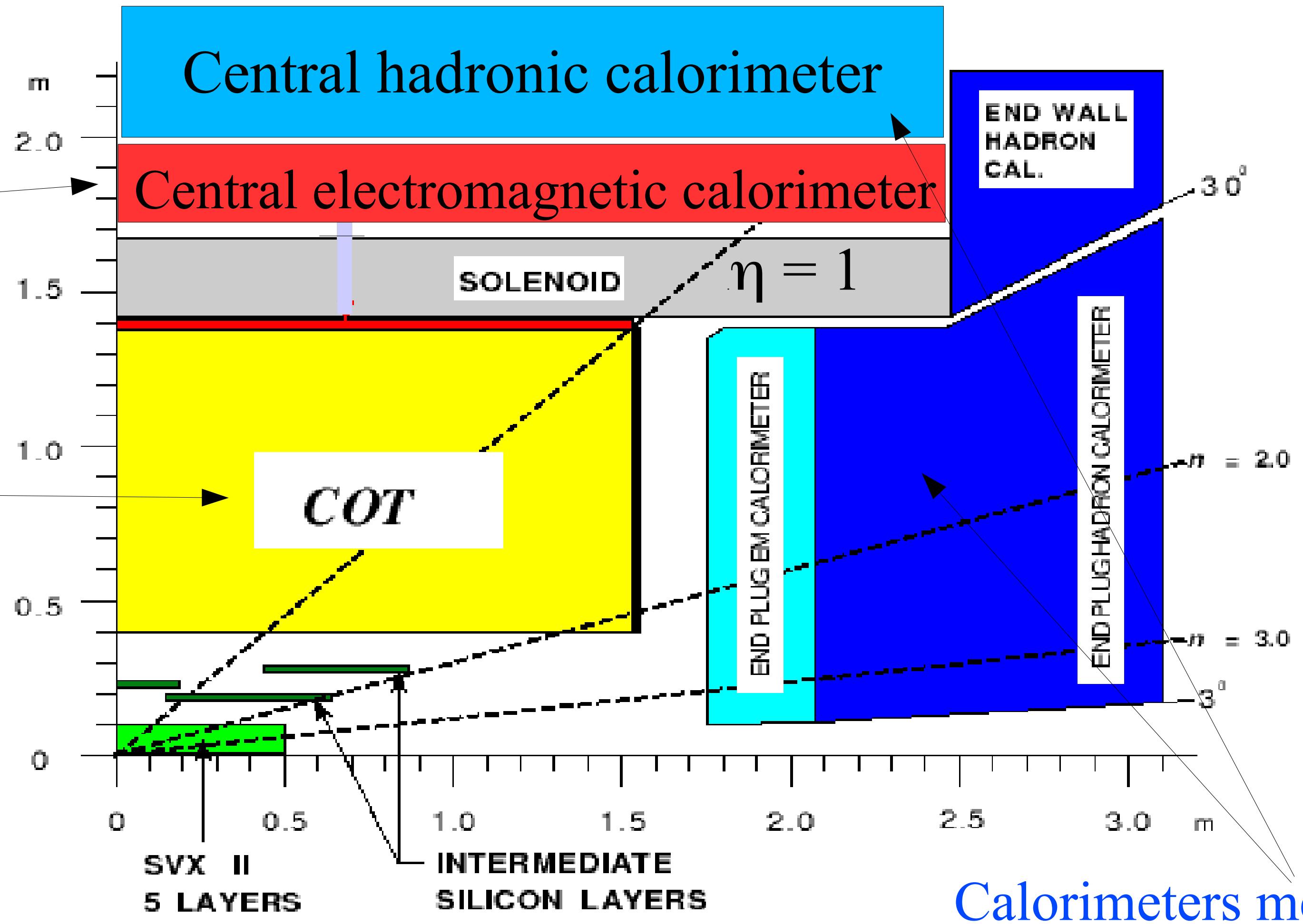

Calorimeters measure hadronic recoil particles

Select W and Z bosons with central (| **η** | < 1) leptons

Collider Detector at Fermilab (CDF)

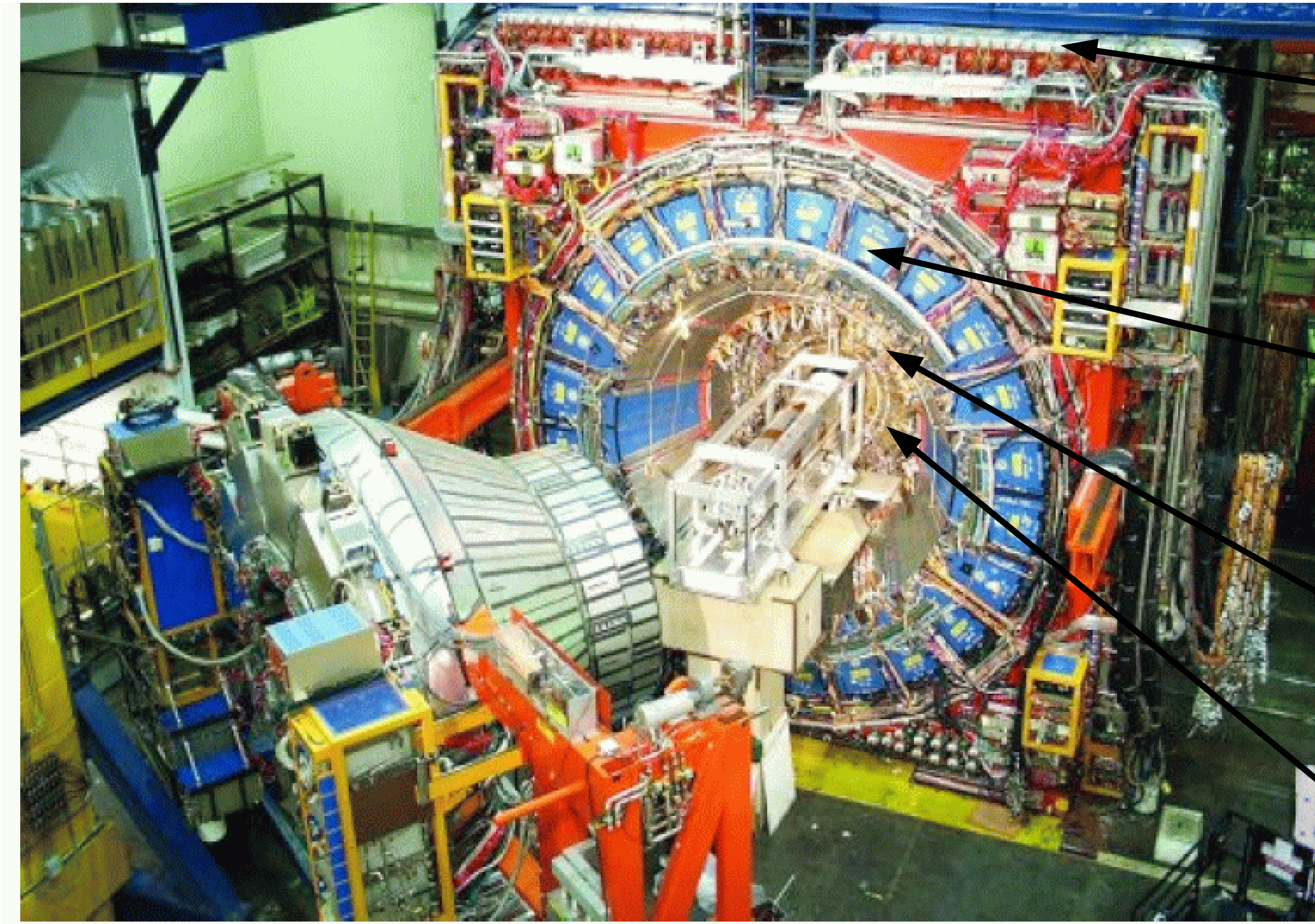

CDF Particle Tracking Chamber

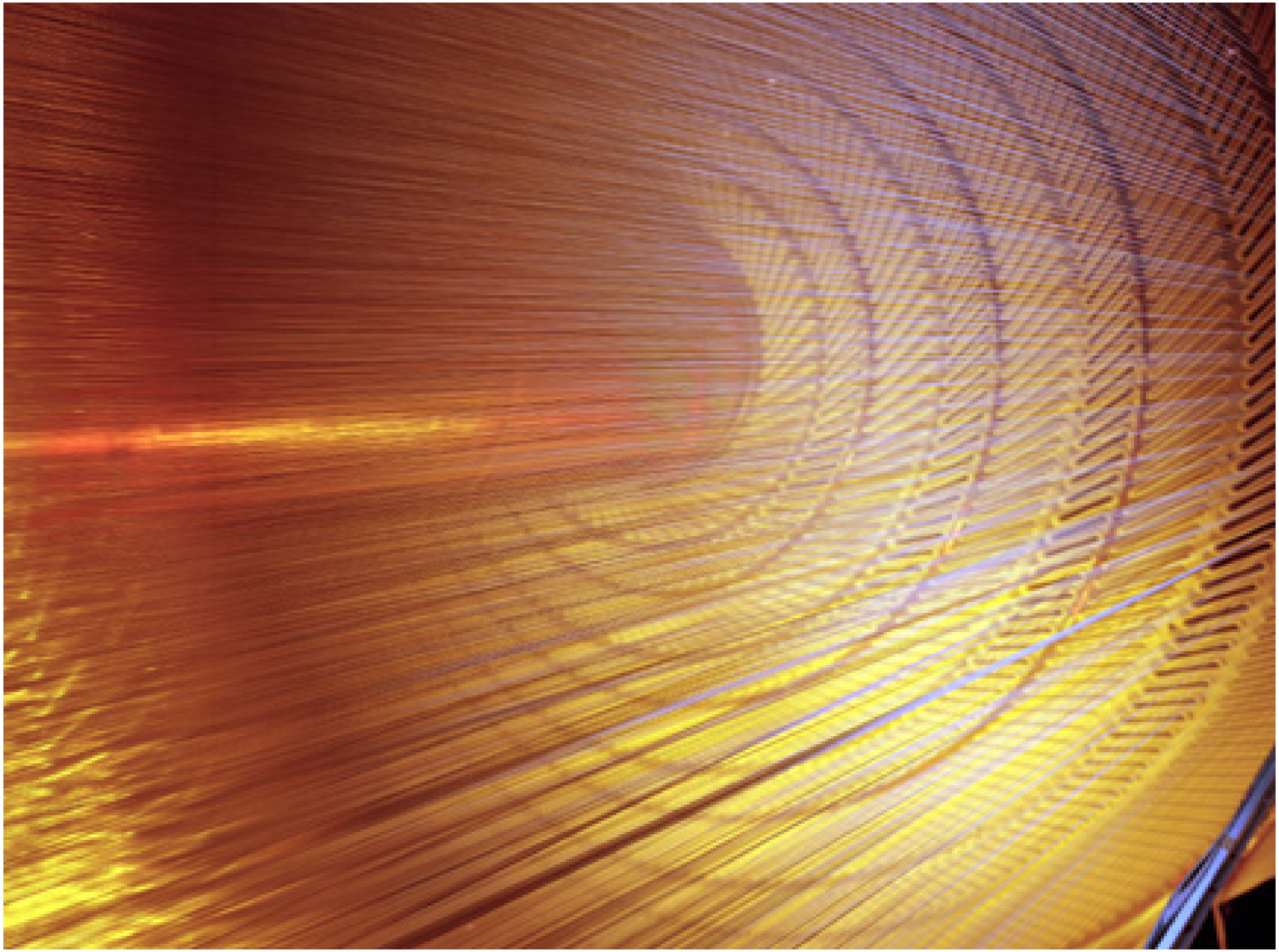

Reconstruction of particle trajectories, calibration to ~1 μm accuracy:

AVK, H. Gerberich and C. Hays, NIM A506, 110 (2003)

C. Hays et al, NIM A538, 249 (2005)

W boson Production Event

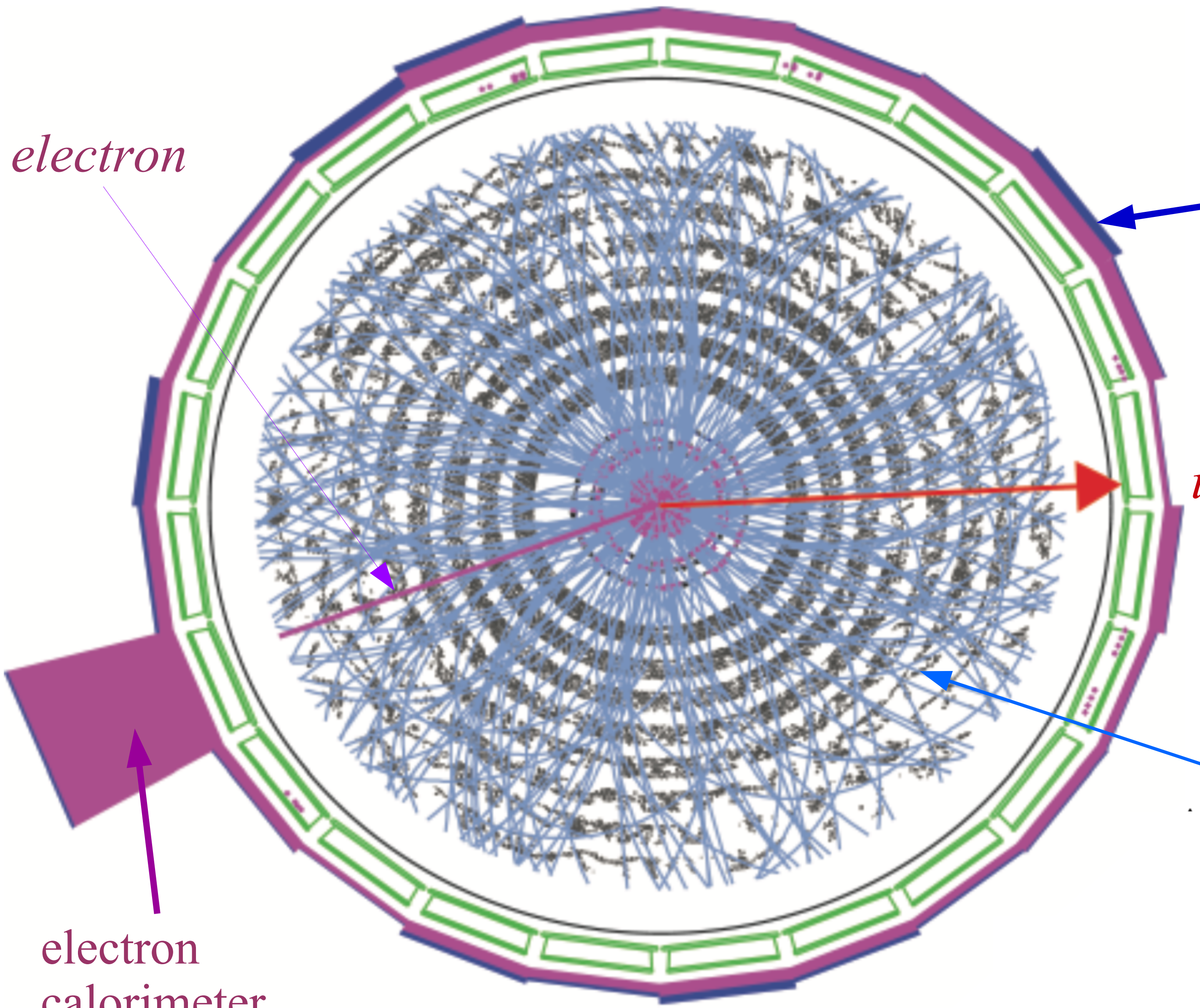

Event Selection

- Goal: Select events with high p_T leptons and small hadronic recoil activity
  - to maximize W mass information content and minimize backgrounds
- Inclusive lepton triggers: loose lepton track and muon stub / calorimeter cluster requirements, with lepton $p_T > 18$ GeV
  - Kinematic efficiency of trigger ~100% for offline selection
- Offline selection requirements:
  - Electron cluster $E_T > 30$ GeV, track $p_T > 18$ GeV
  - Muon track $p_T > 30$ GeV
  - Loose identification requirements to minimize selection bias
- W boson event selection: one selected lepton, $|\boldsymbol{u}| < 15$ GeV & $p_T(\nu) > 30$ GeV
  - Z boson event selection: two selected leptons

W & Z Data Samples

Sample	Candidates
W $\rightarrow$ electron	1 811 700
Z $\rightarrow$ electrons	66 180
W $\rightarrow$ muon	2 424 486
Z $\rightarrow$ muons	238 534

- Integrated Luminosity (collected between February 2002 – September 2011):
  - Electron and muon channels: $L = 8.8\ \text{fb}^{-1}$
  - Identical running conditions for both channels, guarantees cross-calibration
- Event selection gives fairly clean samples
  - Mis-identification backgrounds ~ 0.5%

Analysis Strategy

Strategy

Maximize the number of internal constraints and cross-checks

Driven by three goals:

1) Robustness: constrain the same parameters in as many different ways as possible

2) Precision: combine independent measurements after showing consistency

3) minimize bias: blinded measurements of M_Z and M_W

Outline of Analysis

Energy scale measurements drive the W mass measurement

- Tracker Calibration
  - alignment of the COT (2,520 cells; 30,240 sense wires) using cosmic rays
  - COT momentum scale and tracker non-linearity constrained using $J/\psi \to \mu\mu$ and $\Upsilon \to \mu\mu$ mass fits
  - Confirmed using $Z \to \mu\mu$ mass fit
- EM Calorimeter Calibration
  - COT momentum scale transferred to EM calorimeter using a fit to the peak of the E/p spectrum, around $E/p \sim 1$
  - Calorimeter energy scale confirmed using $Z \to ee$ mass fit
- Tracker and EM Calorimeter resolutions
- Hadronic recoil modeling
  - Characterized using p_T-balance in $Z \to ll$ events

Drift Chamber (COT) Alignment

COT endplate geometry

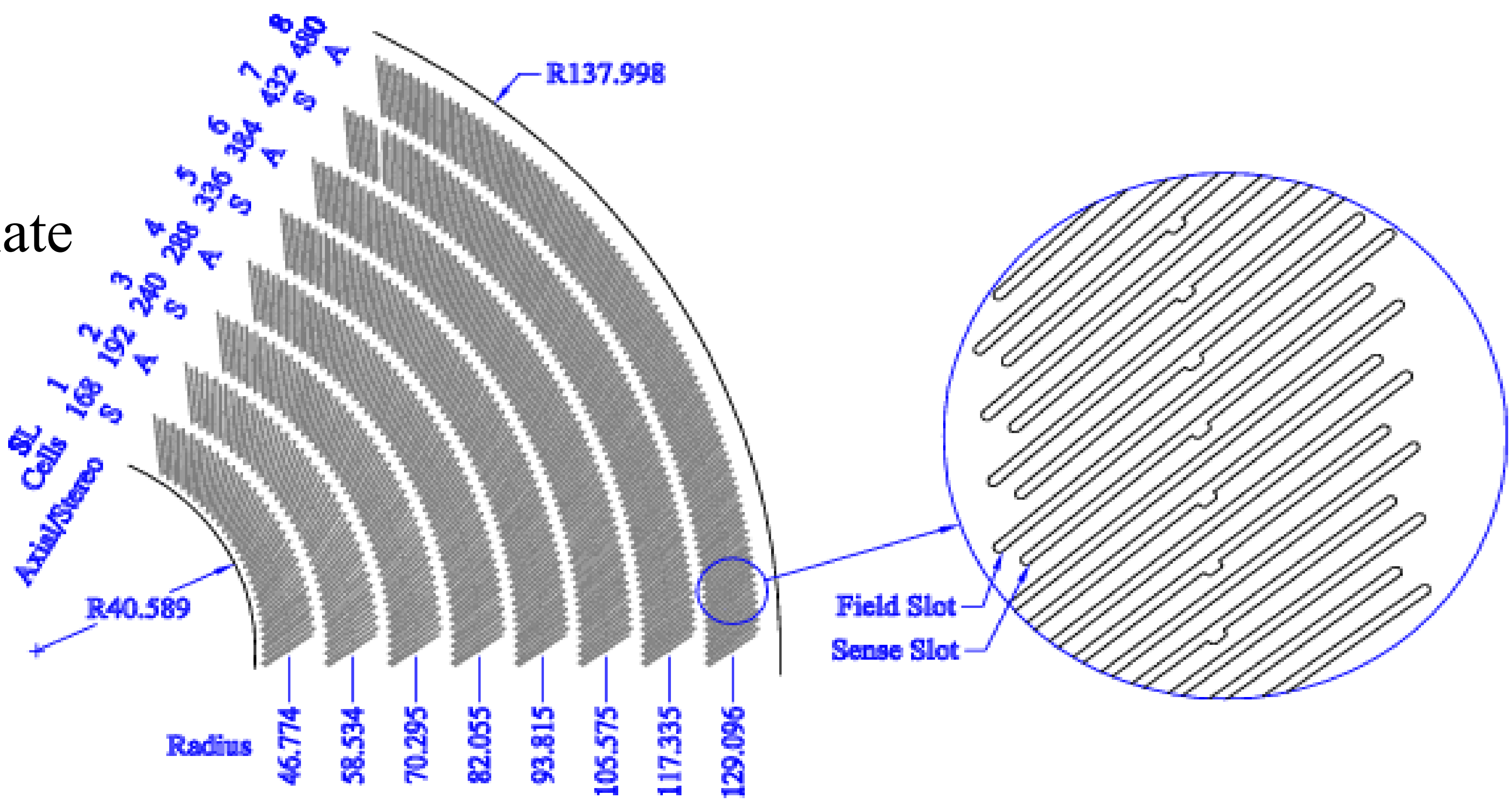

Internal Alignment of COT

- Use a clean sample of ~480k cosmic rays for cell-by-cell internal alignment

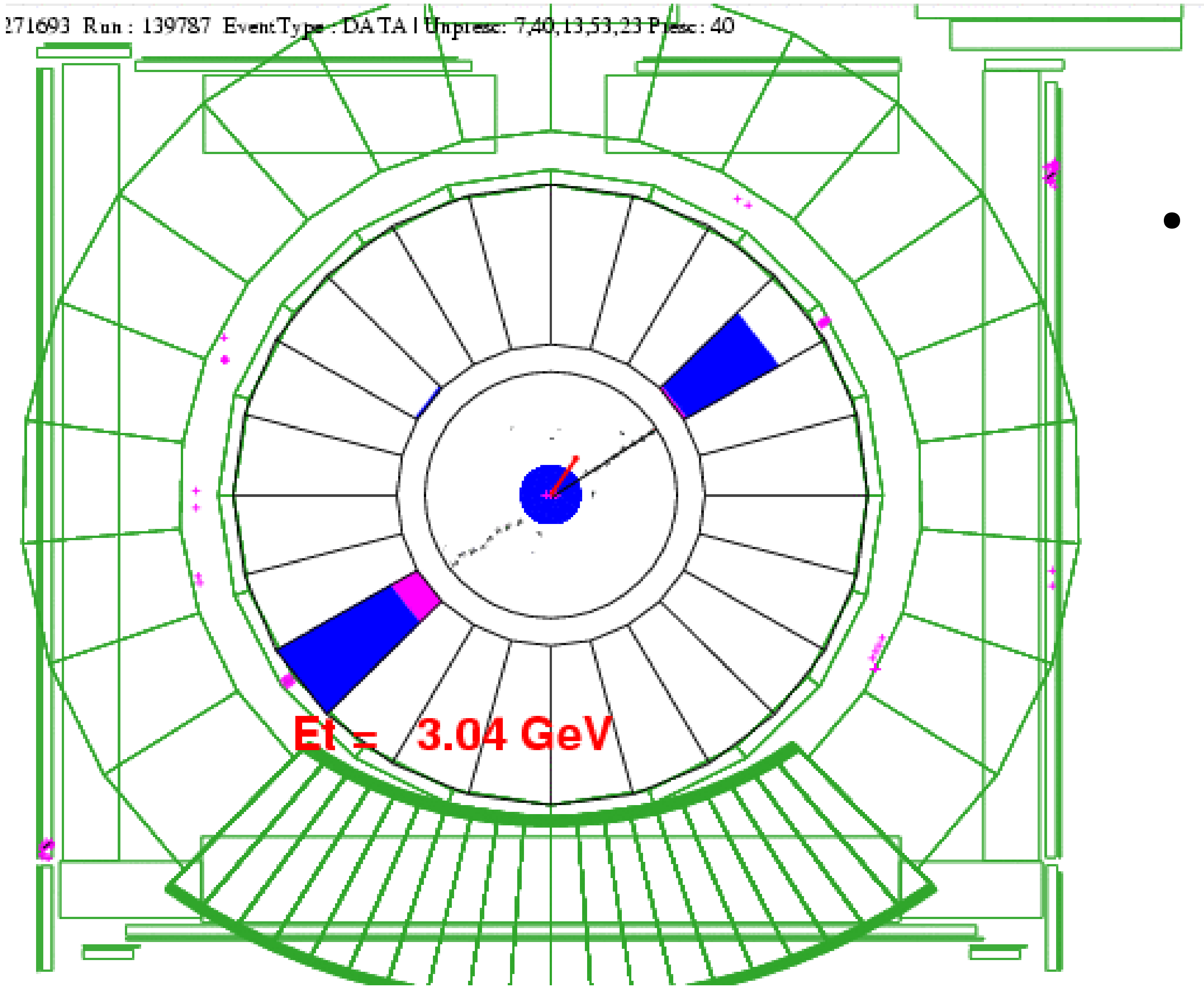

- Fit COT hits on both sides simultaneously to a single helix (AVK, H. Gerberich and C. Hays, NIMA 506, 110 (2003))
  - Time of incidence is a floated parameter in this 'di-cosmic fit'

Residuals of COT cells after alignment

(AVK & CH, *NIM A* 762 (2014) pp 85-99)

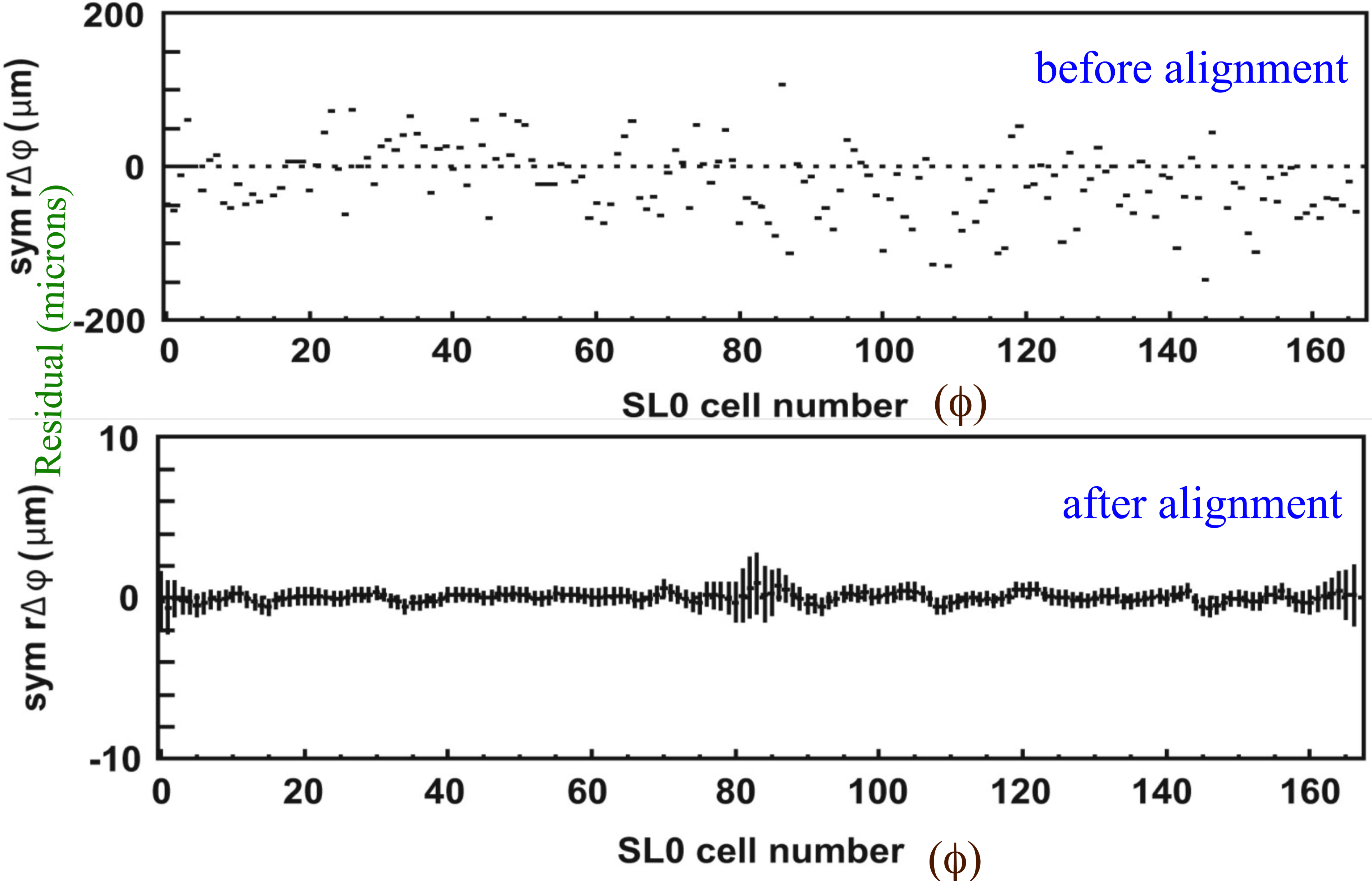

Final relative alignment of cells ~1 μm (initial alignment ~50 μm)

Consistency check of COT alignment procedure

(AVK & CH, *NIM A* 762 (2014) pp 85-99)

Fit separate helices to cosmic ray tracks

Compare track parameters of the two tracks: a measure of track parameter bias

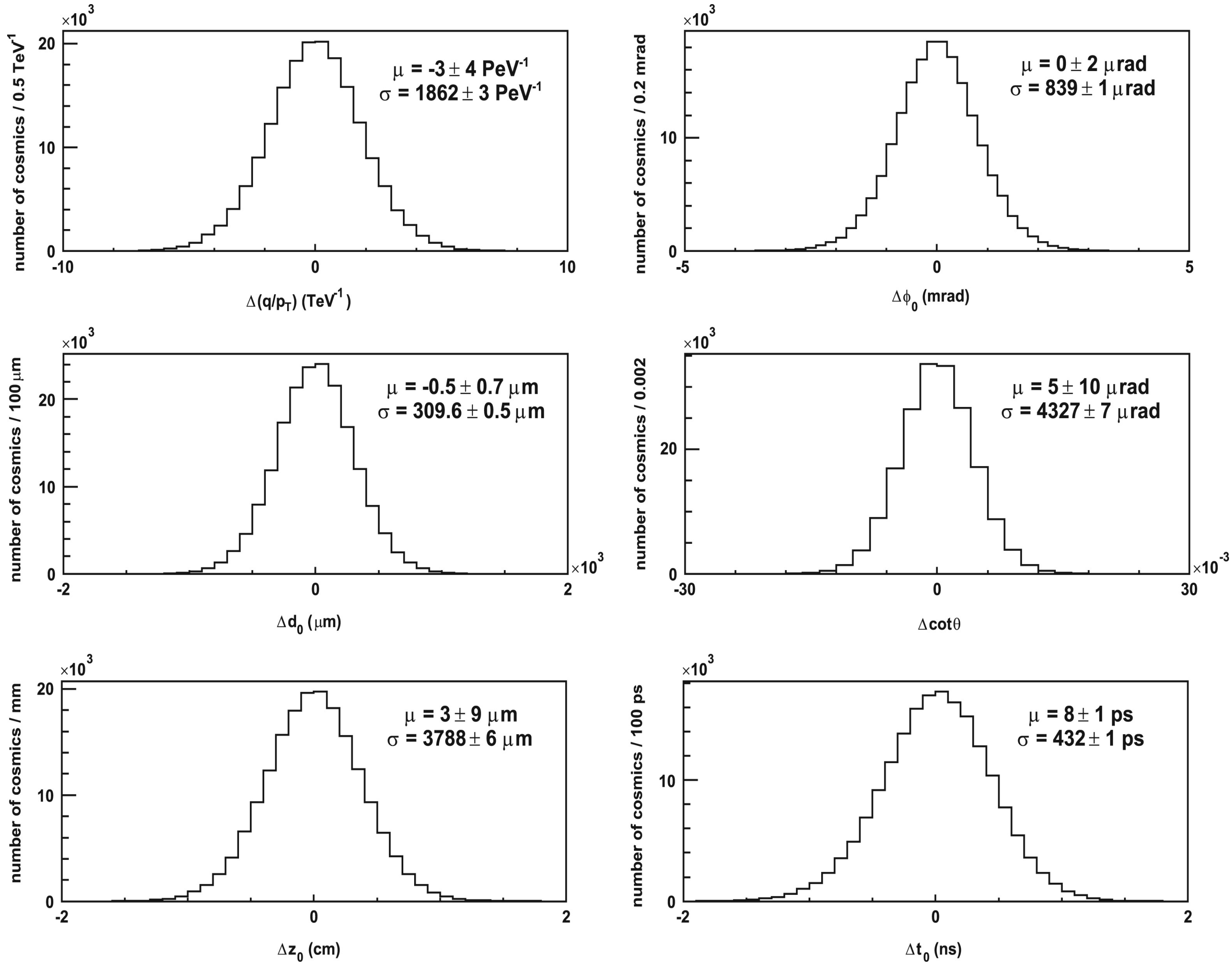

Consistency check of COT alignment procedure

(AVK & CH, *NIM A* 762 (2014) pp 85-99)

track parameter bias versus azimuth

solid = before alignment

open = after alignment

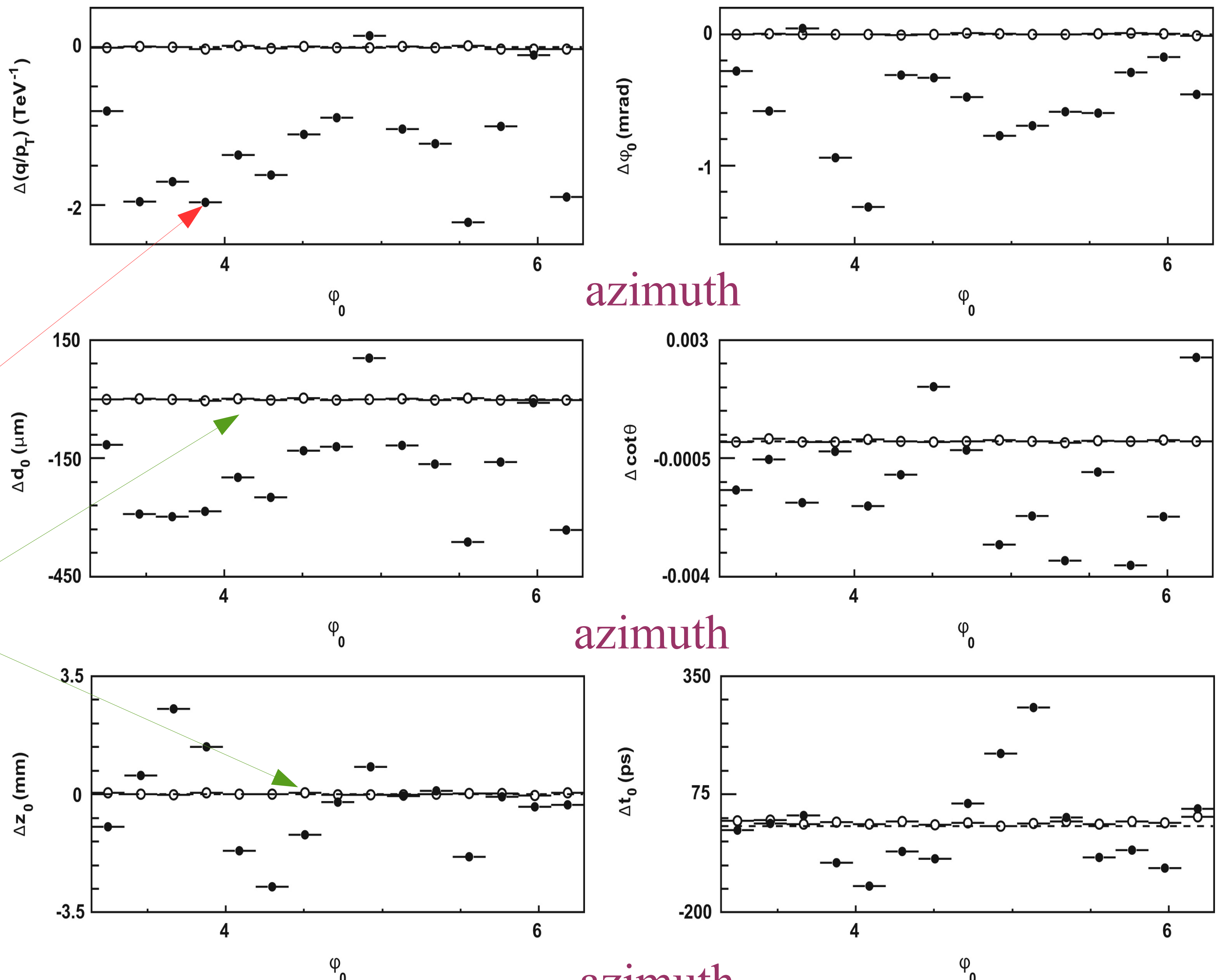

Cross-check of COT alignment

- Cosmic ray alignment removes most deformation degrees of freedom, but "weakly constrained modes" remain
- Final cross-check and correction to beam-constrained track curvature based on difference of <E/p> for positrons *vs* electrons
- Smooth ad-hoc curvature corrections as a function of polar and azimuthal angle: statistical errors => $\Delta M_W = 1$ MeV

q/p_T (measured) =

$c_0 + c_1\, q/p_T + c_2\, (q/p_T)^2$

$+ \ldots$

c_1 measures momentum scale

c_2 includes energy loss

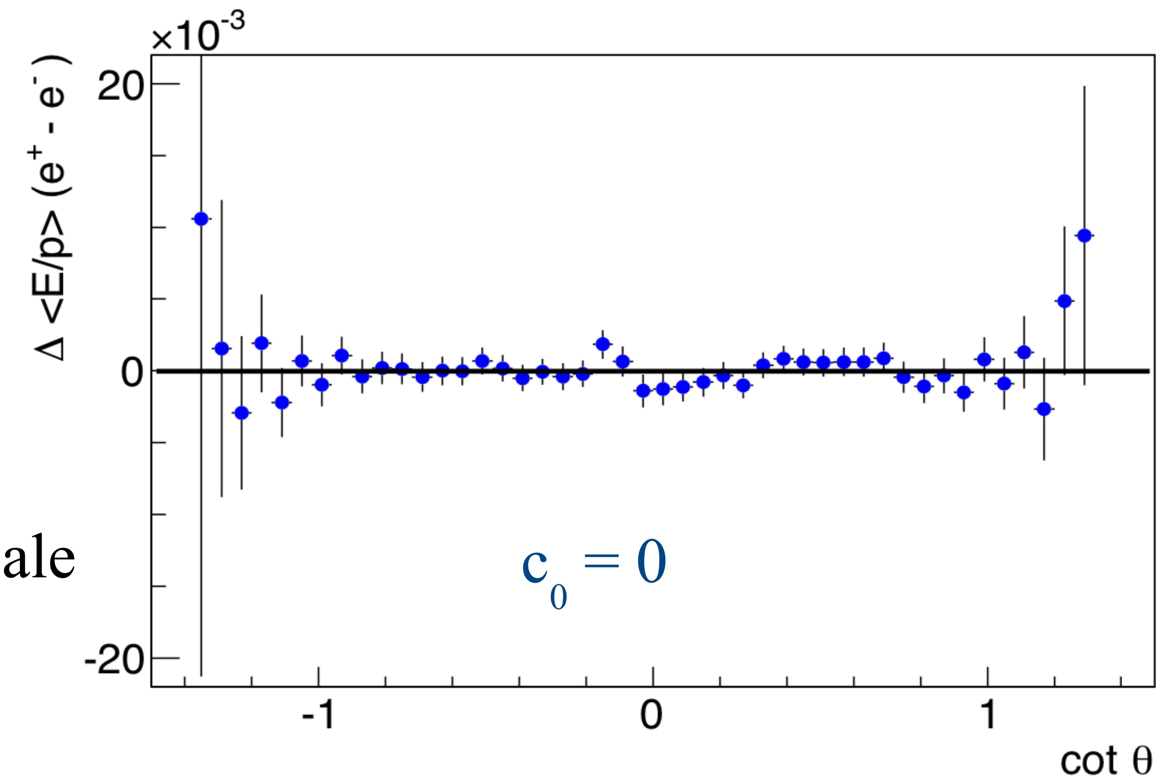

Signal Simulation and Fitting

Generator-level Signal Simulation

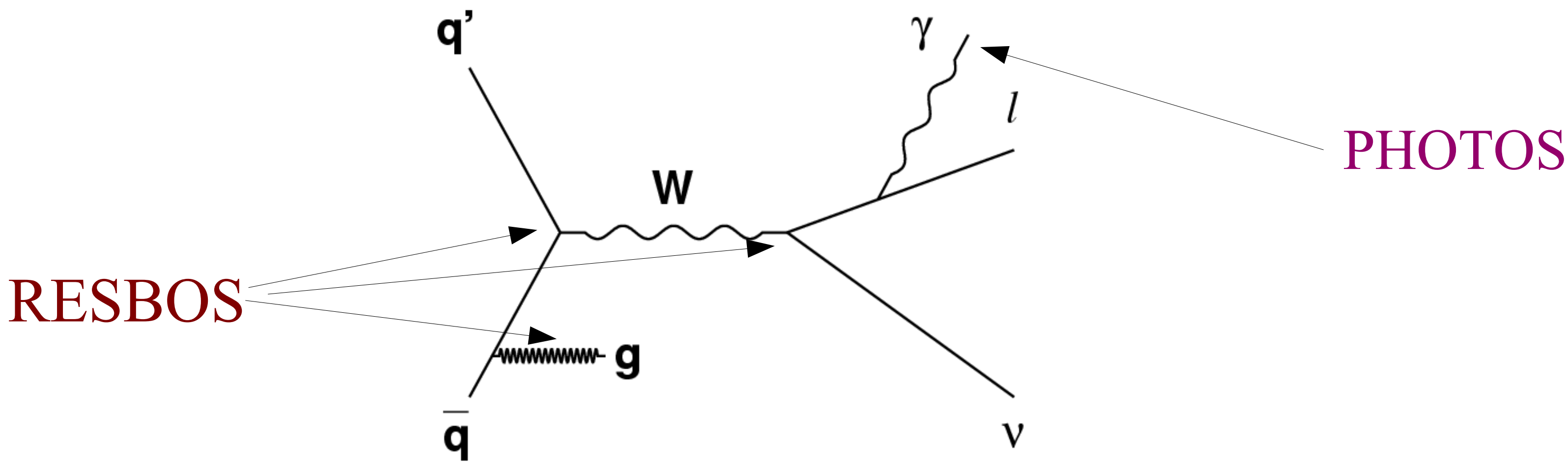

- Generator-level input for W & Z simulation provided by RESBOS (C. Balazs & C.-P. Yuan, PRD56, 5558 (1997) and references therein), which
  - Fully differential production and decay distributions
  - Benchmarked to RESBOS2 (J. Isaacson, Y. Fu & C.-P. Yuan, arXiv:2205.02788)
- Multiple radiative photons generated according to PHOTOS (P. Golonka and Z. Was, Eur. J. Phys. C 45, 97 (2006) and references therein)
  - Calibrated to HORACE (C.M. Carloni Calame, G. Montagna, O. Nicrosini and A. Vicini, JHEP 0710:109,2007)

Constraining Boson p_T Spectrum

- Fit the non-perturbative parameter g_2 and QCD coupling α_s in RESBOS to $p_T(ll)$ spectra:

ΔM_W = 1.8 MeV

Position of peak in boson p_T spectrum depends on g_2

Tail to peak ratio depends on α_s

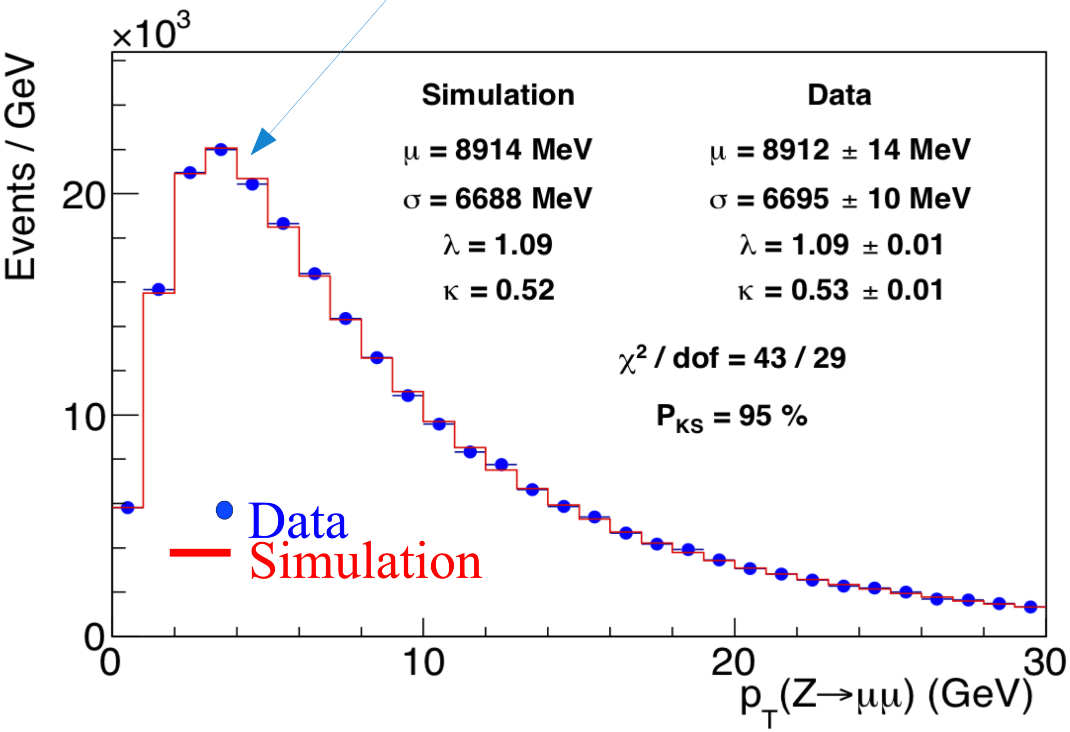

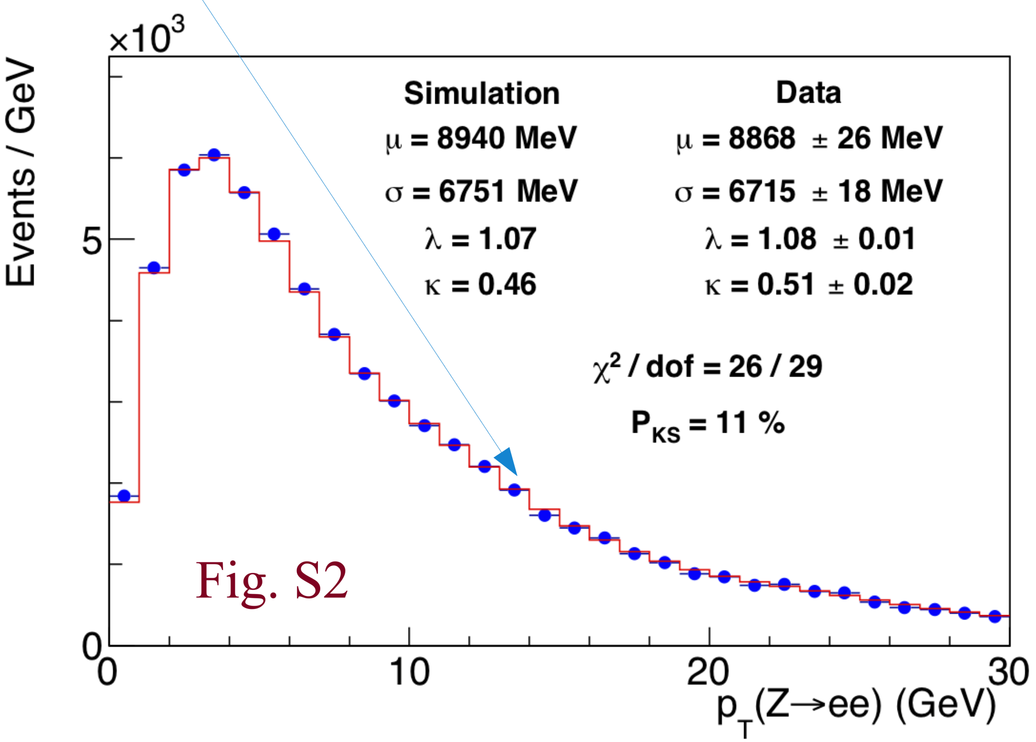

Fig. S2

Outline of Analysis

Energy scale measurements drive the W mass measurement

- Tracker Calibration
  - alignment of the COT (~2400 cells, ~30k sense wires) using cosmic rays
  - COT momentum scale and tracker non-linearity constrained using $J/\psi \rightarrow \mu\mu$ and $\Upsilon \rightarrow \mu\mu$ mass fits
  - Confirmed using $Z \rightarrow \mu\mu$ mass fit
- EM Calorimeter Calibration
  - COT momentum scale transferred to EM calorimeter using a fit to the peak of the E/p spectrum, around $E/p \sim 1$
  - Calorimeter energy scale confirmed using $Z \rightarrow ee$ mass fit
- Tracker and EM Calorimeter resolutions
- Hadronic recoil modeling
  - Characterized using p_T-balance in $Z \rightarrow ll$ events

Custom Monte Carlo Detector Simulation

- A complete detector simulation of all quantities measured in the data
- First-principles simulation of tracking
  - Tracks and photons propagated through a high-resolution 3-D lookup table of material properties for silicon detector and COT
  - At each material interaction, calculate
    - Ionization energy loss according to detailed formulae and Landau distribution
    - Generate bremsstrahlung photons down to 0.4 MeV, using detailed cross section and spectrum calculations
    - Simulate photon conversion and Compton scattering
    - Propagate bremsstrahlung photons and conversion electrons
    - Simulate multiple Coulomb scattering, including non-Gaussian tail
  - Deposit and smear hits on COT wires, perform full helix fit including optional beam-constraint

Custom Monte Carlo Detector Simulation

- A complete detector simulation of all quantities measured in the data
- First-principles simulation of tracking
  - Tracks and photons propagated through a high-resolution 3-D lookup table of material properties for silicon detector and COT

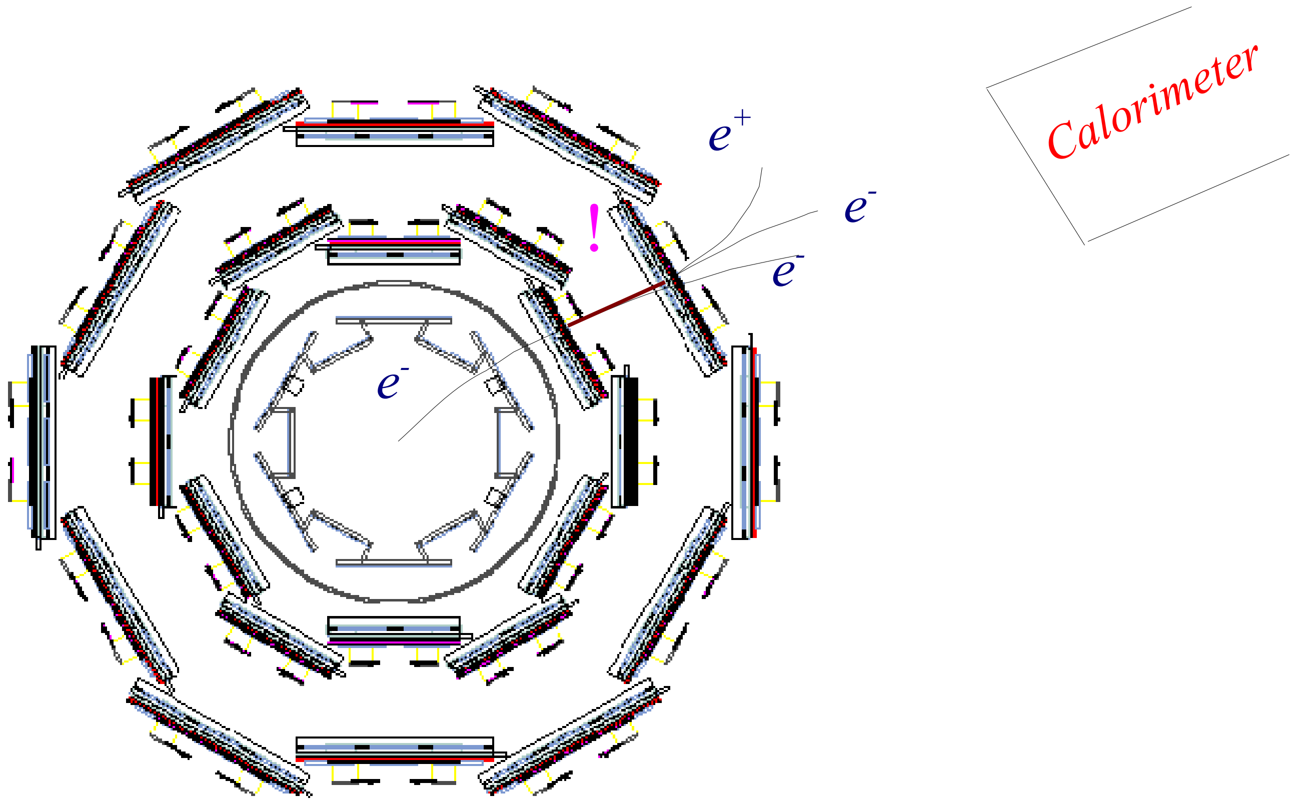

Tracking Momentum Scale

Tracking Momentum Scale

Set using $J/\psi \rightarrow \mu\mu$ and $\Upsilon \rightarrow \mu\mu$ resonance and $Z \rightarrow \mu\mu$ masses

- Extracted by fitting J/ψ mass in bins of $1/p_T(\mu)$, and extrapolating momentum scale to zero curvature
- $J/\psi \rightarrow \mu\mu$ mass independent of $p_T(\mu)$ after 2.6% tuning of energy loss

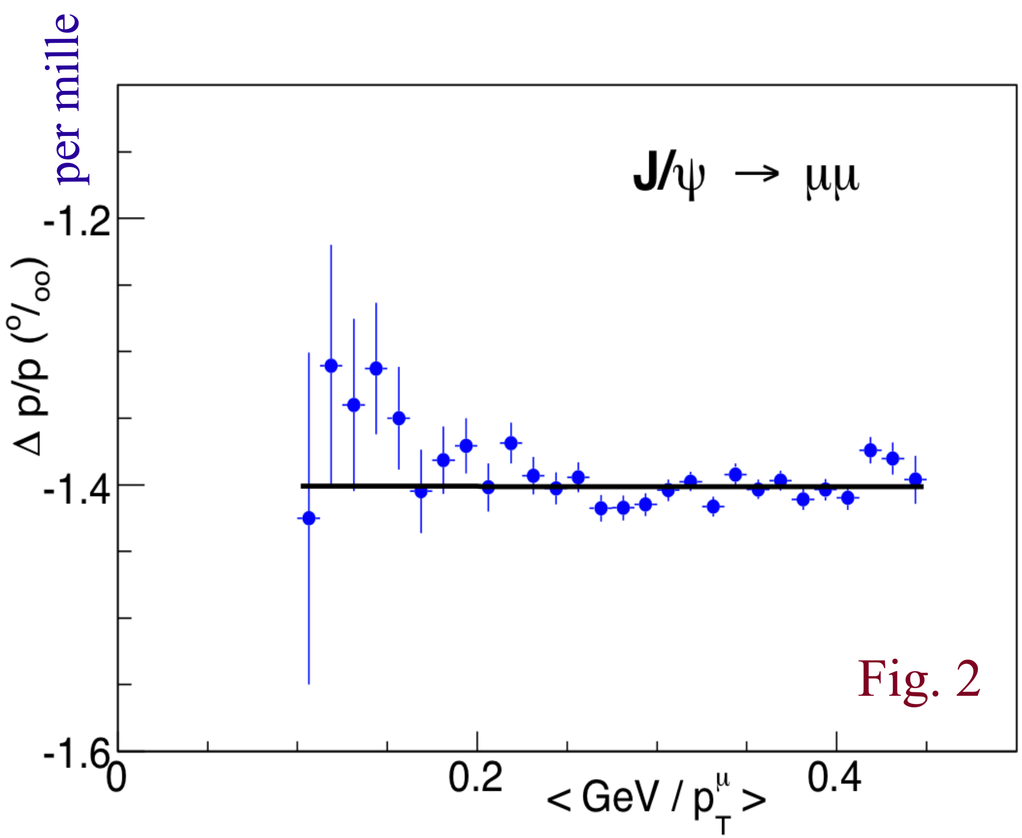

Fig. 2

$J/\psi \rightarrow \mu\mu$ mass fit (bin 8)

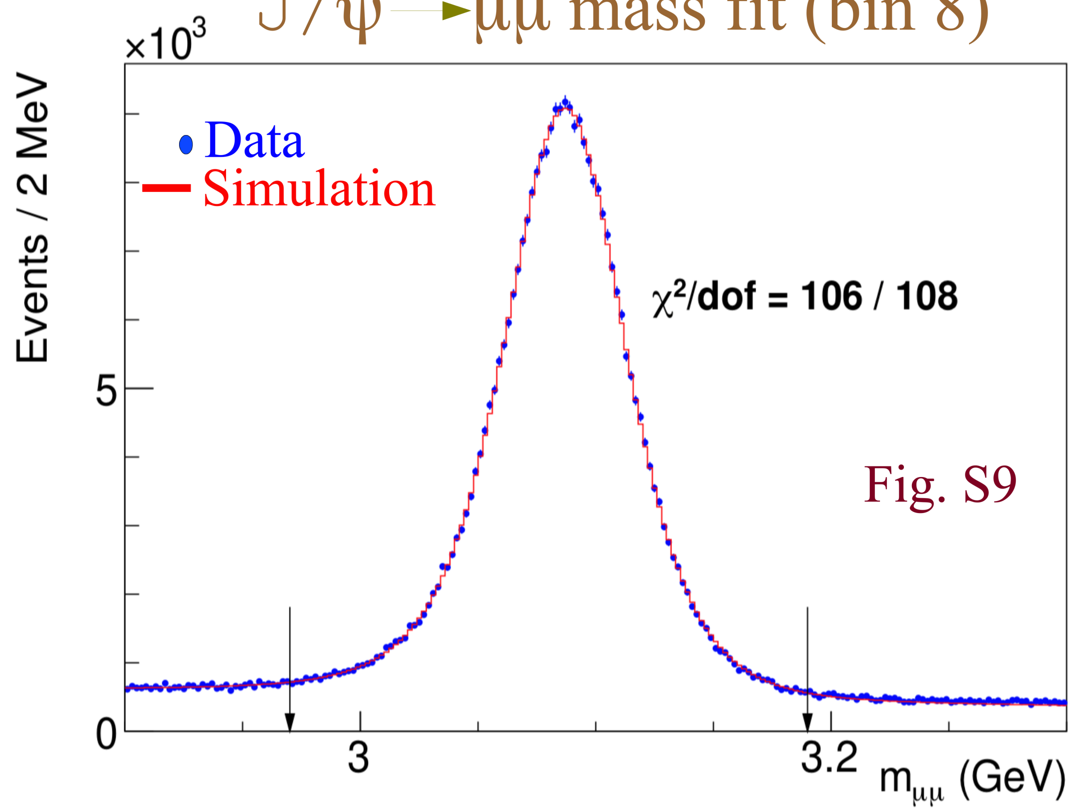

Fig. S9

Tracking Momentum Scale

$\Upsilon \rightarrow \mu\mu$ resonance provides

- Cross-check of non-beam-constrained (NBC) and beam-constrained (BC) fits
- Consistent measurements after incorporating silicon detector passive energy loss in extrapolator code of track reconstruction

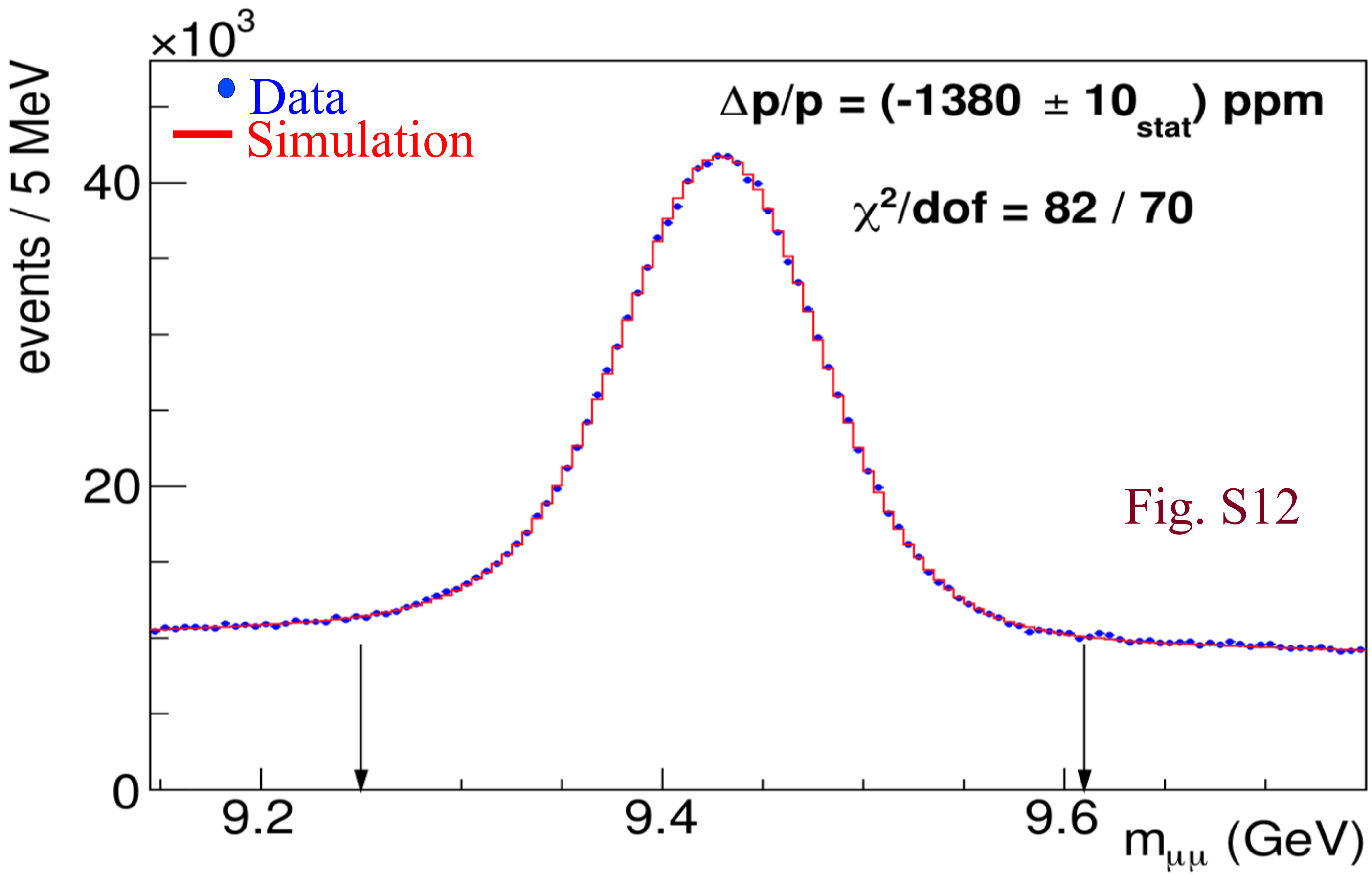

BC $\Upsilon \rightarrow \mu\mu$ mass fit

Tracking Momentum Scale Systematics

Systematic uncertainties on momentum scale (parts per million)

Source	J/ψ (ppm)	Υ (ppm)	Correlation (%)
QED	1	1	100
Magnetic field non-uniformity	13	13	100
Ionizing material correction	11	8	100
Resolution model	10	1	100
Background model	7	6	0
COT alignment correction	4	8	0
Trigger efficiency	18	9	100
Fit range	2	1	100
$\Delta p/p$ step size	2	2	0
World-average mass value	4	27	0
Total systematic	29	34	16 ppm
Statistical NBC (BC)	2	13(10)	0
Total	29	36	16 ppm

$\Delta M_{W,Z}$ = 2 MeV

Uncertainty dominated by magnetic field non-uniformity, passive material energy loss, low p_T modeling and Υ mass world average

$Z \rightarrow \mu\mu$ Mass Cross-check & Combination

- Using the J/ψ and ϒ momentum scale, performed "blinded" measurement of *Z* boson mass
  - *Z* mass consistent with PDG value (91188 MeV) (0.7σ statistical)
  - $M_Z = 91192.0 \pm 6.4_{stat} \pm 2.3_{momentum} \pm 3.1_{QED} \pm 1_{alignment}$ MeV

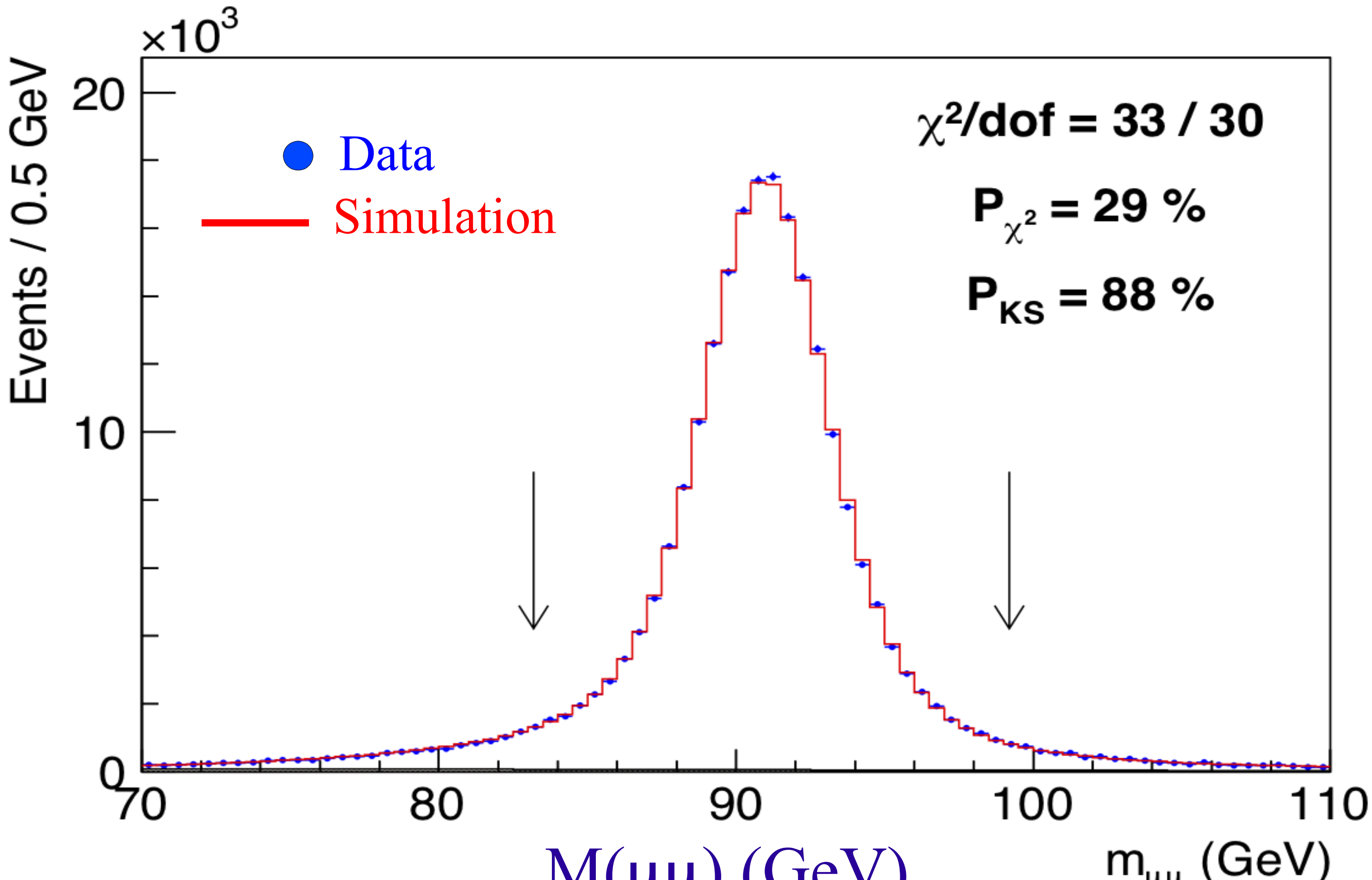

M(μμ) (GeV)

Tracker Linearity Cross-check & Combination

- Final calibration using the J/ψ, ϒ and Z bosons for calibration
- Combined momentum scale correction :

$$\Delta p/p = (-1389 \pm 25_{syst}) \text{ parts per million}$$

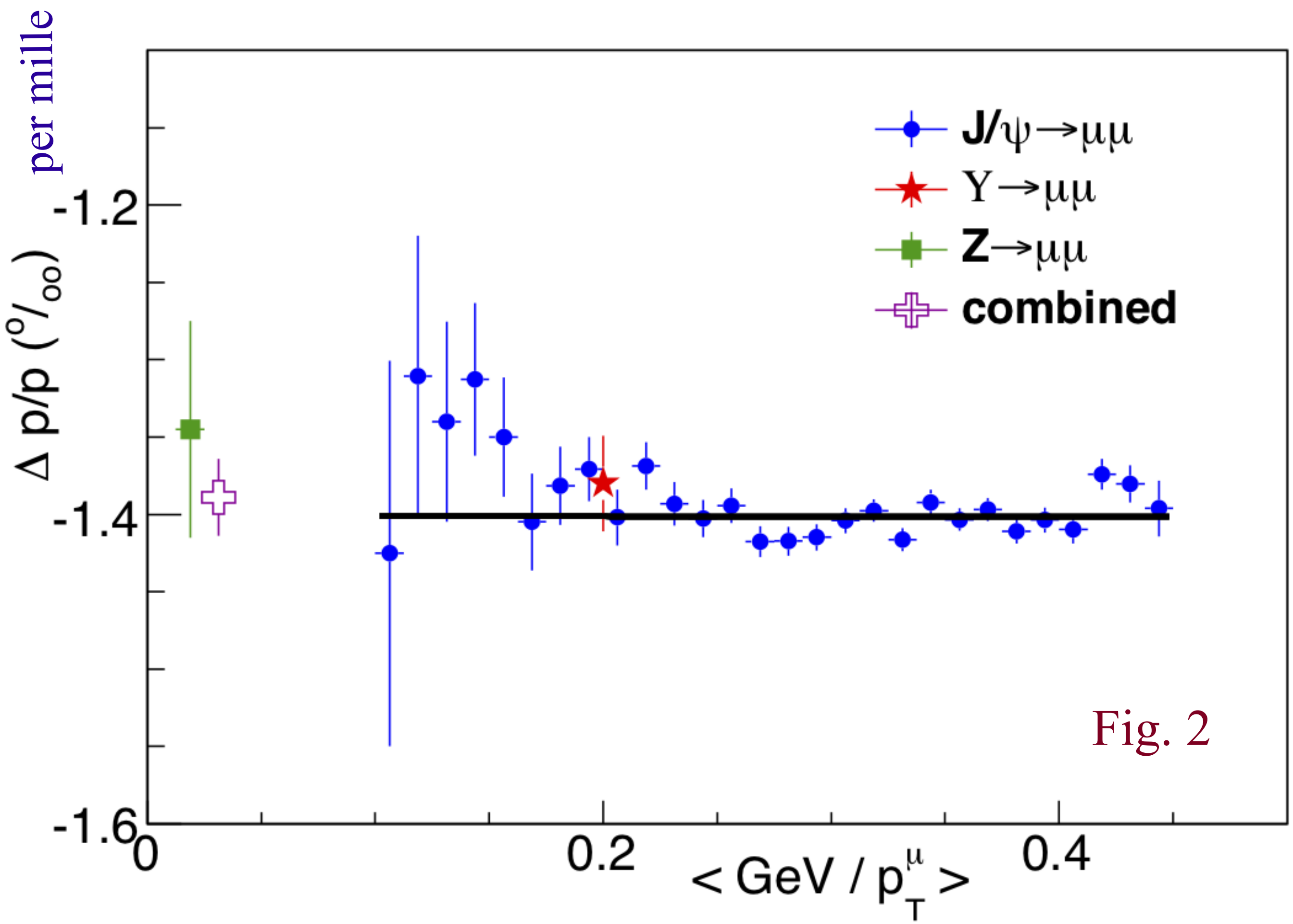

Fig. 2

ΔM_W = 2 MeV

EM Calorimeter Response

EM Calorimeter Scale

- E/p peak from $W \rightarrow e\upsilon$ decays provides measurements of EM calorimeter scale and its (E_T-dependent) non-linearity

$$\Delta S_E = (43_{\mathrm{stat}} \pm 30_{\mathrm{non\text{-}linearity}} \pm 34_{X0} \pm 45_{\mathrm{Tracker}})\ \text{parts per million}$$

Setting S_E to 1 using E/p calibration from combined $W \rightarrow e\upsilon$ and $Z \rightarrow ee$ samples

$\Delta M_W = 6\ \mathrm{MeV}$

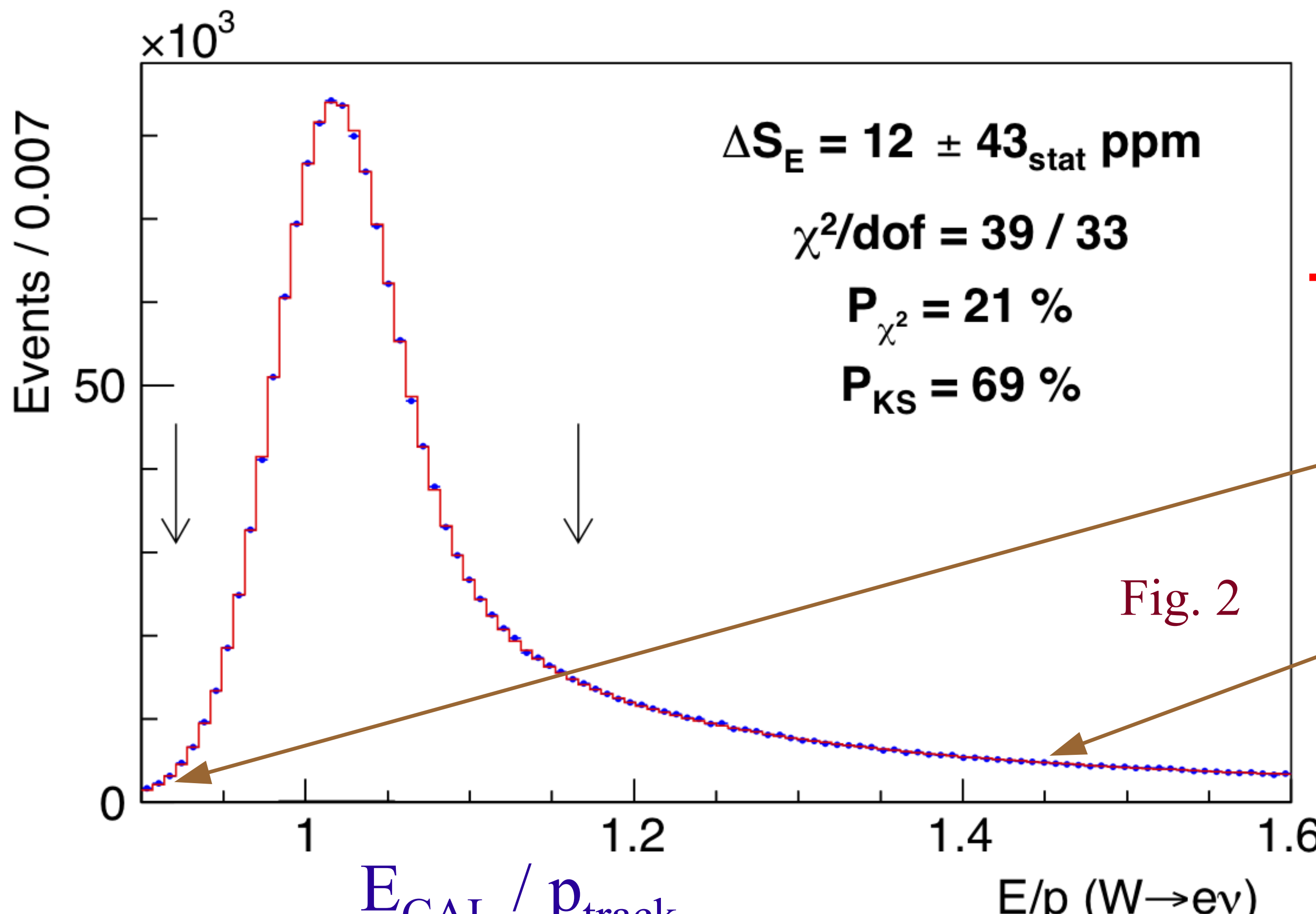

● Data

Simulation

Low tail used for tuning calorimeter thickness

High tail of used for tuning model of radiative material

Measurement of EM Calorimeter Non-linearity

- Perform E/p fit-based calibration in bins of electron E_T
- GEANT-motivated parameterization of non-linear response:

$$S_E = 1 + \beta \log(E_T / 39\ \text{GeV})$$

- Tune on W and Z data: $\beta = (7.2 \pm 0.4_{stat}) \times 10^{-3}$

=> $\Delta M_W = 2$ MeV

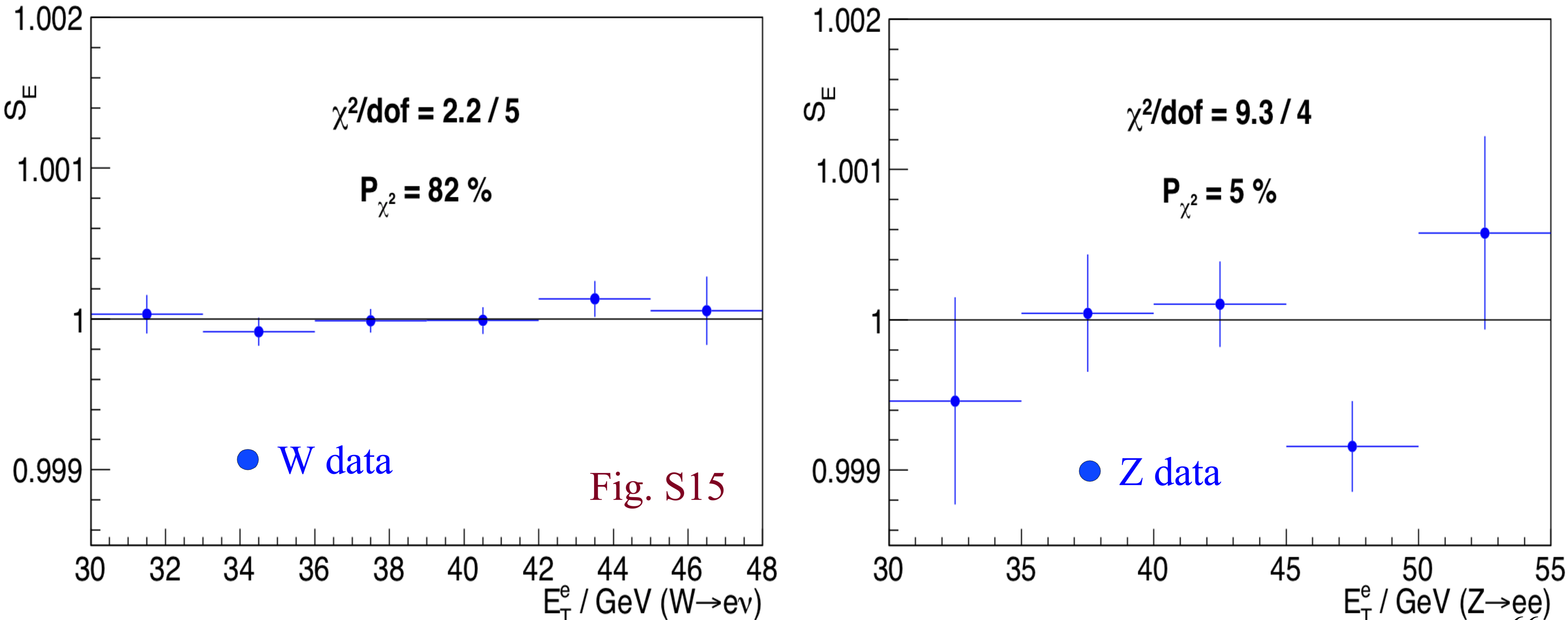

Fig. S15

$Z \rightarrow ee$ Mass Cross-check and Combination

- Performed "blind" measurement of Z mass using E/p-based calibration
  - Consistent with PDG value (91188 MeV) within 0.5σ (statistical)
  - M_Z=91194.3±13.8$_{stat}$ ±6.5$_{calorimeter}$ ±2.3$_{momentum}$ ±3.1$_{QED}$ ±0.8$_{alignment}$ MeV
- Combine E/p-based calibration with $Z \rightarrow ee$ mass for maximum precision

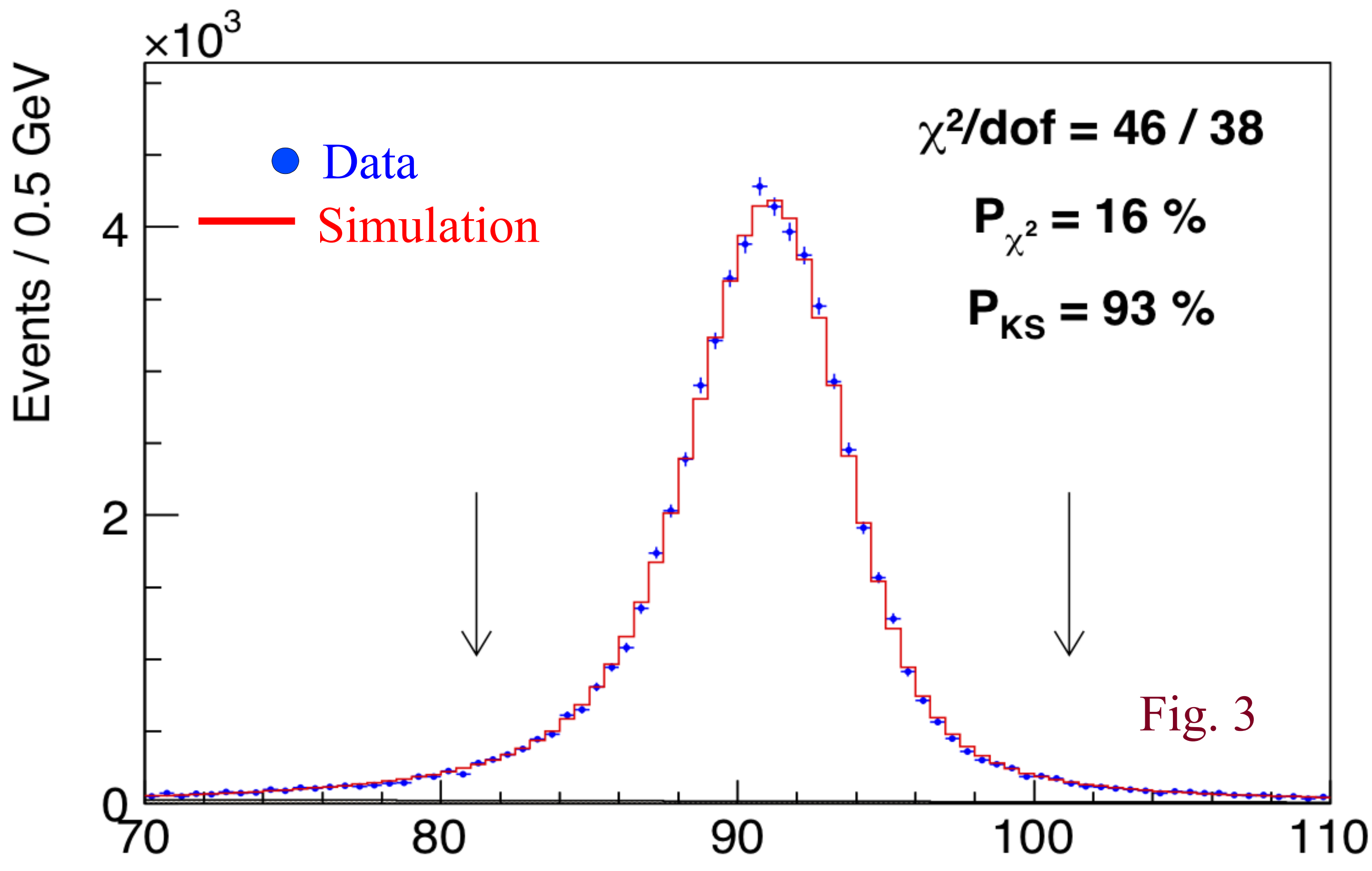

M(ee) (GeV)

ΔM_W = 5.8 MeV

ΔS_E = -14 ± 72 ppm

Hadronic Recoil Model

Constraining the Hadronic Recoil Model

Exploit similarity in production and decay of *W* and *Z* bosons

Detector response model for hadronic recoil tuned using p_T-balance in $Z \rightarrow ll$ events

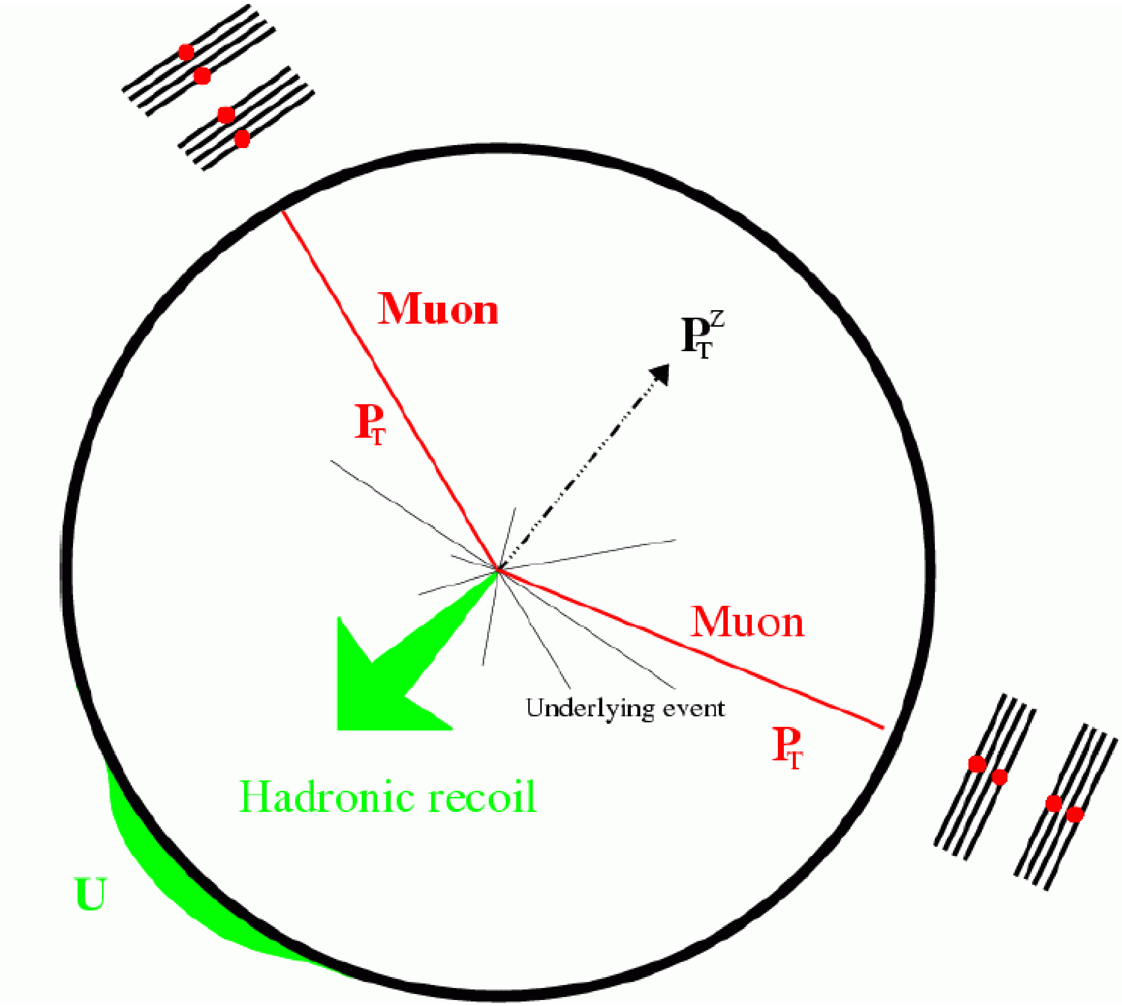

Transverse momentum of Hadronic recoil (***u***) calculated as 2-vector-sum over calorimeter towers

Lepton Tower Removal

- We remove the calorimeter towers containing lepton energy from the hadronic recoil calculation
  - Lost underlying event energy is measured in ϕ-rotated windows in W boson data

$$\Delta M_W = 1\ \mathrm{MeV}$$

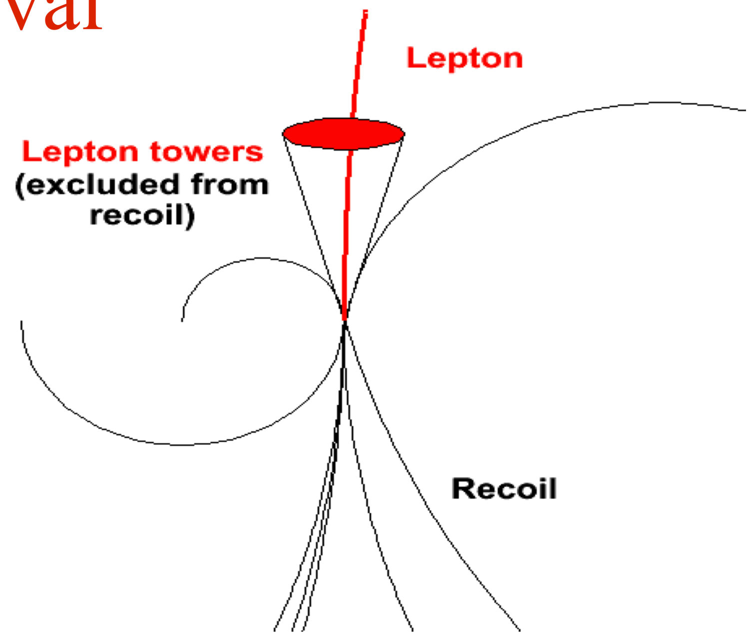

Figs. S17 & S18

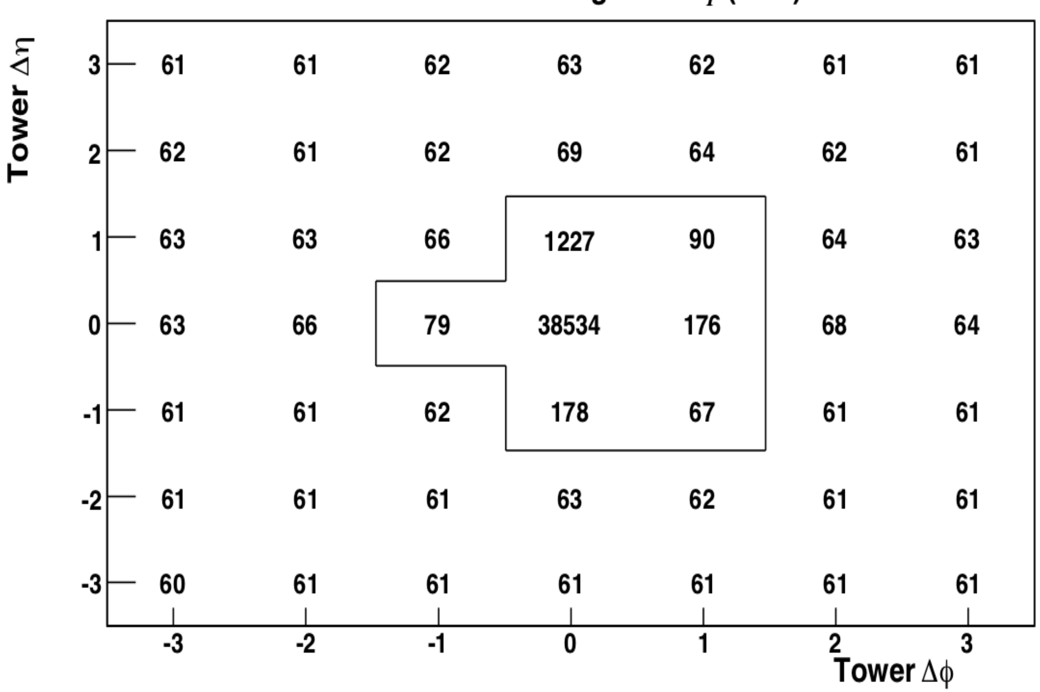

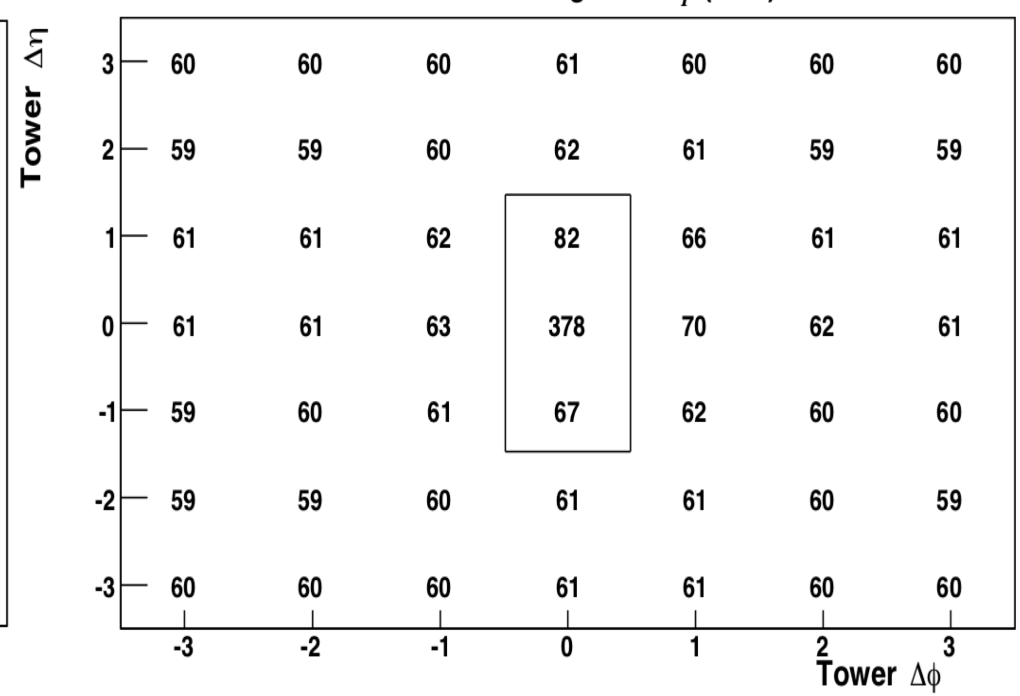

Lepton Tower Removal

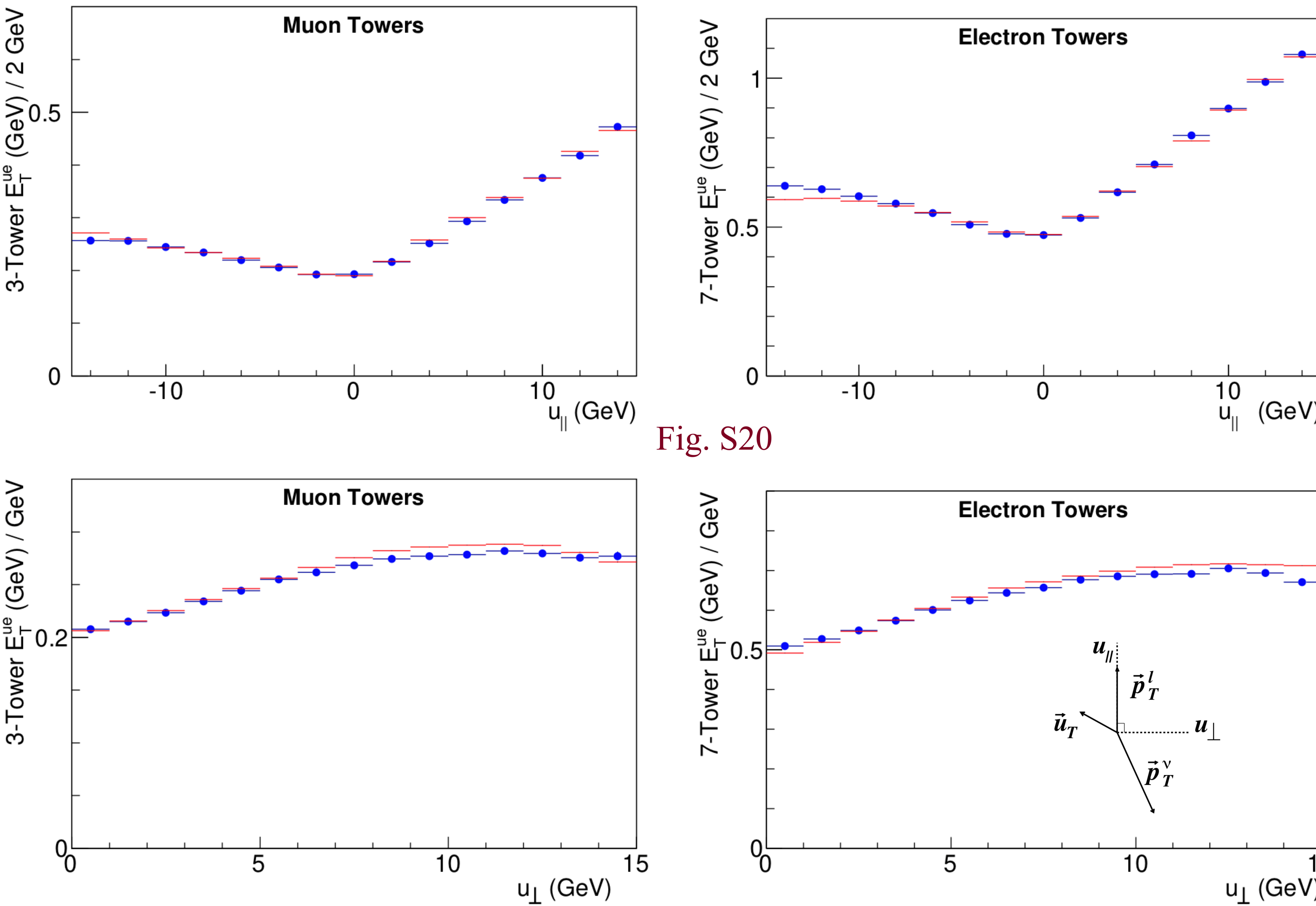

Fig. S20

Constraining the Hadronic Recoil Model

Exploit similarity in production and decay of *W* and *Z* bosons

Detector response model for hadronic recoil tuned using p_T-balance in $Z \rightarrow ll$ events

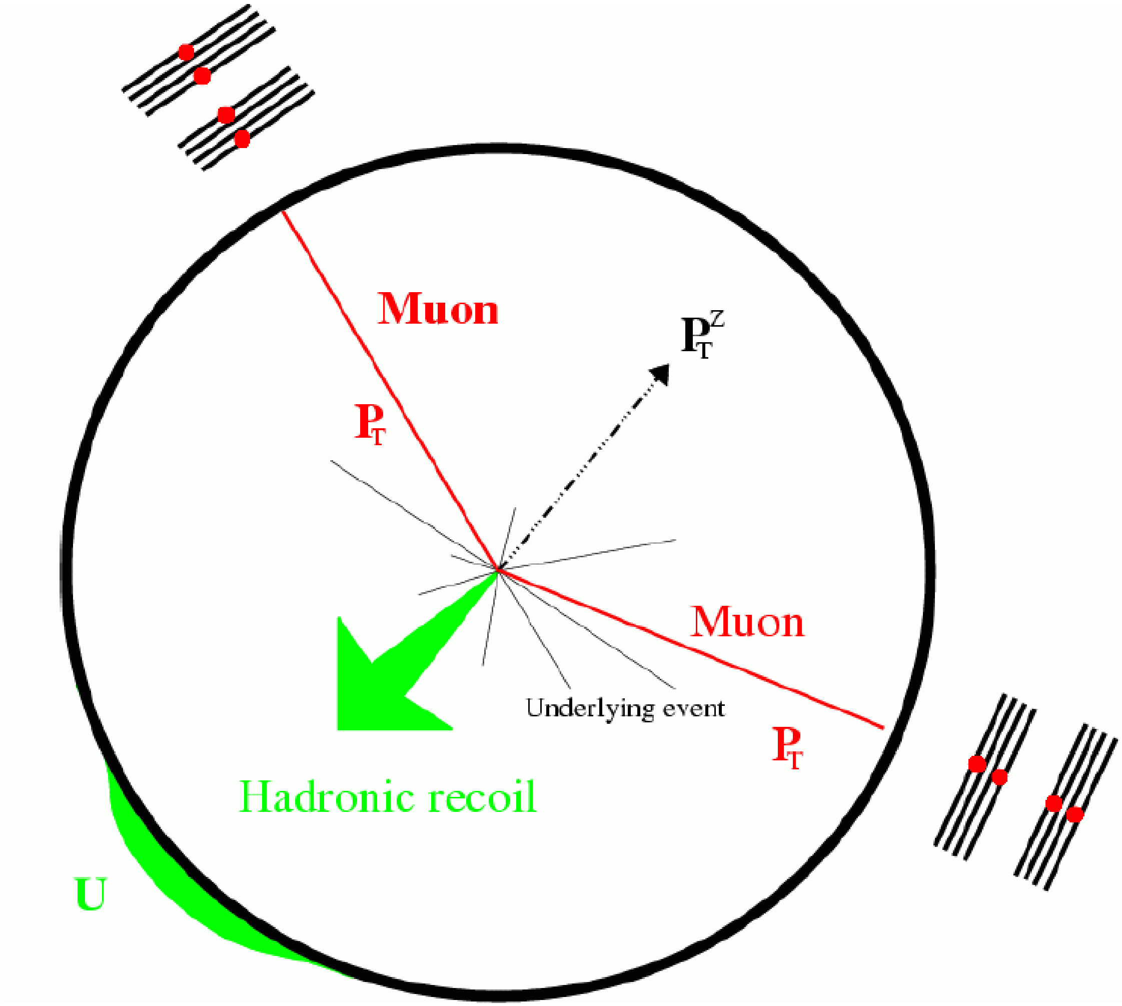

Transverse momentum of Hadronic recoil (***u***) calculated as 2-vector-sum over calorimeter towers

Hadronic Recoil Simulation

Recoil momentum 2-vector ***u*** has

- a soft 'spectator interaction' component, randomly oriented
  - Modeled using minimum-bias data with tunable magnitude
- A hard 'jetty' component, directed opposite the boson p_T
  - P_T-dependent response and resolution parameterizations
  - Hadronic response $R = \boldsymbol{u}_{\text{reconstructed}} / \boldsymbol{u}_{\text{true}}$ parameterized as a logarithmically increasing function of boson p_T motivated by Z boson data

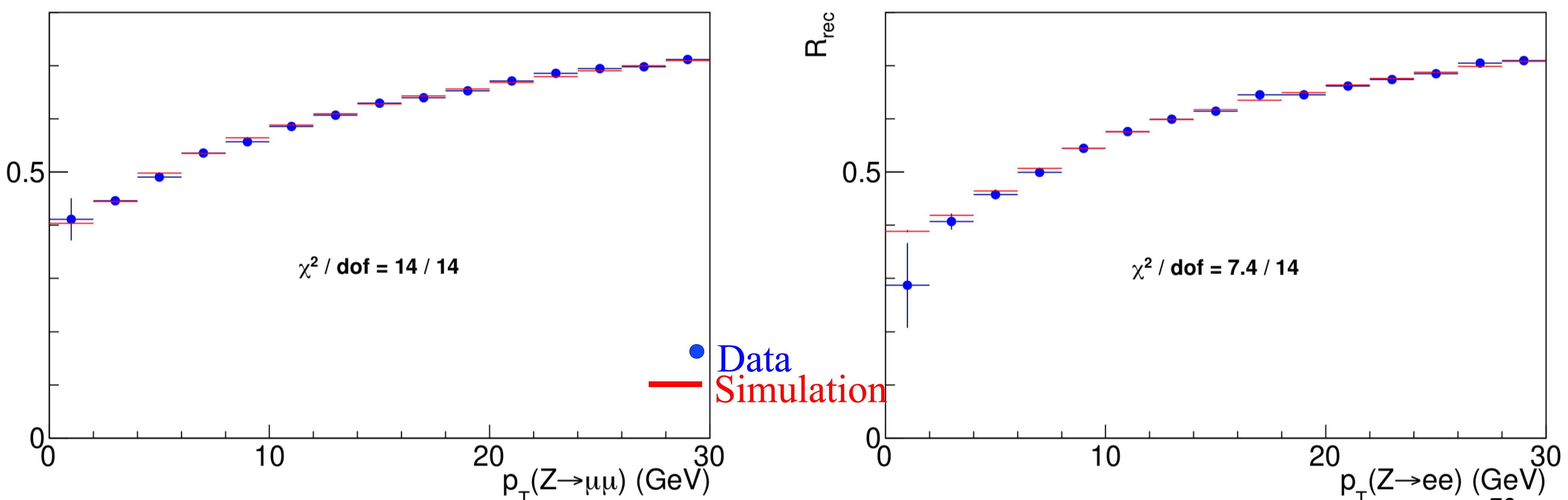

Tuning Recoil Response Model with Z events

Project the vector sum of $p_T(ll)$ and $\boldsymbol{u}$ on a set of orthogonal axes defined by boson p_T

Mean and rms of projections as a function of $p_T(ll)$ provide information on hadronic model parameters

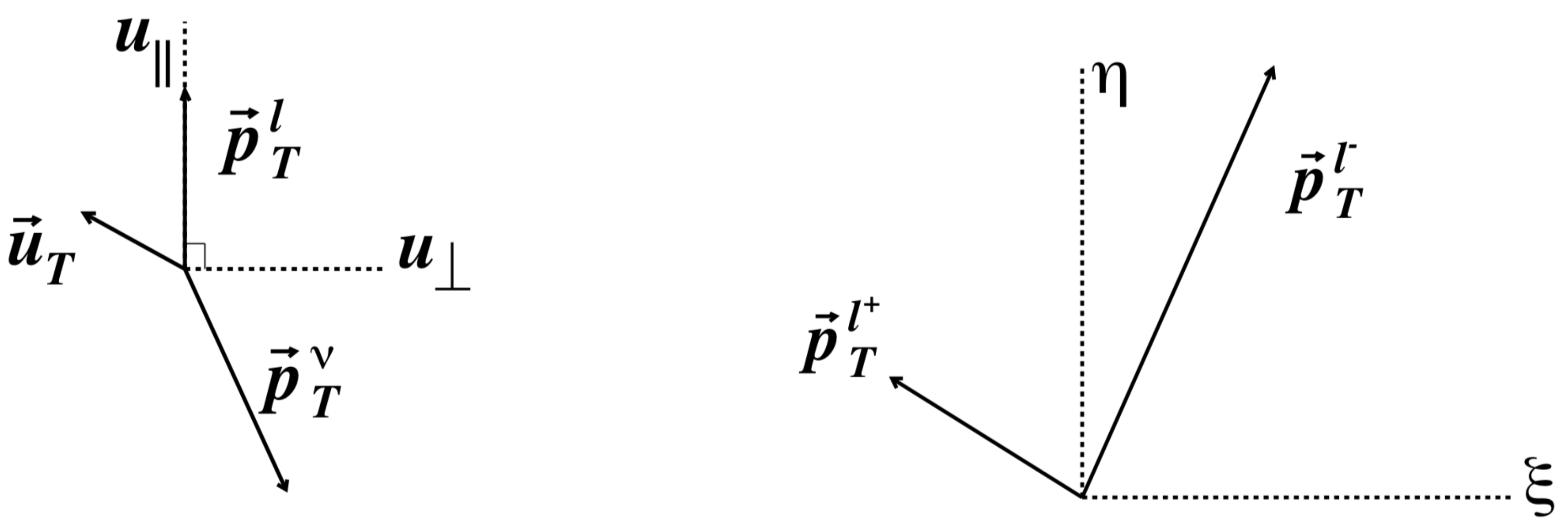

FIG. S3: (left) Sketches of typical transverse vectors associated to quantities reconstructed in a W-boson event, with the recoil hadron momentum ($\vec{u}_T$) separated into axes parallel ($u_{||}$) and perpendicular ($u_\perp$) to the charged lepton. (right) Illustration of the η and ξ axes in Z boson events.

Tuning Recoil Response Model with Z events

Project the vector sum of $p_T(ll)$ and $\boldsymbol{u}$ on a set of orthogonal axes defined by boson p_T

Mean and rms of projections as a function of $p_T(ll)$ provide information on hadronic model parameters

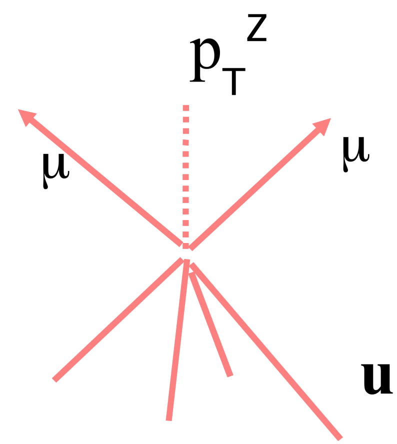

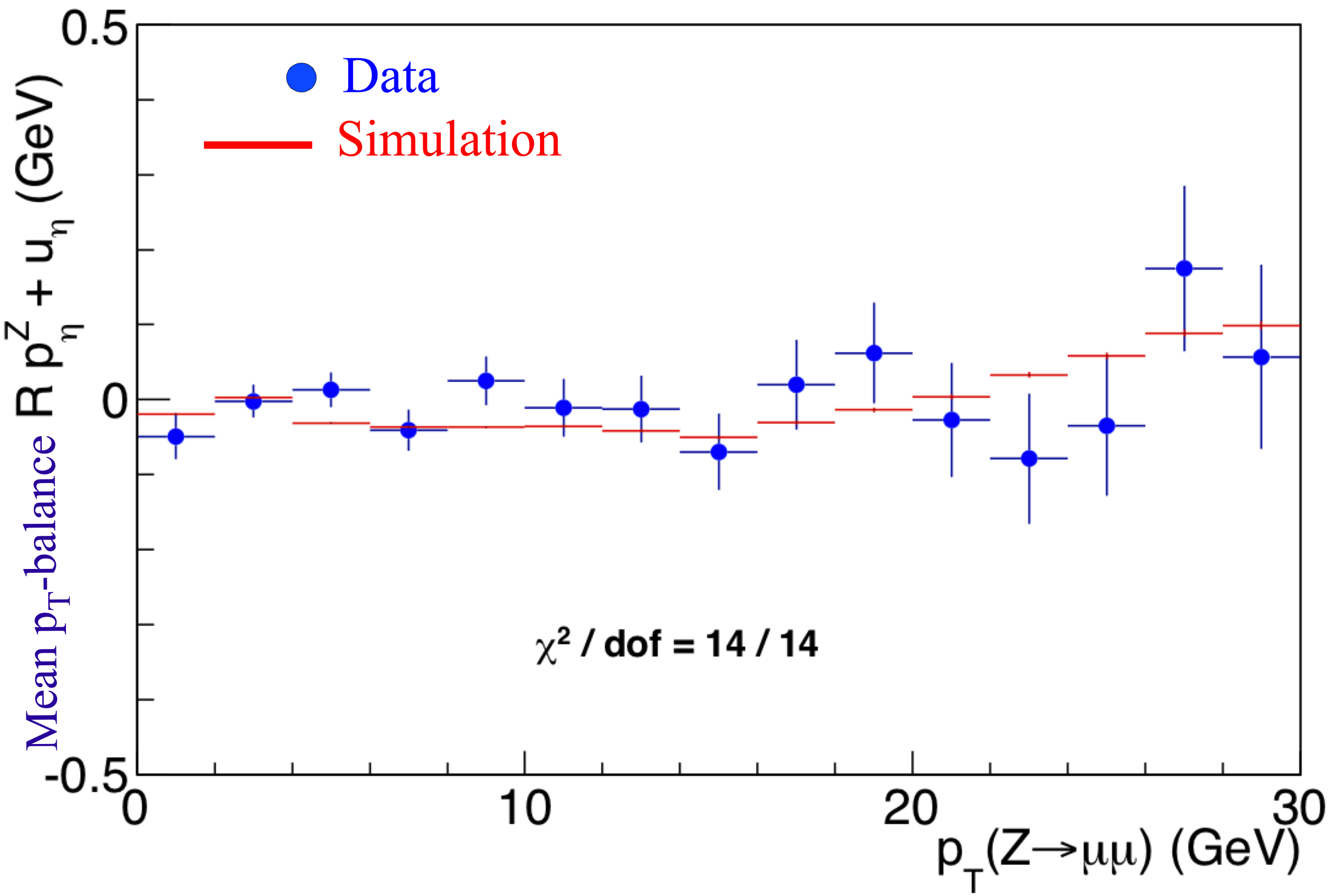

Hadronic model parameters tuned by minimizing χ^2 between data and simulation

$\Delta M_W = 2$ MeV

Tuning Recoil Resolution Model with Z events

At low $p_T(Z)$, p_T-balance constrains hadronic resolution due to underlying event

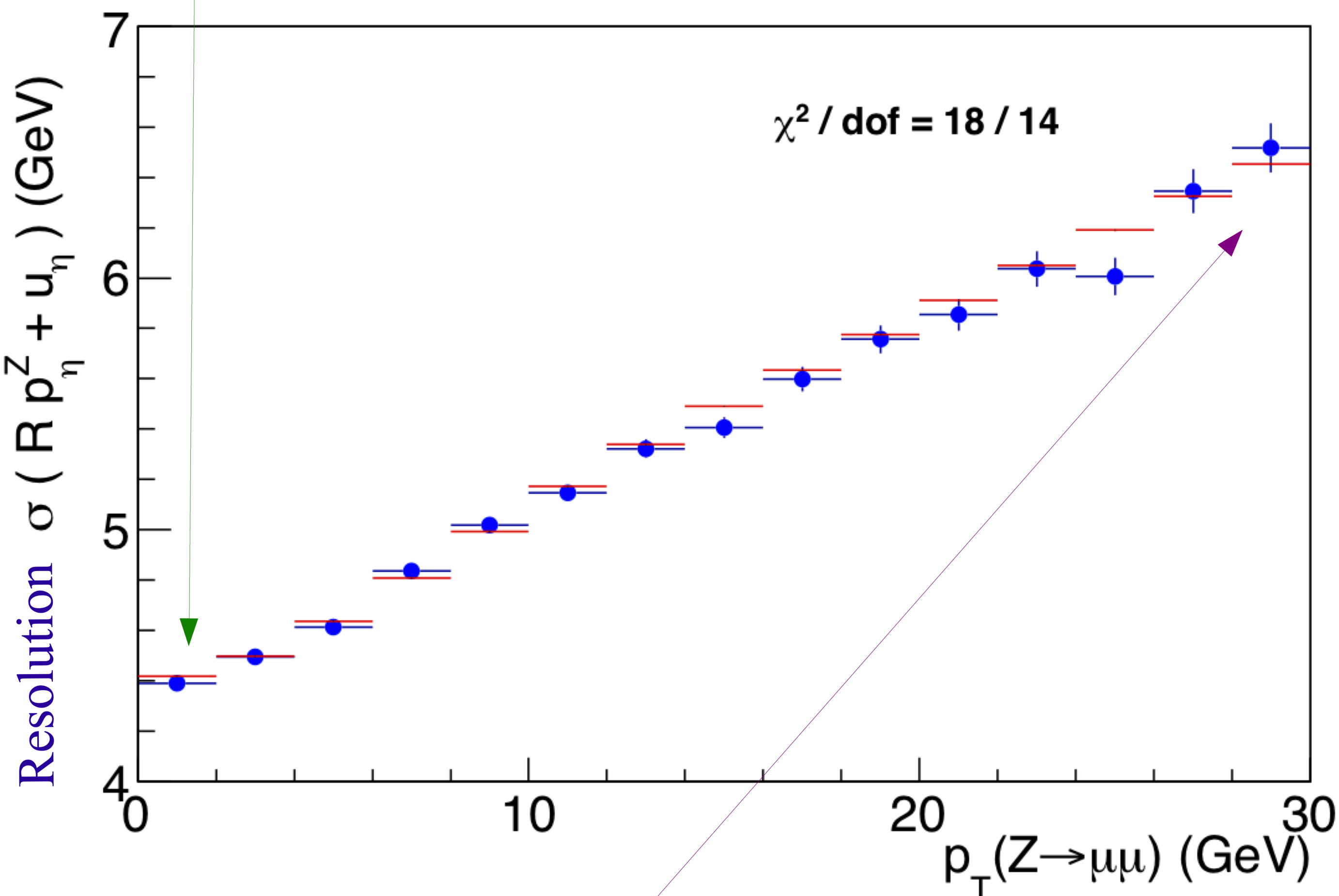

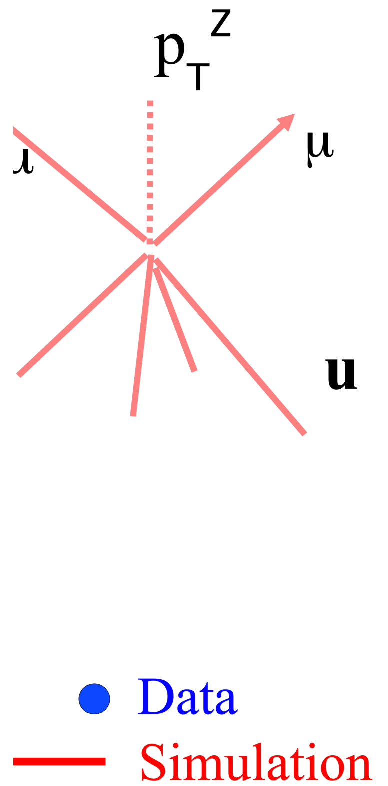

At high $p_T(Z)$, p_T-balance constrains jet resolution

Tuning Recoil Resolution Model with Z events

NEW: model of boson + dijet events

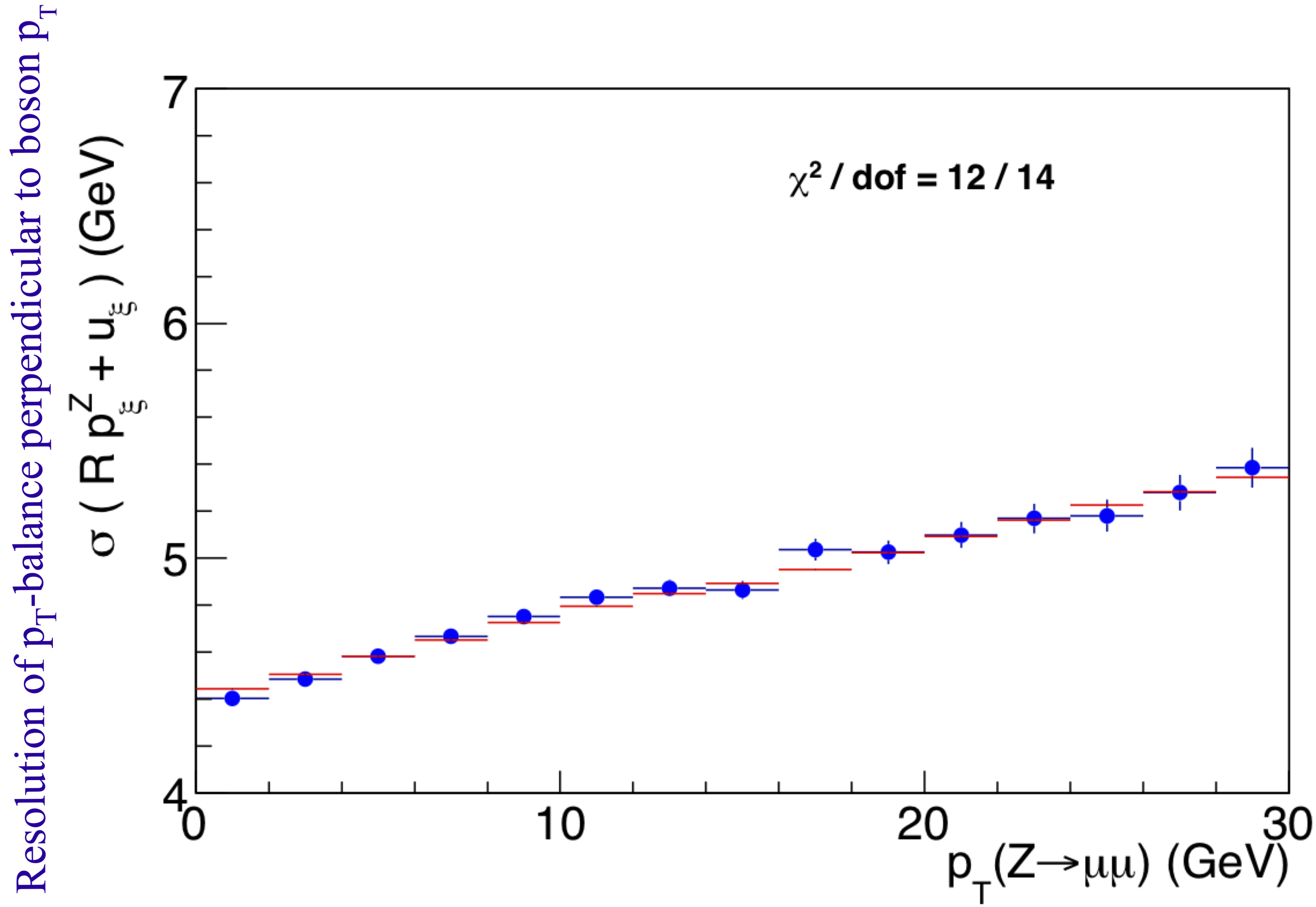

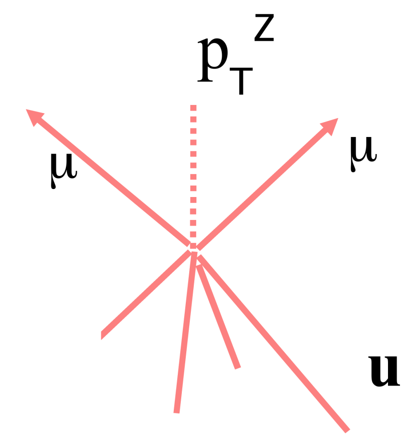

$\Delta M_W = 1.8$ MeV

Data
Simulation

As a function of $p_T(Z)$, dijet event fraction varies between 0.4 % & 1.2 %

Tuning Recoil Resolution Model with *Z* events

Model of p_T-dependent collimation of jet(s) recoiling against boson

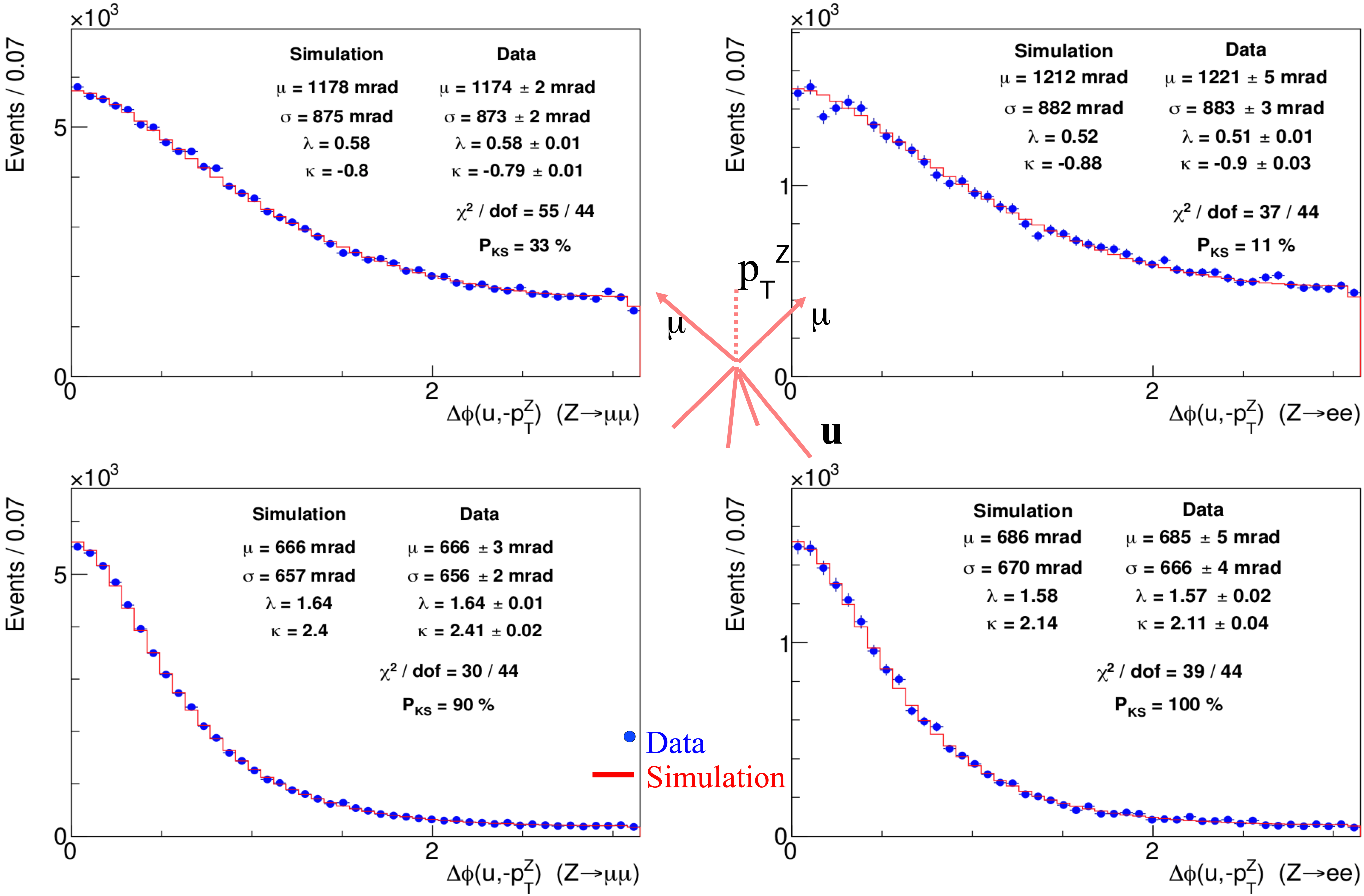

Tuning Recoil Resolution Model with *Z* events

NEW: Fine-tuning model for resolution along $p_T(Z)$ axis

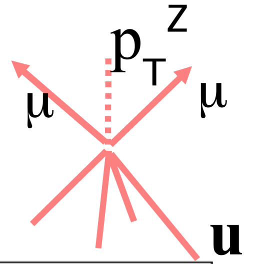

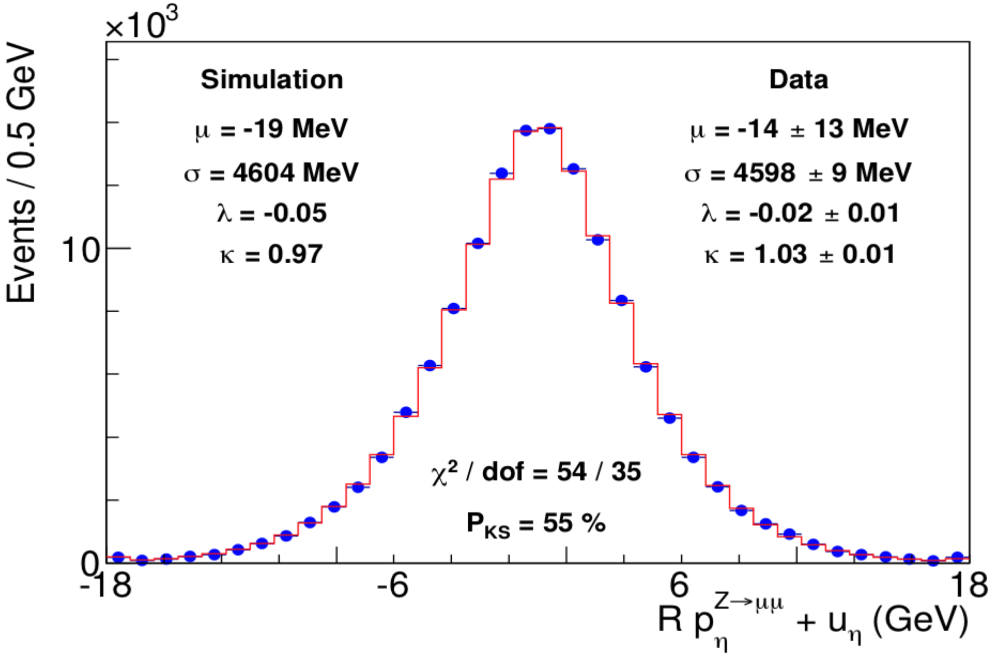

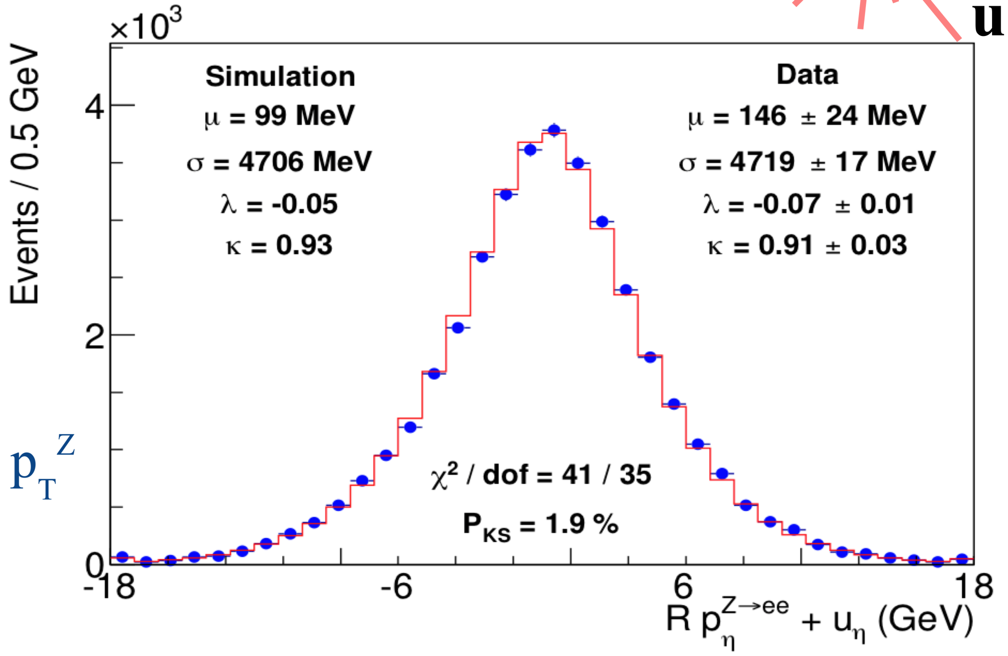

low p_T^Z

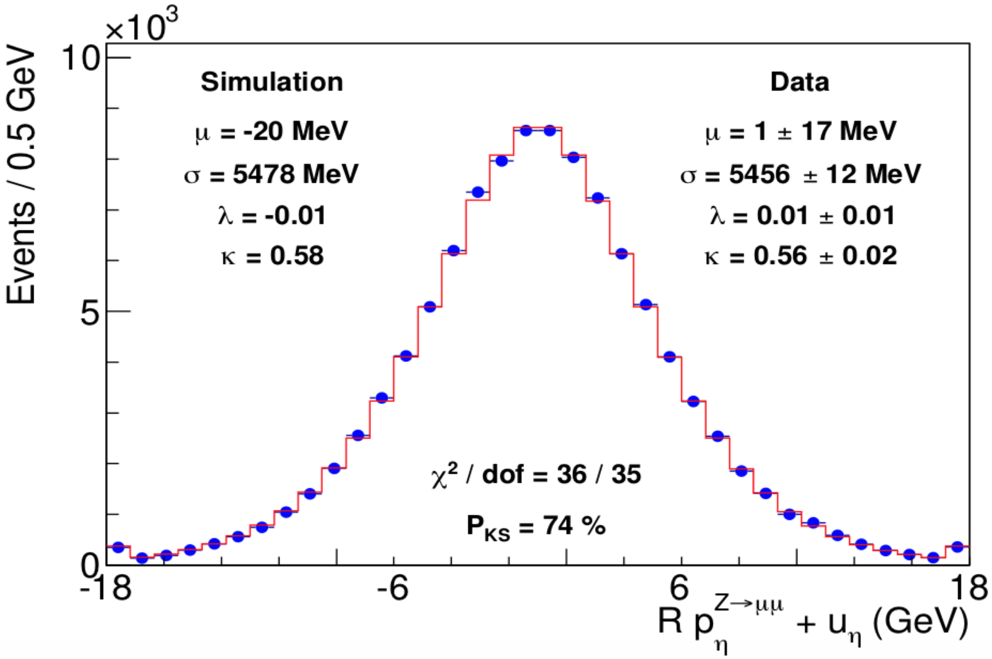

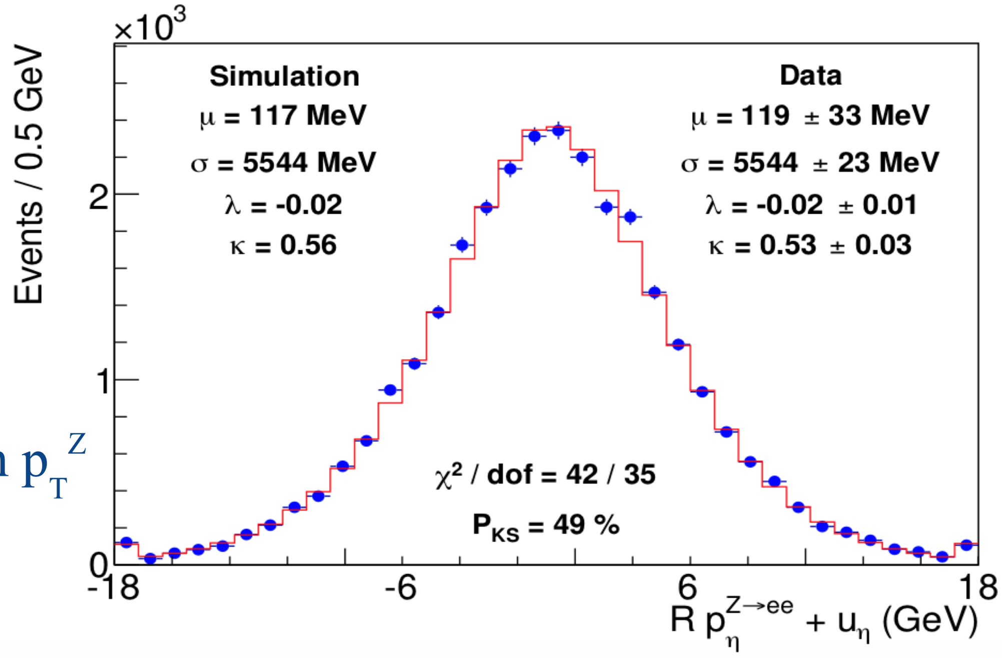

high p_T^Z

Tuning Recoil Resolution Model with *Z* events

NEW: Fine-tuning model for resolution perpendicular to p_T(Z) axis

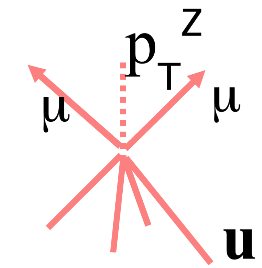

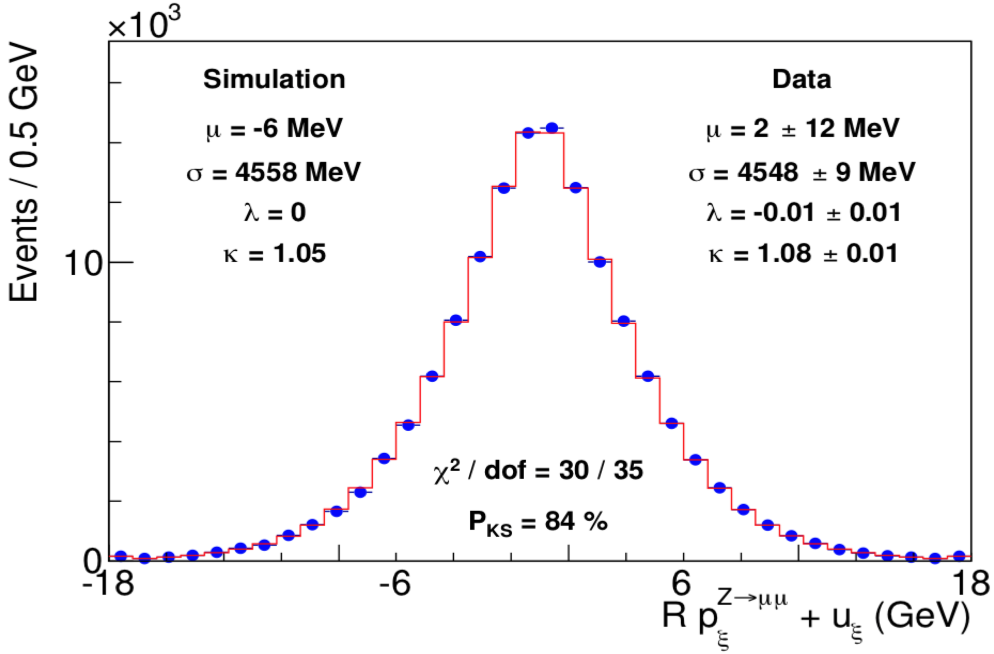

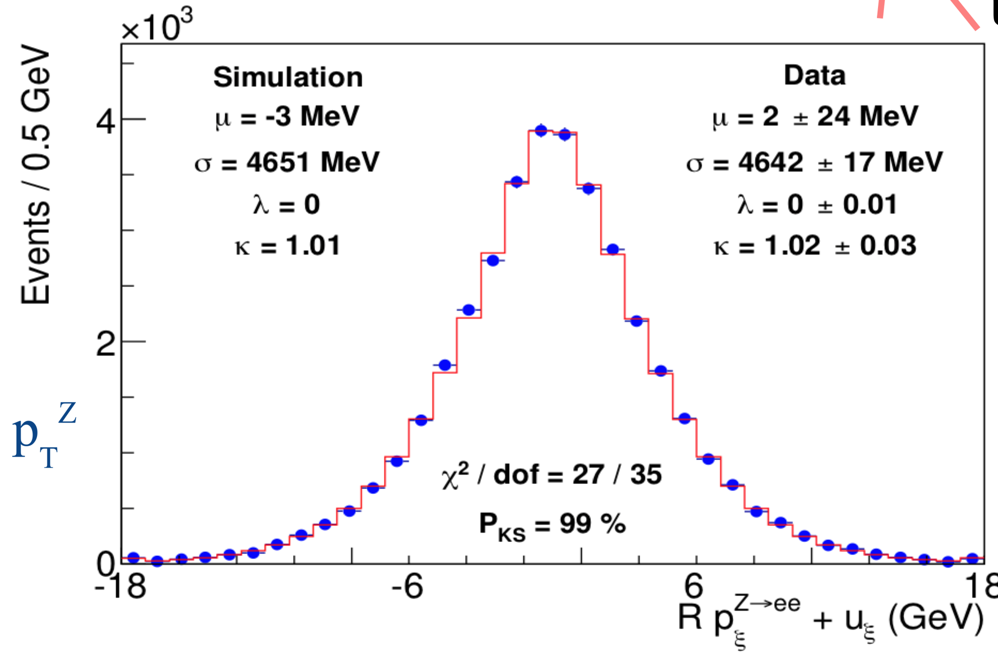

low p_T^Z

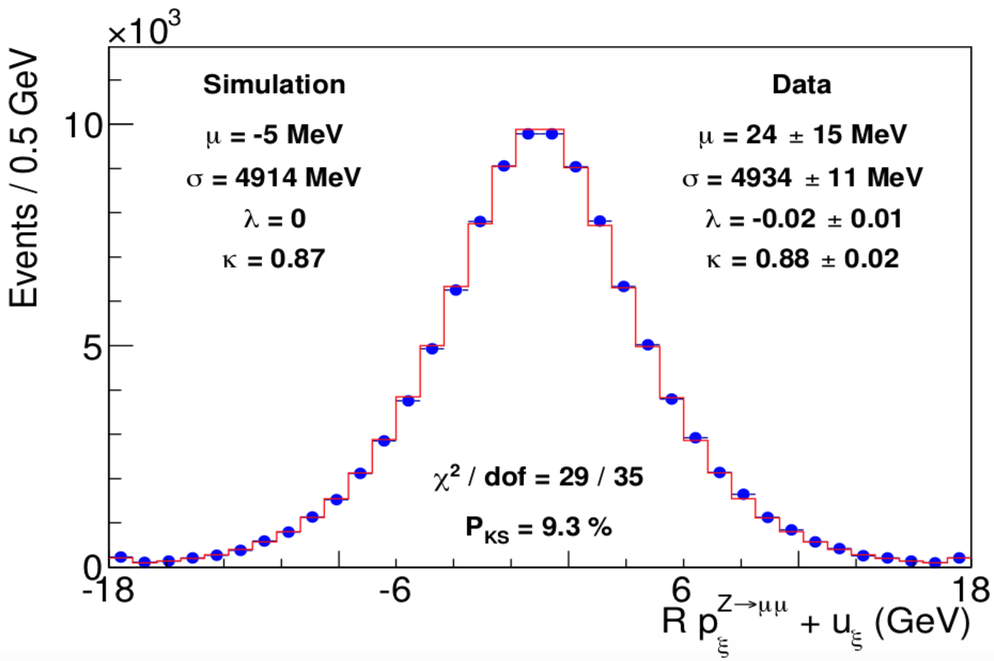

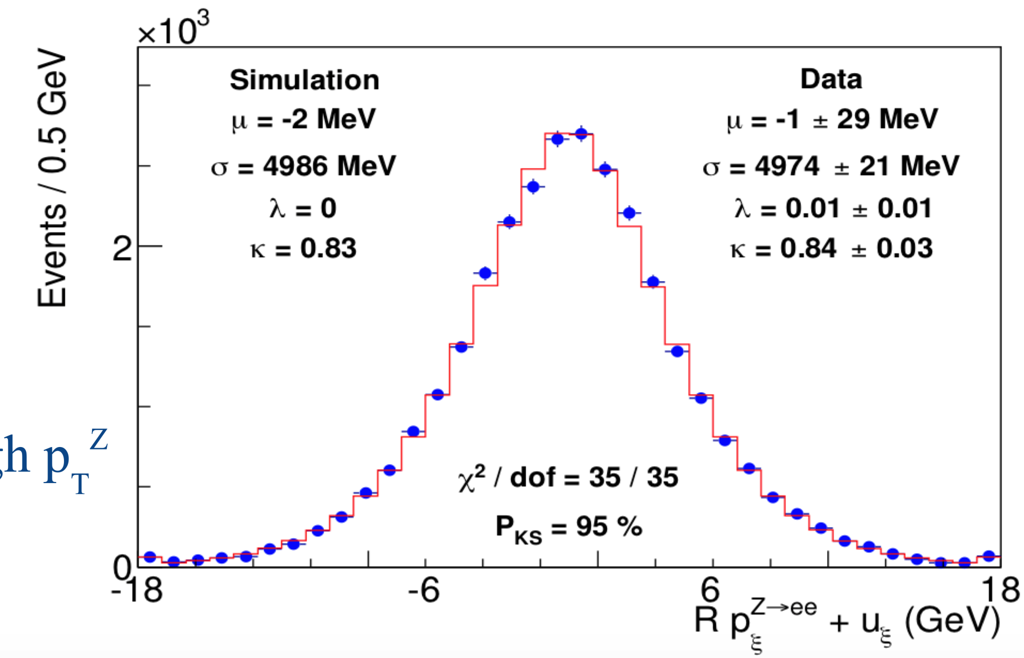

high p_T^Z

Testing Hadronic Recoil Model with *W* boson events

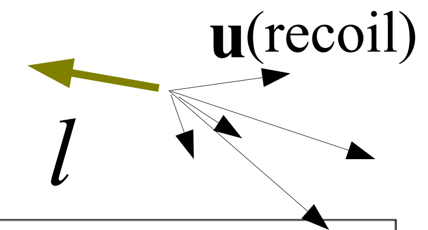

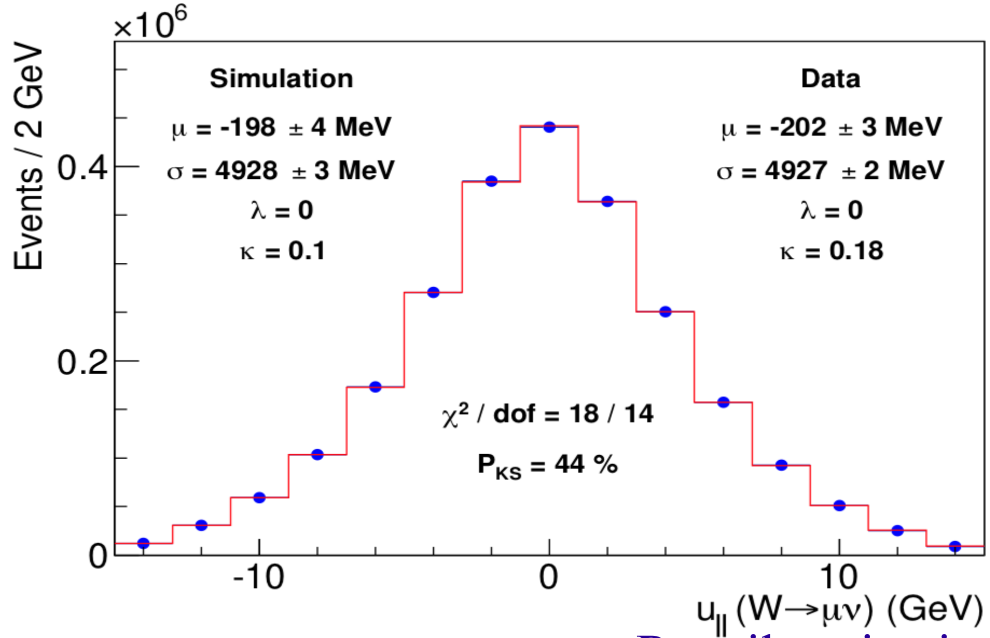

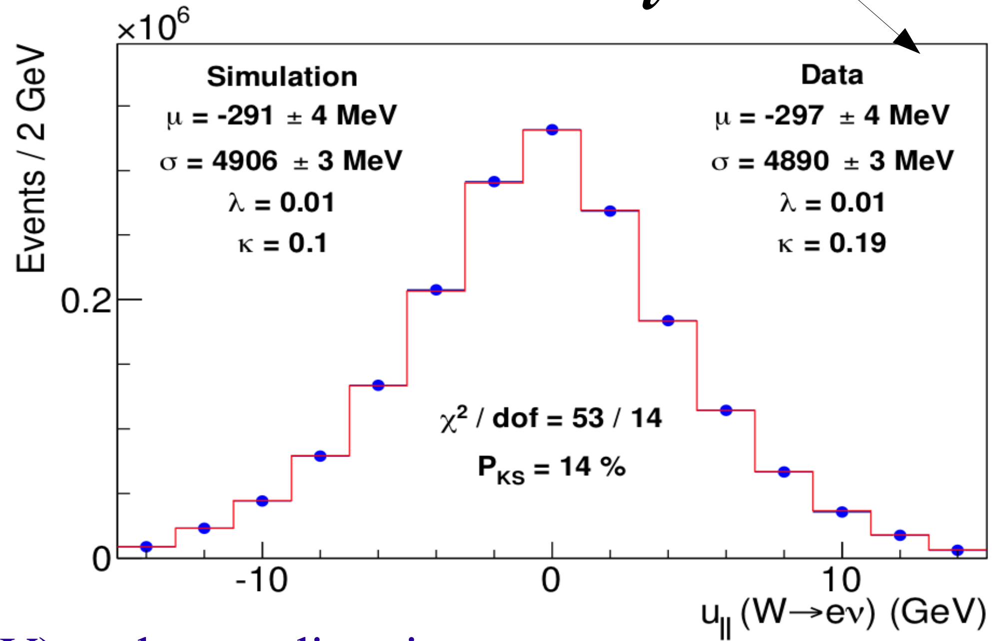

Recoil projection (GeV) on lepton direction

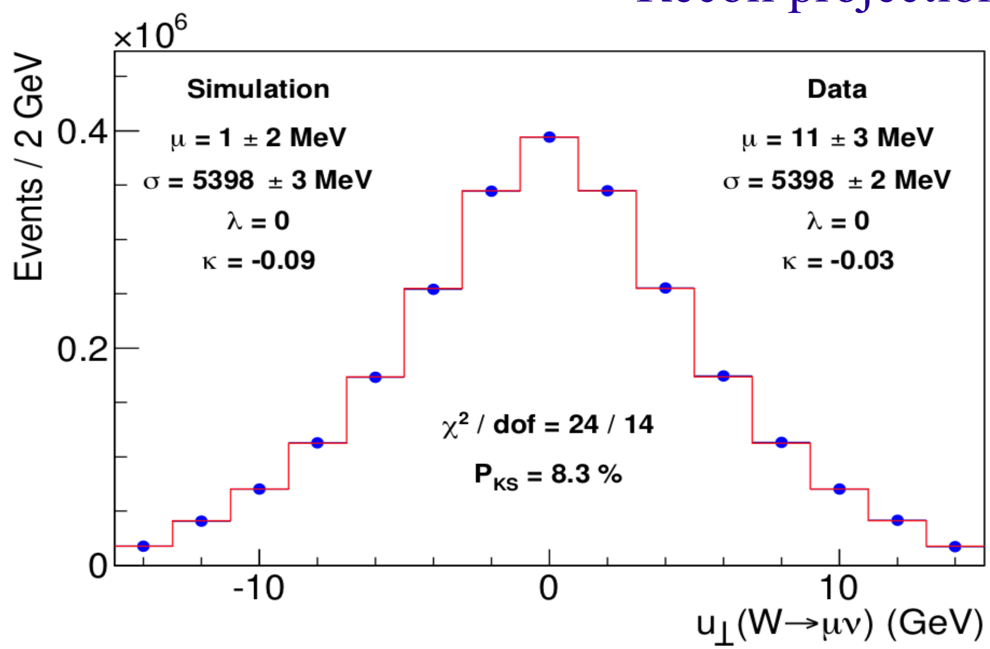

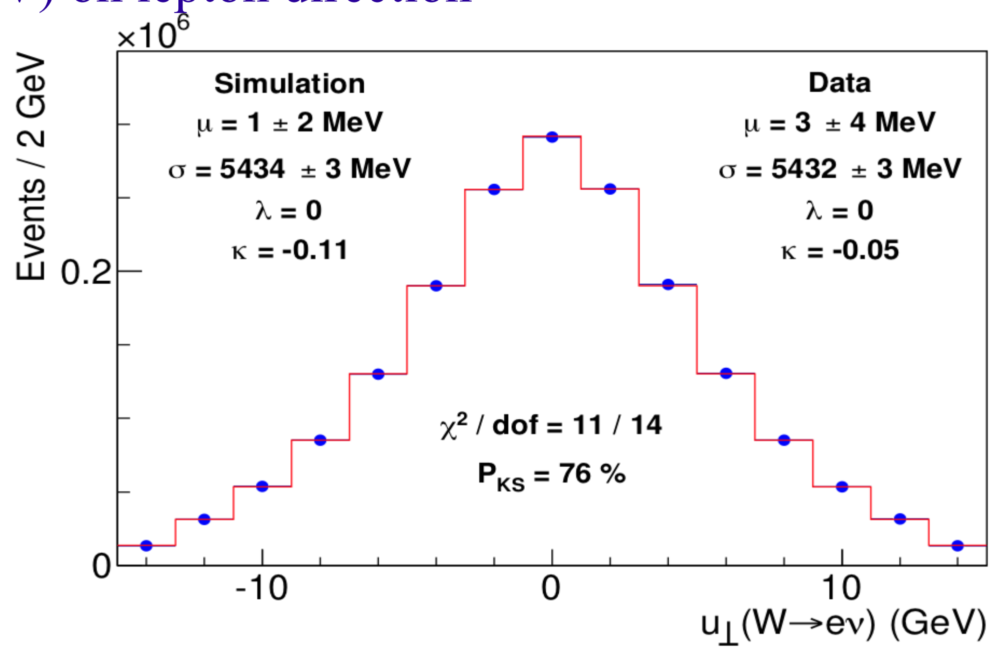

Recoil projection (GeV) perpendicular to lepton

Additional Constraint on $p_T(W)$ Model with *W* boson events

- NEW: In addition to the $p_T(Z)$ data constrain on the boson p_T spectrum, the ratio of the $p_T(W)$ / $p_T(Z)$ spectra is also constrained from the $p_T(W)$ data
  - DyqT : triple-differential cross section calculation at NNLO-QCD used to model scale variation of ratio
  - $p_T(W)$ data is used as constraint on ratio model
  - correlation with hadronic recoil model is taken into account

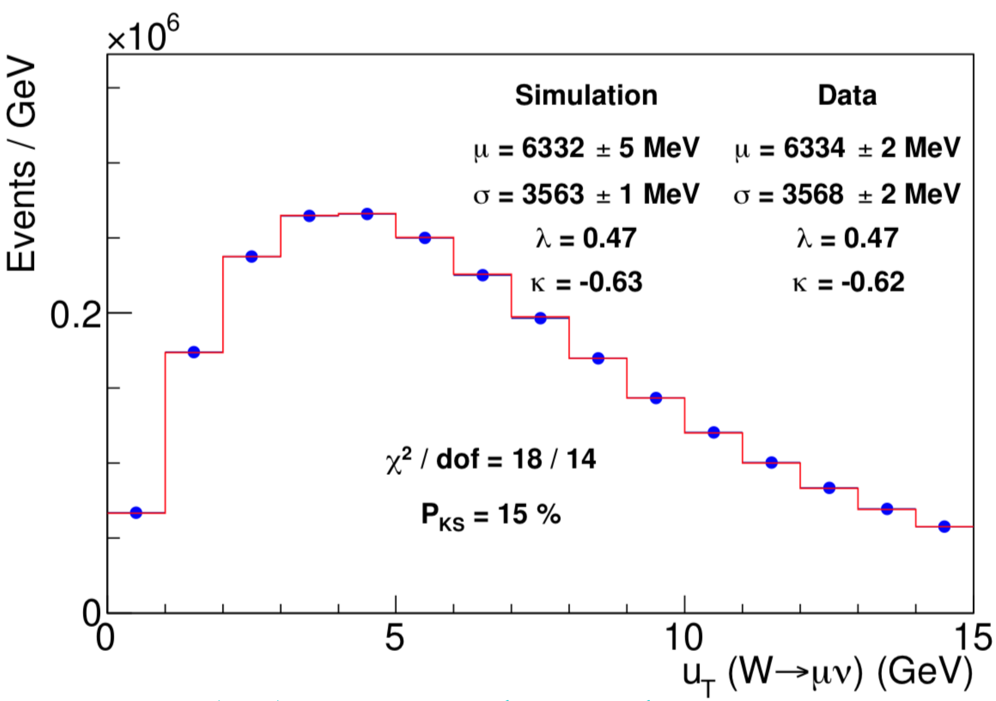

$p_T(W)$, muon channel

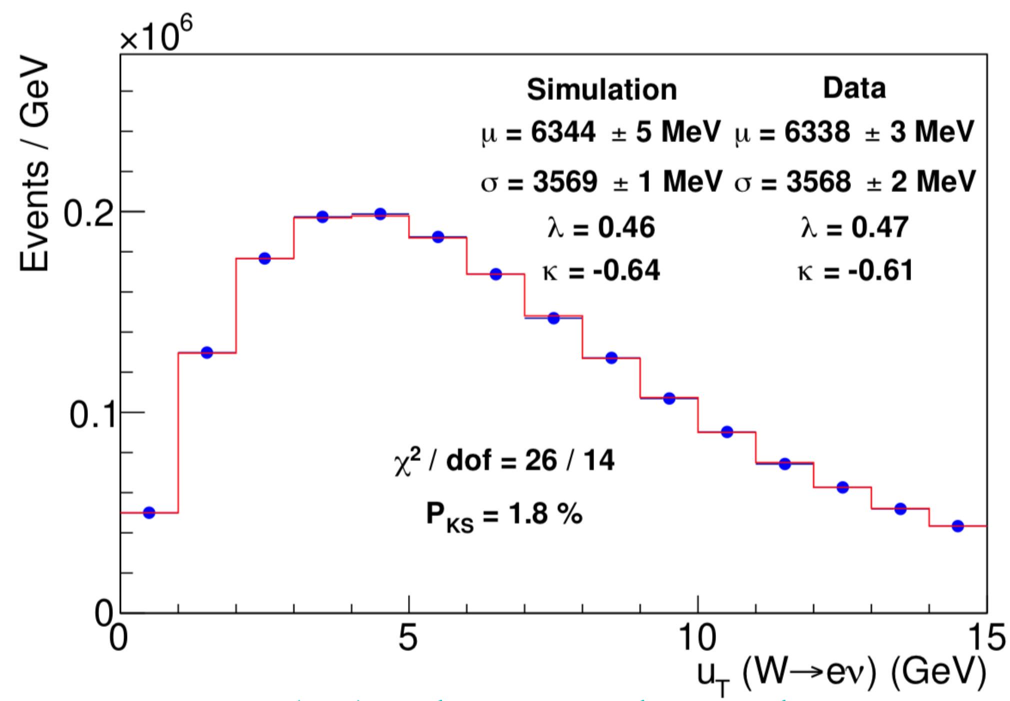

$p_T(W)$, electron channel

• Data
Simulation

Parton Distribution Functions and Backgrounds

Parton Distribution Functions

- Affect W kinematic lineshapes through acceptance cuts
- In the rest frame, $p_T = m \sin \theta^* / 2$
- Longitudinal cuts on lepton in the lab frame sculpt the distribution of θ^*, hence biases the distribution of lepton p_T
  - Relationship between lab frame and rest frame depends on the boost of the W boson along the beam axis
- Parton distribution functions control the longitudinal boost
- Uncertainty due to parton distribution functions evaluated by fitting pseudo-experiments (simulated samples with the same statistics and selection as data) with varied parton distribution functions

Parton Distribution Functions

- Affect W boson kinematic line-shapes through acceptance cuts
- We use NNPDF3.1 as the default NNLO PDFs
- Use ensemble of 25 'uncertainty' PDFs => 3.9 MeV
  - Represent variations of eigenvectors in the PDF parameter space
  - compute δM_W contribution from each error PDF
- Central values from NNLO PDF sets CT18, MMHT2014 and NNPDF3.1 agree within 2.1 MeV of their midpoint
- As an additional check, central values from NLO PDF sets ABMP16, CJ15, MMHT2014 and NNPDF3.1 agree within 3 MeV of their midpoint
- Missing higher-order QCD effects estimated to be 0.4 MeV
  - varying the factorization and renormalization scales
  - comparing two event generators with different resummation and non-perturbative schemes.

Backgrounds in the *W* boson sample

- $Z \to ll$ events with only one reconstructed leptons:
  - efficiency and calorimeter response mapped using control samples of $Z \to ll$ data, and modeled in the custom simulation
  - background estimates validated using a full GEANT-based CDF detector simulation
  - the only large background is $Z \to \mu\mu$ with geometrical acceptance loss of forward muons

- $W \to \tau\upsilon \to l\upsilon\bar{\upsilon}\upsilon$ background estimated using custom simulation

- QCD jet background estimated using control samples of data, anti-selected on lepton quality requirements

- Pion and kaon decays-in-flight to mis-reconstructed muons
  - Estimated using control samples of data, anti-selected on muon track-quality requirements

- Cosmic ray muons estimated using a dedicated track-finding algorithm

Backgrounds in the *W* boson sample

Muon channel

Source	Fraction (%)	δM_W (MeV) m_T fit	p_T^μ fit	p_T^ν fit
$Z/\gamma^* \to \mu\mu$	7.37 ± 0.10	1.6 (0.7)	3.6 (0.3)	0.1 (1.5)
$W \to \tau\nu$	0.880 ± 0.004	0.1 (0.0)	0.1 (0.0)	0.1 (0.0)
Hadronic jets	0.01 ± 0.04	0.1 (0.8)	-0.6 (0.8)	2.4 (0.5)
Decays in flight	0.20 ± 0.14	1.3 (3.1)	1.3 (5.0)	-5.2 (3.2)
Cosmic rays	0.01 ± 0.01	0.3 (0.0)	0.5 (0.0)	0.3 (0.3)
Total	8.47 ± 0.18	2.1 (3.3)	3.9 (5.1)	5.7 (3.6)

Electron channel

Source	Fraction (%)	δM_W (MeV) m_T fit	p_T^e fit	p_T^ν fit
$Z/\gamma^* \to ee$	0.134 ± 0.003	0.2 (0.3)	0.3 (0.0)	0.0 (0.6)
$W \to \tau\nu$	0.94 ± 0.01	0.6 (0.0)	0.6 (0.0)	0.6 (0.0)
Hadronic jets	0.34 ± 0.08	2.2 (1.2)	0.9 (6.5)	6.2 (-1.1)
Total	1.41 ± 0.08	2.3 (1.2)	1.1 (6.5)	6.2 (1.3)

Backgrounds are small (except $Z \to \mu\mu$ with a forward muon)

W Mass Fits

Blind Analysis Technique

- All W and Z mass fit results were blinded with a random [-50,50] MeV offset hidden in the likelihood fitter

- Blinding offset removed after the analysis was declared frozen

- Technique allows to study all aspects of data while keeping Z boson mass and W boson mass result unknown within ±50 MeV

W Transverse Mass Fits

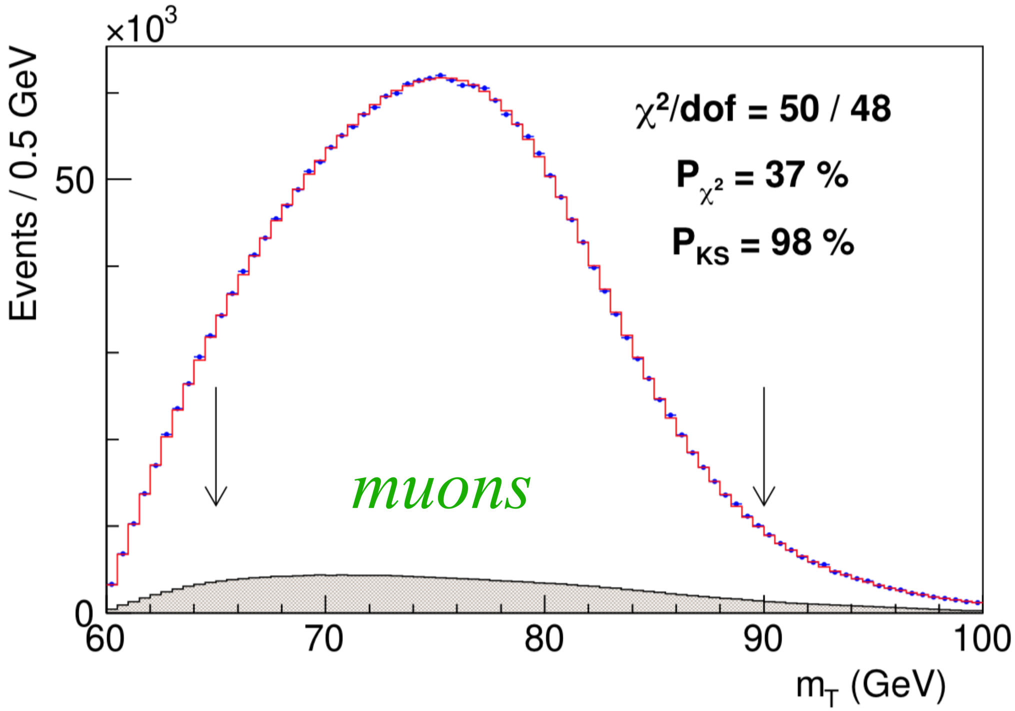

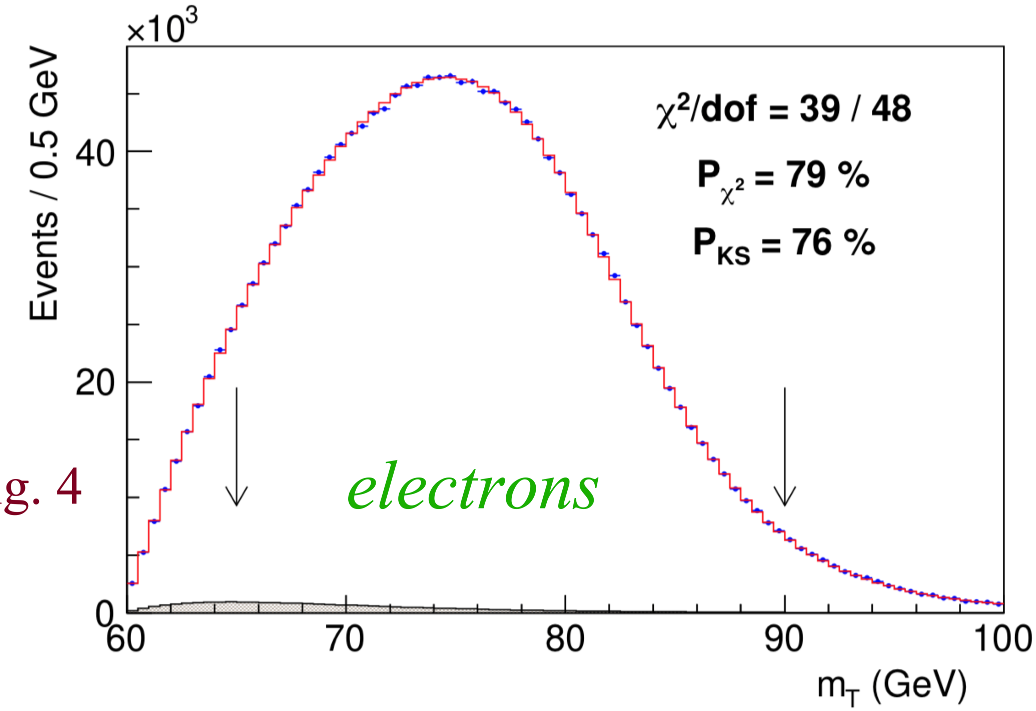

Fig. 4

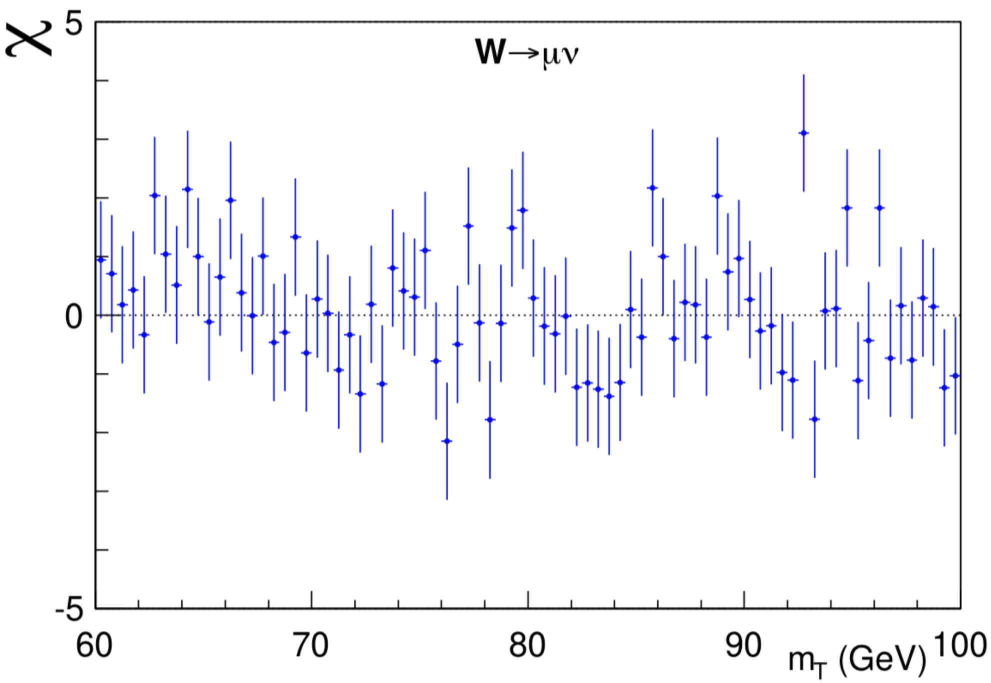

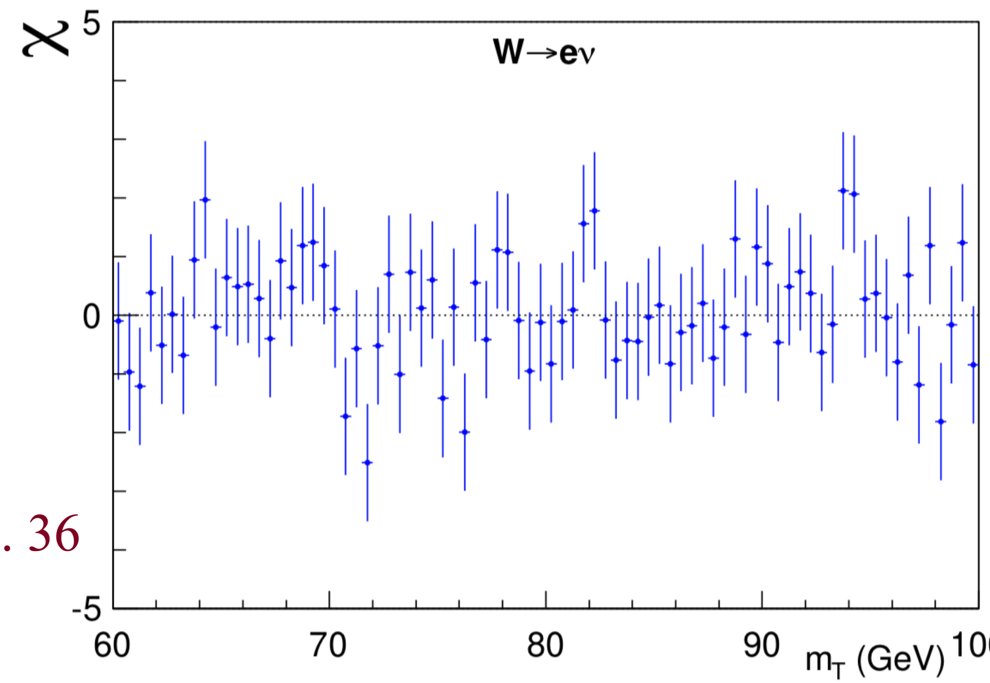

Fig. 36

W Charged Lepton p_T Fits

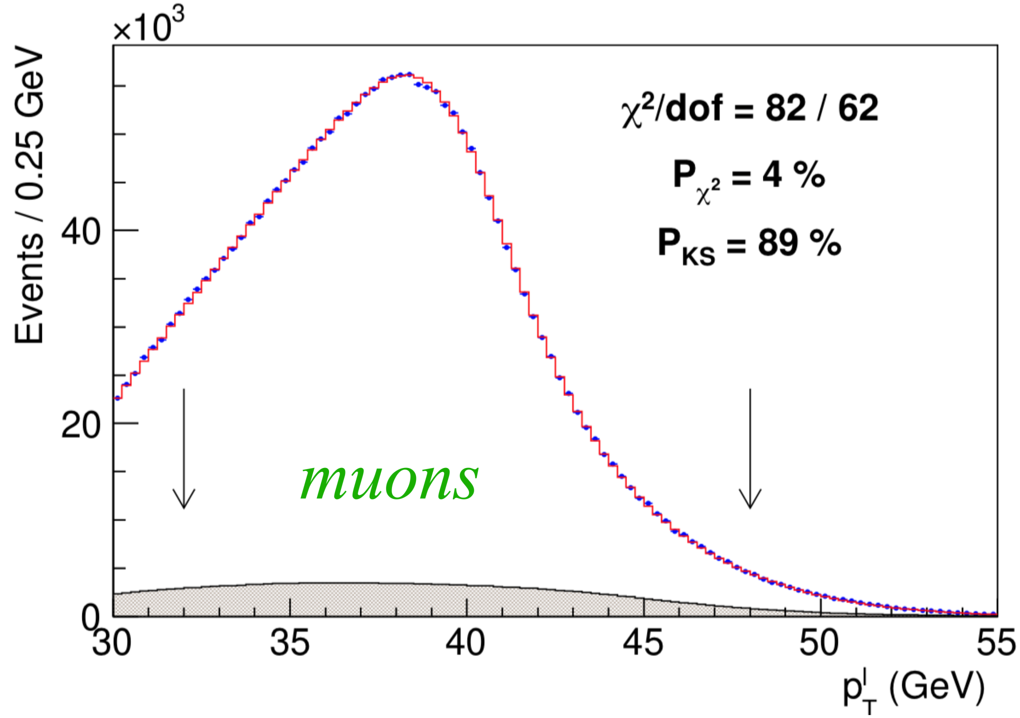

Fig. 4

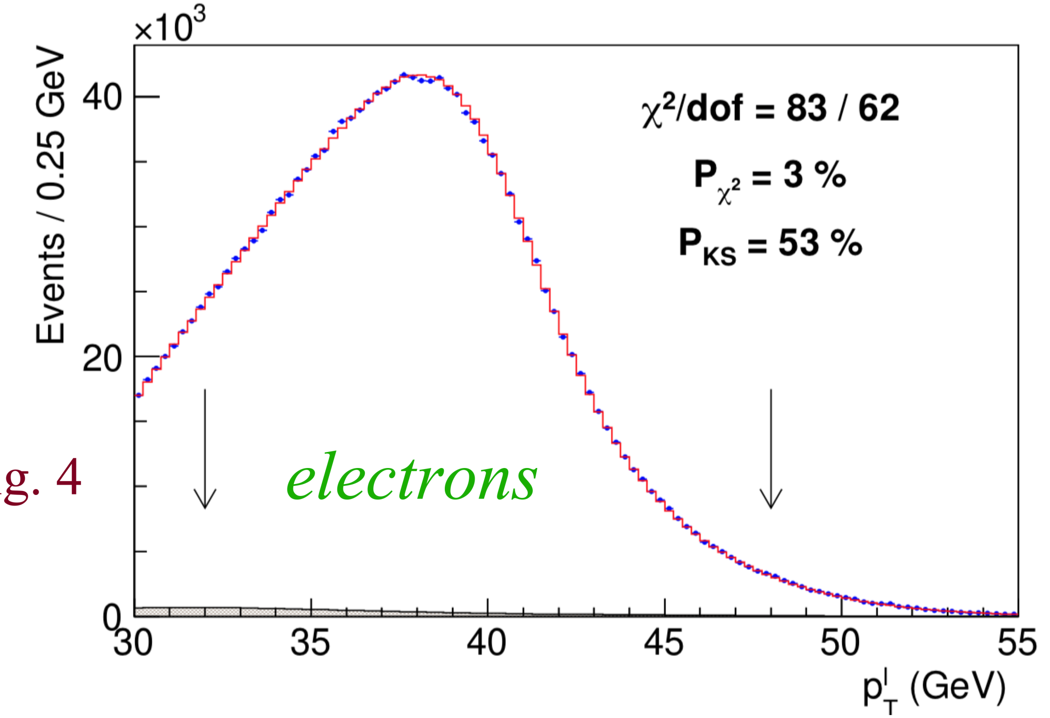

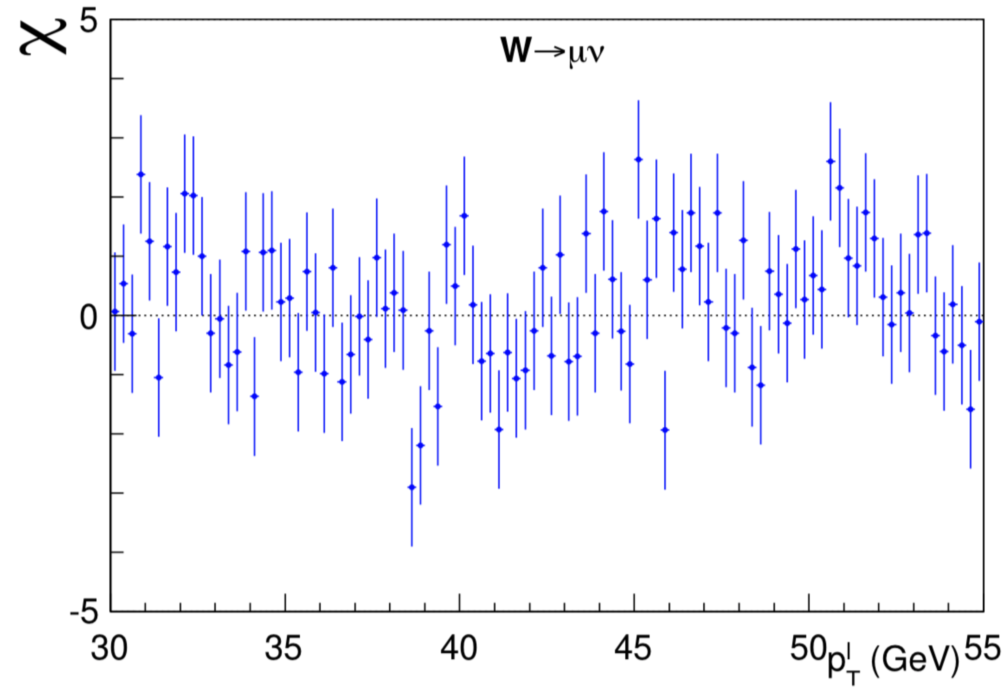

Fig. 37

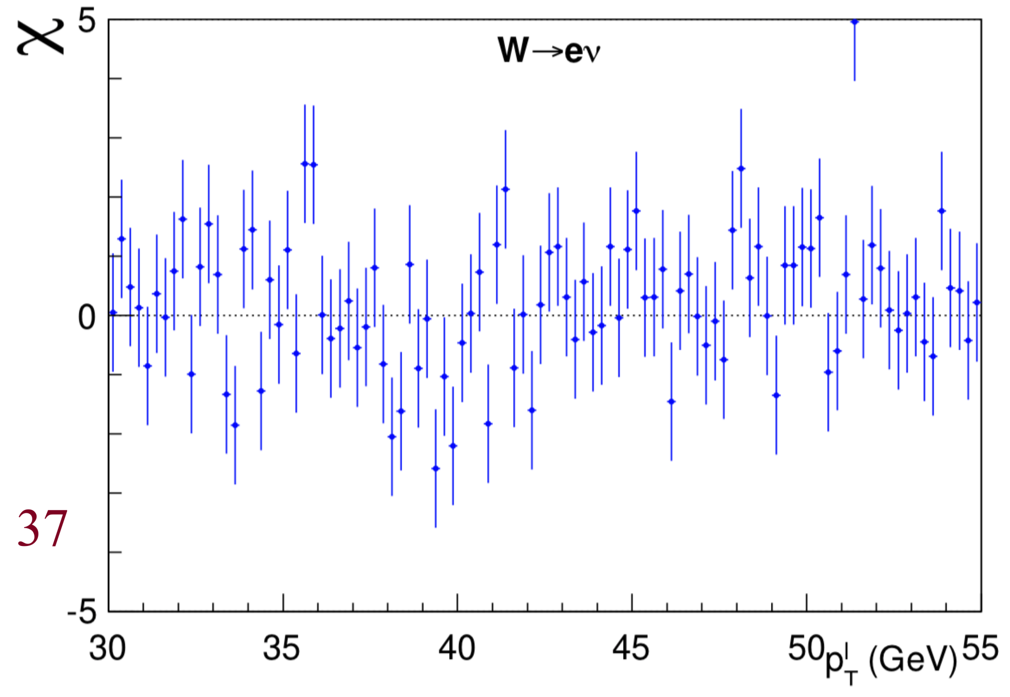

W Neutrino p_T Fits

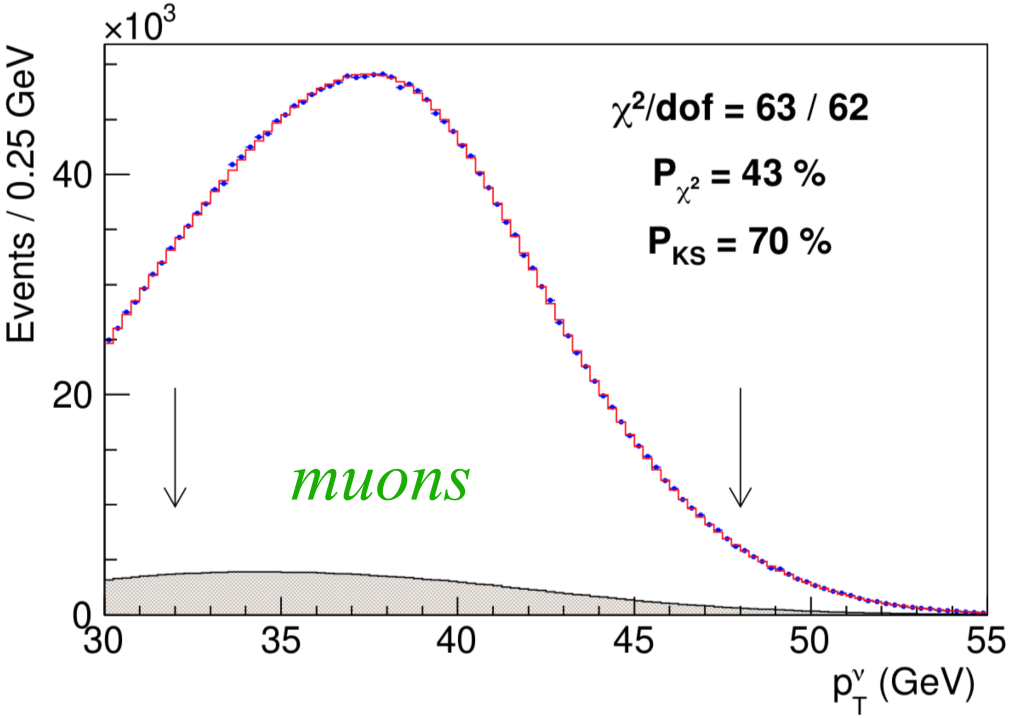

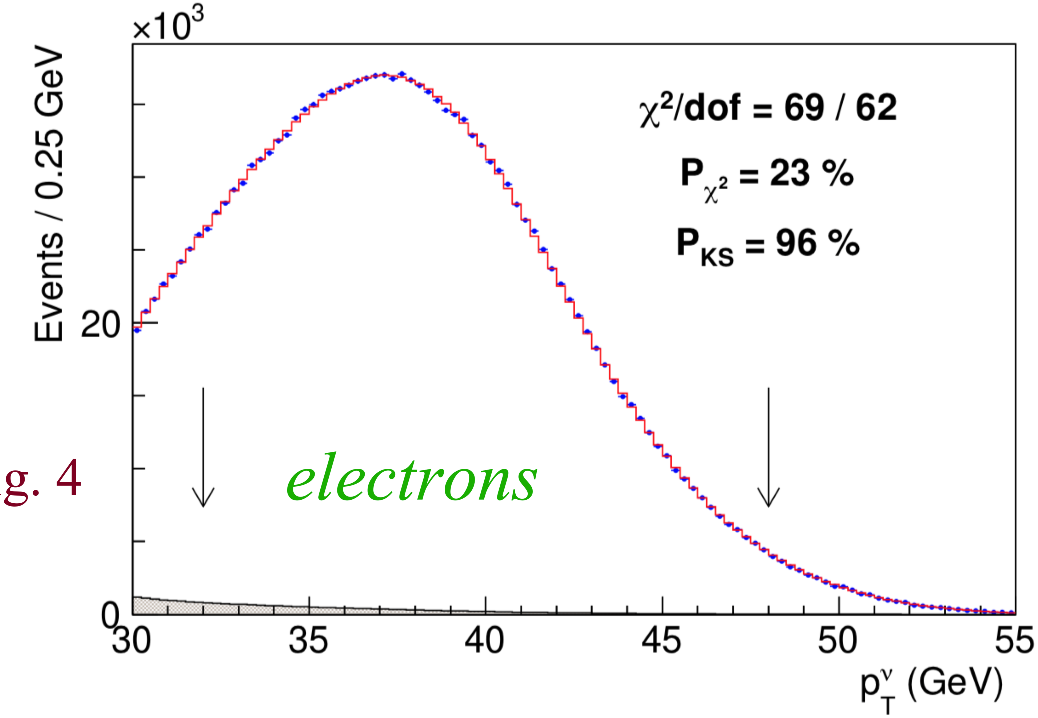

Fig. 4

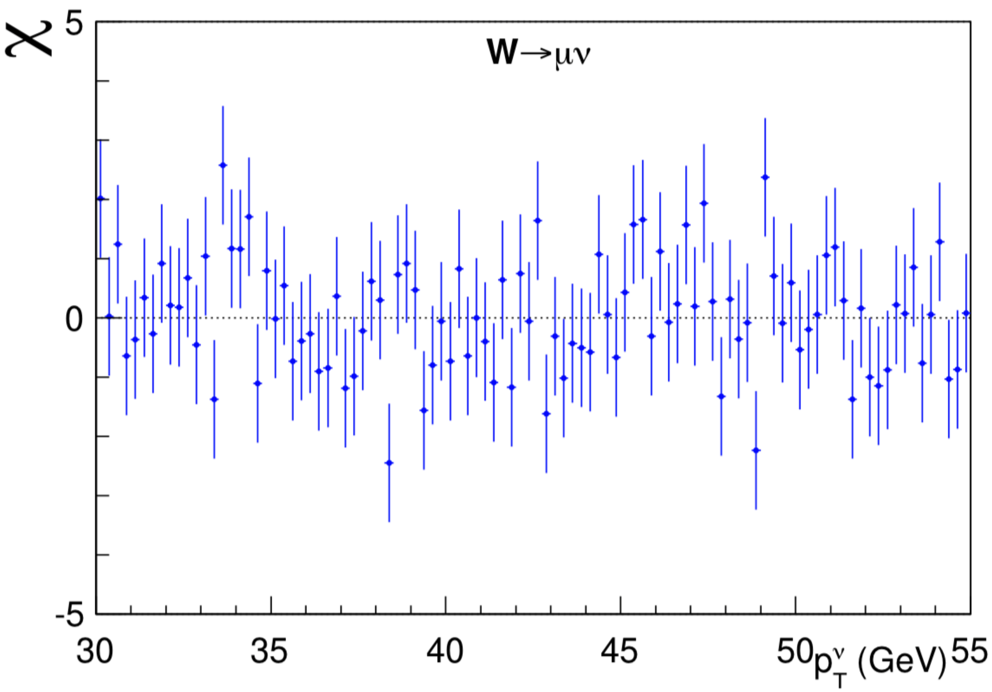

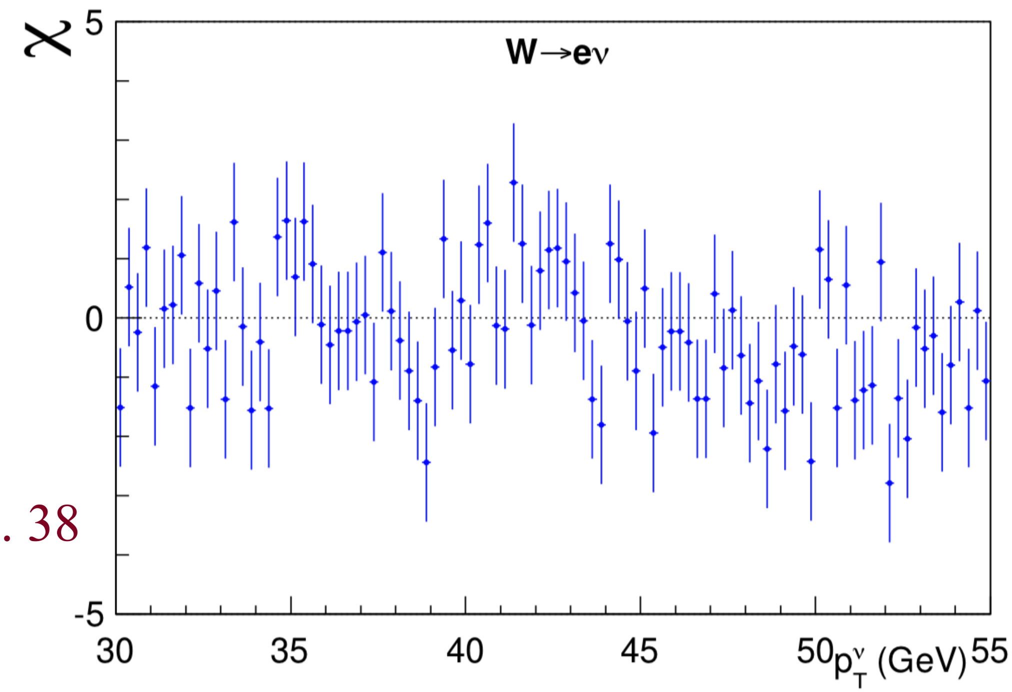

Fig. 38

Summary of *W* Mass Fits

Distribution	W-boson mass (MeV)	χ^2/dof
$m_T(e,\nu)$	$80\ 429.1 \pm 10.3_{\mathrm{stat}} \pm 8.5_{\mathrm{syst}}$	$39/48$
$p_T^\ell(e)$	$80\ 411.4 \pm 10.7_{\mathrm{stat}} \pm 11.8_{\mathrm{syst}}$	$83/62$
$p_T^\nu(e)$	$80\ 426.3 \pm 14.5_{\mathrm{stat}} \pm 11.7_{\mathrm{syst}}$	$69/62$
$m_T(\mu,\nu)$	$80\ 446.1 \pm 9.2_{\mathrm{stat}} \pm 7.3_{\mathrm{syst}}$	$50/48$
$p_T^\ell(\mu)$	$80\ 428.2 \pm 9.6_{\mathrm{stat}} \pm 10.3_{\mathrm{syst}}$	$82/62$
$p_T^\nu(\mu)$	$80\ 428.9 \pm 13.1_{\mathrm{stat}} \pm 10.9_{\mathrm{syst}}$	$63/62$
combination	$80\ 433.5 \pm 6.4_{\mathrm{stat}} \pm 6.9_{\mathrm{syst}}$	$7.4/5$

Consistency between two channels and three kinematic fits

Combinations of Fit Results

Combination	m_T fit Electrons	m_T fit Muons	p_T^ℓ fit Electrons	p_T^ℓ fit Muons	p_T^ν fit Electrons	p_T^ν fit Muons	Value (MeV)	χ^2/dof	Probability (%)
m_T	✓	✓					$80\ 439.0 \pm 9.8$	1.2 / 1	28
p_T^ℓ			✓	✓			$80\ 421.2 \pm 11.9$	0.9 / 1	36
p_T^ν					✓	✓	$80\ 427.7 \pm 13.8$	0.0 / 1	91
m_T & p_T^ℓ	✓	✓	✓	✓			$80\ 435.4 \pm 9.5$	4.8 / 3	19
m_T & p_T^ν	✓	✓			✓	✓	$80\ 437.9 \pm 9.7$	2.2 / 3	53
p_T^ℓ & p_T^ν			✓	✓	✓	✓	$80\ 424.1 \pm 10.1$	1.1 / 3	78
Electrons	✓		✓		✓		$80\ 424.6 \pm 13.2$	3.3 / 2	19
Muons		✓		✓		✓	$80\ 437.9 \pm 11.0$	3.6 / 2	17
All	✓	✓	✓	✓	✓	✓	$80\ 433.5 \pm 9.4$	7.4 / 5	20

- Combined electrons (3 fits): $M_W = 80424.6 \pm 13.2$ MeV, $P(\chi^2) = 19\%$
- Combined muons (3 fits): $M_W = 80437.9 \pm 11.0$ MeV, $P(\chi^2) = 17\%$
- All combined (6 fits): $M_W = 80433.5 \pm 9.4$ MeV, $P(\chi^2) = 20\%$

citation: *Science* **376**, 170 (April 7, 2022); DOI: 10.1126/science.abk1781

Previous CDF Result (2.2 fb^{-1})
Combined Fit Systematic Uncertainties

Source	Uncertainty (MeV)
Lepton Energy Scale	7
Lepton Energy Resolution	2
Recoil Energy Scale	4
Recoil Energy Resolution	4
$u_{\|\|}$ efficiency	0
Lepton Removal	2
Backgrounds	3
$p_T(W)$ model	5
Parton Distributions	10
QED radiation	4
W boson statistics	12
Total	19

New CDF Result (8.8 fb^{-1})
Combined Fit Systematic Uncertainties

Source	Uncertainty (MeV)
Lepton energy scale	3.0
Lepton energy resolution	1.2
Recoil energy scale	1.2
Recoil energy resolution	1.8
Lepton efficiency	0.4
Lepton removal	1.2
Backgrounds	3.3
p_T^Z model	1.8
p_T^W/p_T^Z model	1.3
Parton distributions	3.9
QED radiation	2.7
W boson statistics	6.4
Total	9.4

CDF M_W *vs* m_{top}

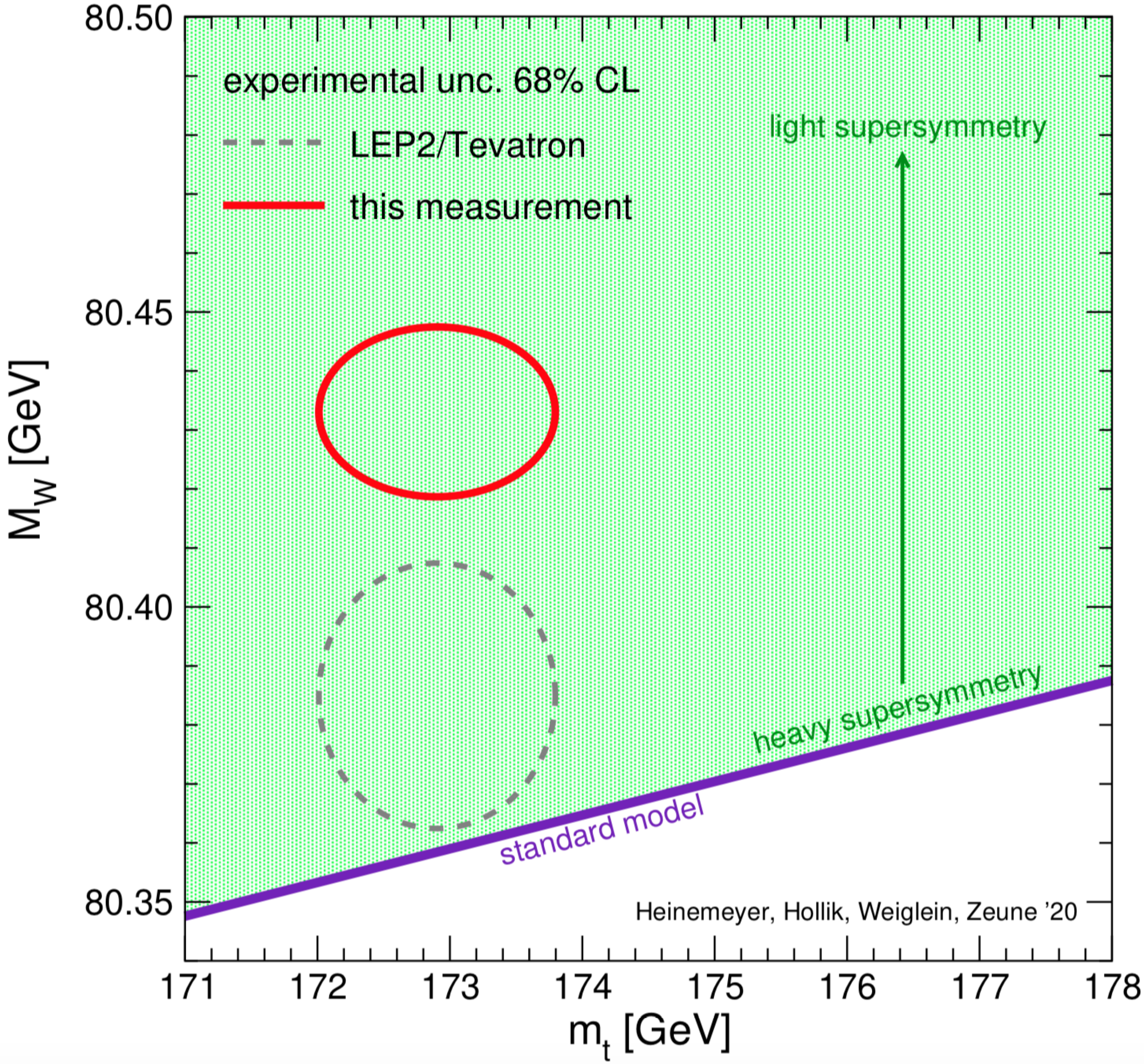

Understanding Tevatron-LHC correlations and combination with ATLAS in progress

W Boson Mass Measurements from Different Experiments

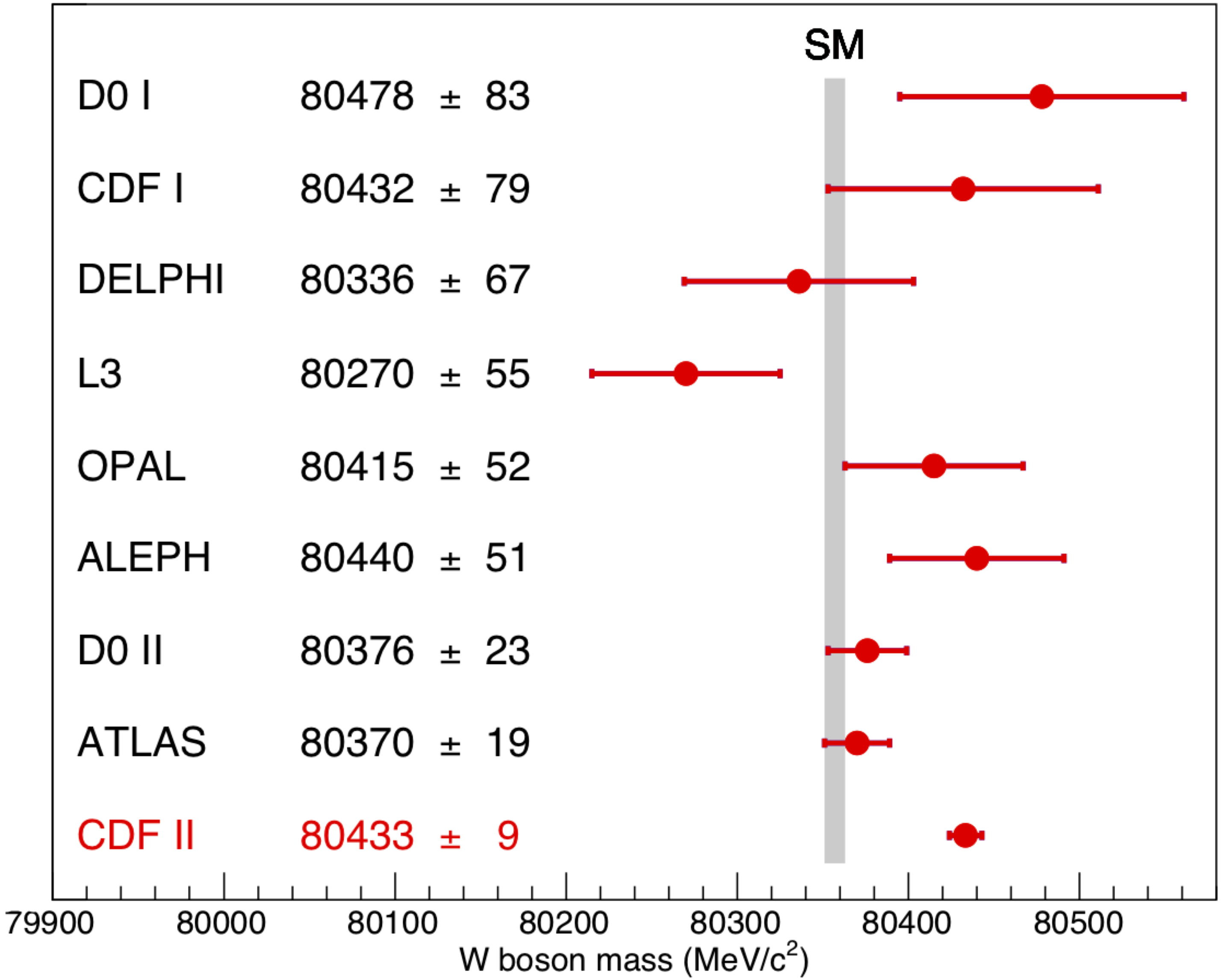

Fig. 5

SM expectation: $M_W = 80{,}357 \pm 4_{\text{inputs}} \pm 4_{\text{theory}}$ (PDG 2020)

LHCb measurement : $M_W = 80{,}354 \pm 23_{\text{stat}} \pm 10_{\text{exp}} \pm 17_{\text{theory}} \pm 9_{\text{PDF}}$ [*JHEP* **2022,** 36 (2022)]

1998 Status of M_W *vs* M_{top}

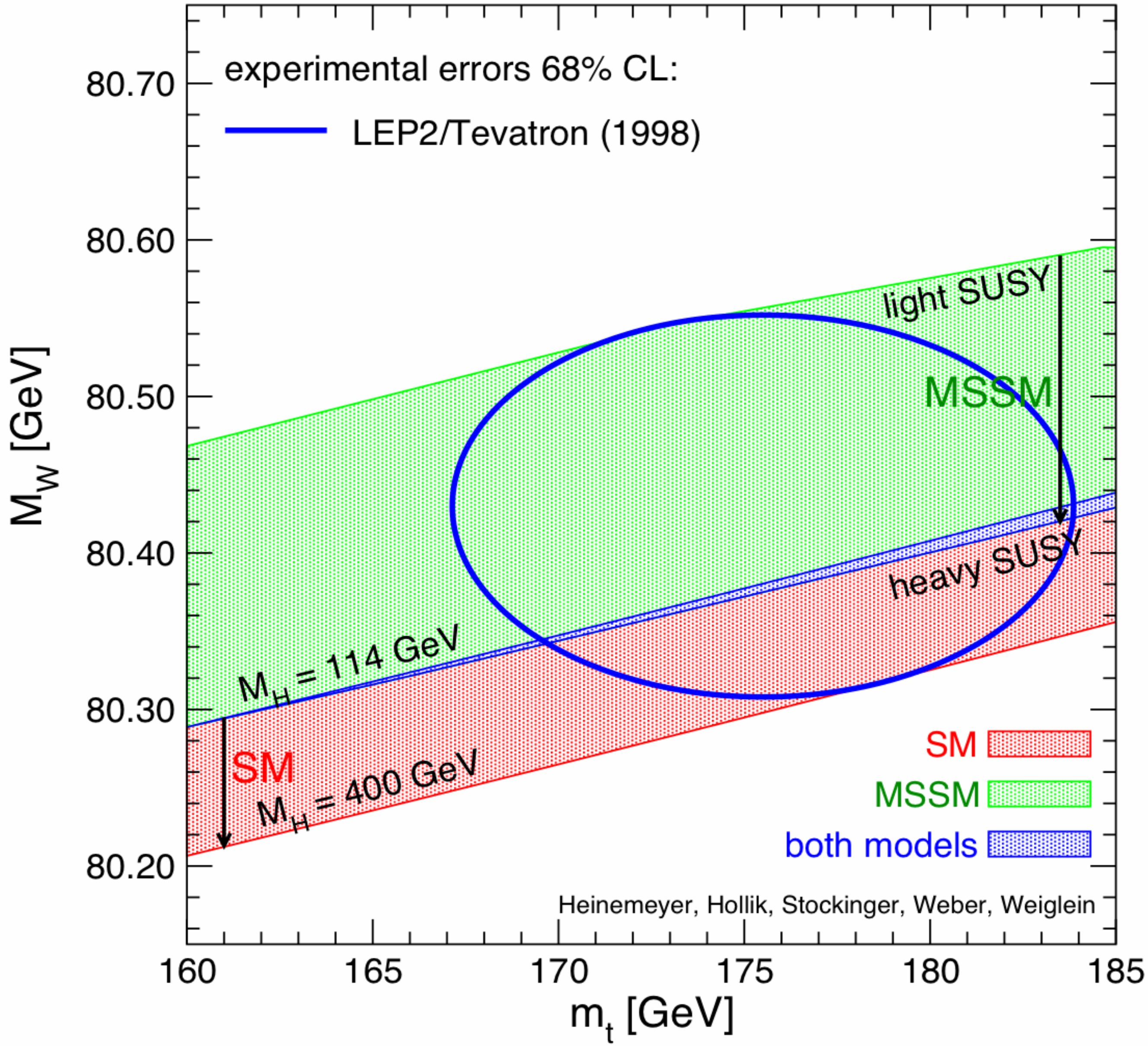

2022 Status of M_W *vs* M_{top}

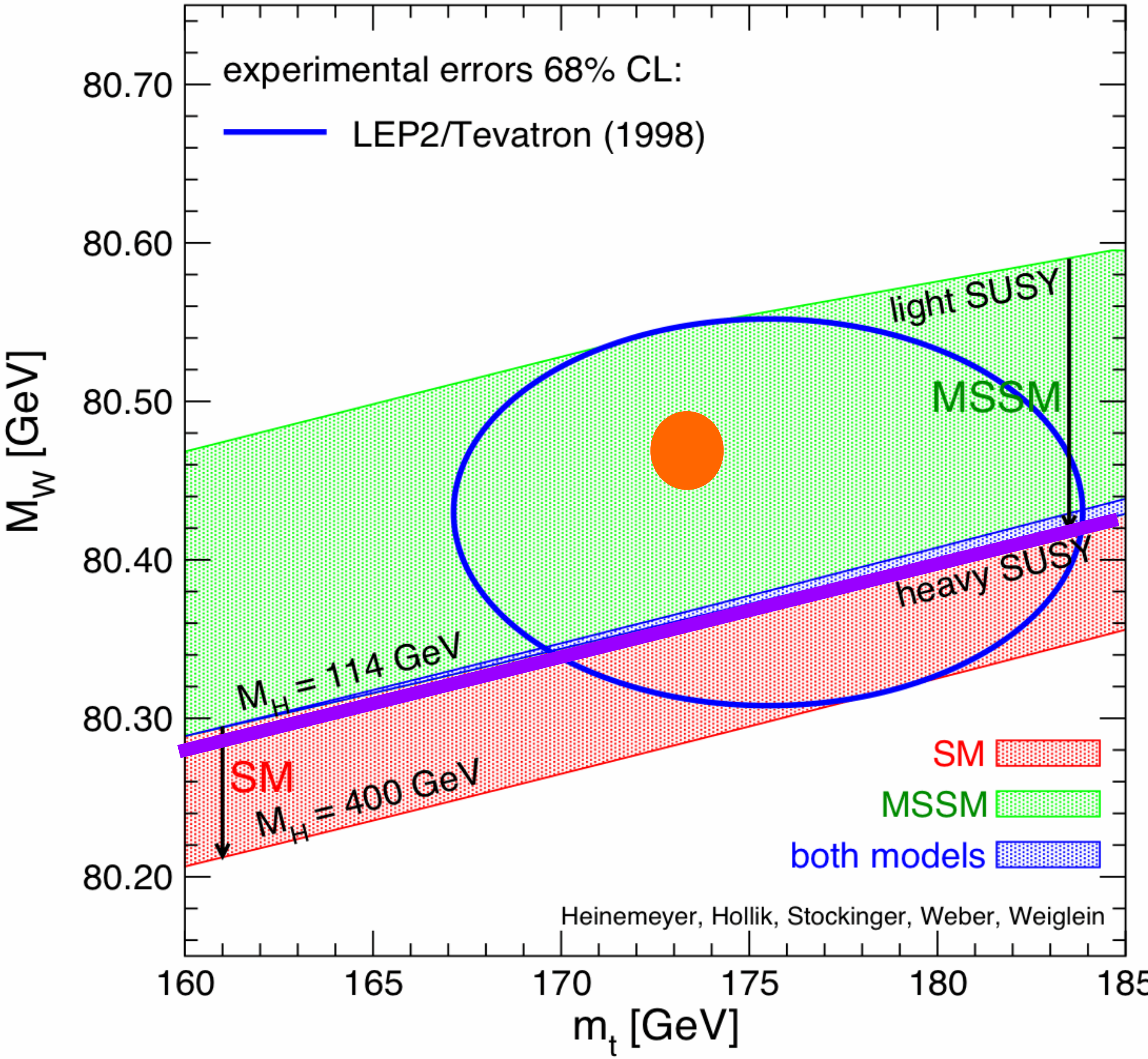

Standard Model after 2012 Higgs discovery

Epilogue

CDF W mass

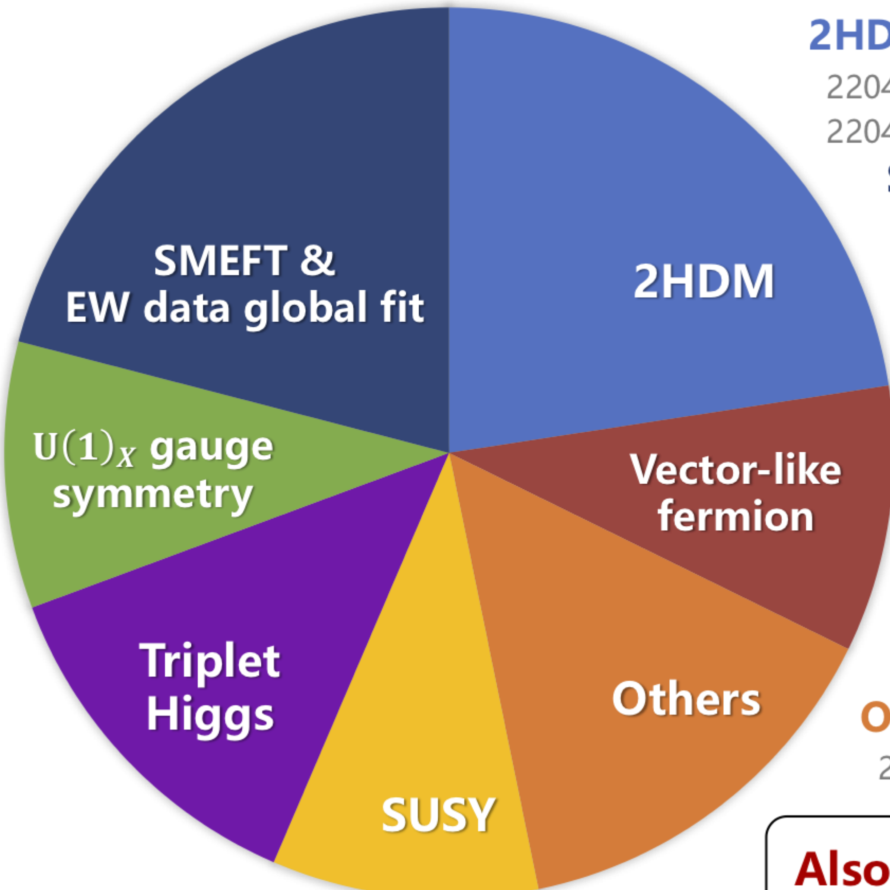

Total number: 62*

2HDM: 14

2204.03693/03767/04834/04688/06485/05085/05269/05303
2204.05975/09001/05728/08406/08390/10338

SMEFT & EW data global fit: 13

2204.04805/05260/05284/05267/05992/05965/05965/08546
2204.08440/10130/04191/05283/04204

Triplet Higgs: 8

2204.05031/05760/07144/07511/07844/08266/10274/10315

SUSY: 6

2204.04286/04356/04202/05285/06541/07138

$U(1)_X$ gauge symmetry: 6

2204.07100/08067/09487/09024/09585/10156

Vector-like fermion: 6

2204.07022/07411/08568/09477/09671/05024

Others: 9 (Non-unitarity, leptoquark, singlet scalar, ...)

2204.04559/04672/04770/04514/05302/06327/03996/05942/09031

* Preprints as of April 25th are counted.

Also related to
dark matter, neutrino masses/seesaw, flavor violation, muon g-2, flavor anomalies, gravitational waves, ...

The Future of the M_W Measurement

- The experiments at the LHC have collected and are collecting a lot of data.
  - While W bosons are produced slightly differently at the LHC (*pp* collider) than the Tevatron ($p\bar{p}$ collider), the LHC experiments have the opportunity to make this measurement.

- If built, a new electron-positron collider can also measure the W boson mass very precisely.

- The LHC as well as smaller, specialized experiments are sensitive to the kinds of new particles and interactions that can influence the W boson mass.
  - If there is new physics which could explain the tension of our result with the SM expectation, this new physics could show up directly in these experiments.

Summary

- The *W* boson mass is a very interesting parameter to measure with increasing precision

- New CDF result is twice as precise as previous measurements:

  - $M_W = 80433.5 \pm 6.4_{stat} \pm 6.9_{syst}$ MeV
    $= 80433.5 \pm 9.4$ MeV

- Difference from SM expectation of $M_W = 80{,}357 \pm 6$ MeV

  - significance of 7.0σ
  - suggests the possibility of improvements to the SM calculation or of extensions to the SM

Thank you for your attention !